Audun Røsjorde

Minimization of entropy production in separate and connected process units

This thesis has been submitted to
Department of Chemistry
Norwegian University of Science and Technology

in partial fulfillment of the requirements for
the Norwegian academic degree
DOKTOR INGENIØR
August 2004

Institutt for kjemi
Norges teknisk-naturvitenskapelige universitet
N-7491 Trondheim
Norway

Doktoringeniøravhandling 2004:111
ISBN 82-471-6443-4
ISSN 1503-8181

In the beginning the Universe was created. This has made a lot of people very angry and been widely regarded as a bad move.

- The Restaurant at the End of the Universe

Acknowledgments

This thesis would not have existed were it not for the financial support offered by VISTA, the program for fundamental research sponsored by the Norwegian Academy of Science and Letters and Statoil. I thank all of those involved for providing me the opportunity to work on this thesis.

For being my supervisor during the four and a half year it took to finish this project, I sincerely thank Prof. Signe Kjelstrup. She taught me the art of scientific research in general and the field of nonequilibrium thermodynamics in particular. Her never-ending effort to understand the fundamental mechanisms of Nature is a source of great inspiration! I hope we may continue working together in the years to come.

I would also like to thank Prof. Dick Bedeaux for acting as my co-supervisor and for sharing happily of his seemingly infinite knowledge of physics and mathematics! Furthermore, I am grateful for the assistance I have gotten from Prof. Bjørn Hafskjold on classical thermodynamics in times of confusion.

For giving the project an industrial input, I thank Roger Hansen at Statoil Research Center at Rotvoll, Trondheim. He supplied necessary information about the propane dehydrogenation process and helped keeping the right focus on the process optimization part.

All the results that are presented in this thesis were obtained by performing numerical calculations, and a stable and well-equipped computer facility at Department of Chemistry made the calculations possible. I am deeply grateful to Terje Bruvoll for appreciating the value of computers in scientific work, as well as for creating a friendly atmosphere among the staff at Department of Chemistry.

Among my colleagues, I wish to thank Eivind Johannessen in particular. Our countless scientific discussions really contributed to shape my thoughts on matters related to entropy production minimizations. Gelein de Koeijer and Lars Nummedal, who both worked on subjects related to my thesis, lay the foundation for the present work. I thank them both for their effort: It really made a difference!

Thanks to all of my former and present colleagues at the Department of Chemistry for their effort in making the daily life at the department more enjoyable. Lars Erik: I miss those daily chess and cake sessions we used to have before

life got too serious. I also wish to thank my parents for teaching me the value of education. Without it, I would not have gone to a university in the first place.

Finally, I had the great fortune to work as a guest researcher at the National Institute of Advanced Industrial Science and Technology in Tsukuba, Japan. In the Energy-efficient Chemical Systems Group, lead by Dr. Nakaiwa, I spent five wonderful months. The hospitality and generosity I received from my colleagues and friends there was truly incredible! To them I say:

いろいろ あいがと ございました. にほん の こと を わすれません.

Summary

The objective of this thesis was to further develop a methodology for minimizing the entropy production of single and connected chemical process units. When chemical process equipment is designed and operated at the lowest entropy production possible, the energy efficiency of the equipment is enhanced. We have found for single process units that the entropy production could be reduced with up to 20-40%, given the degrees of freedom in the optimization. In processes, our results indicated that even bigger reductions were possible. The states of minimum entropy production were studied and important parameters for obtaining significant reductions in the entropy production were identified. Both from sustainability and economical viewpoints knowledge of energy efficient design and operation are important.

In some of the systems we studied, nonequilibrium thermodynamics was used to model the entropy production. In Chapter 2, we gave a brief introduction to different industrial applications of nonequilibrium thermodynamics. The link between local transport phenomena and overall system description makes nonequilibrium thermodynamics a useful tool for understanding design of chemical process units.

We developed the methodology of minimization of entropy production in several steps. First, we analyzed and optimized the entropy production of single units: Two alternative concepts of adiabatic distillation; diabatic and heat-integrated distillation, were analyzed and optimized in Chapter 3 to 5. In diabatic distillation, heat exchange is allowed along the column, and it is this feature that increases the energy efficiency of the distillation column. In Chapter 3, we found how a given area of heat transfer should be optimally distributed among the trays in a column separating a mixture of propylene and propane. The results showed that heat exchange was most important on the trays close to the reboiler and condenser. In Chapter 4 and 5, we studied how the entropy production of a heat-integrated distillation column separating benzene and toluene was influenced by changing two important system parameters. The two parameters were the ratio between the pressure in the rectifying and stripping section and the total rate of heat transfer per Kelvin (UA_{total}). In Chapter 4, UA_{total} was evenly distributed in the column. The results showed that there was an upper and a lower bound on the pressure ratio, for which the heat-integrated column had a lower entropy production than the adiabatic column. A lower bound was also found on UA_{total}. In Chapter 5, we allowed the UA_{total} to distribute itself in an optimal way. This enabled even lower en-

tropy productions and widened the range of the two parameters for which the heat-integrated distillation column performed better than the adiabatic. As in Chapter 3, we found that heat exchange was most important close to the condenser and reboiler. This made us propose a new design for the heat-integrated distillation column, with heat transfer between the topmost and bottommost trays only. This enabled further reductions in the entropy production.

The next step in the development was to study several units in connection. In Chapter 6, we minimized the entropy production of a heat exchanger, a plug-flow reactor, and a heat exchanger in series. This was a preparatory study for the larger process optimization in Chapter 7. By shifting heat transfer from the reactor to the heat exchanger up-front, the entropy production was reduced. It was also found that the ambient temperature profile along the reactor was of less important to the entropy production.

Finally, in Chapter 7, we were able to minimize the entropy production of a process, producing propylene from propane. We showed that it is meaningful to use the entropy production in a chemical process as objective function in an optimization that aims to find the most energy efficient state of operation and, in some aspects, design. By reducing the recycle stream, increasing the pressure of the separation section, and increasing the conversion and selectivity of the reactor, a large reduction in the entropy production of the process was obtained. The results showed that the most inefficient units were the reactor, partial condenser and the two distillation columns, even after the optimization was carried out. This may motivate further work along these lines in the chemical process industry.

Nomenclature

A	Heat transfer area / m^2
B	Bottoms molar flow rate / mol/s
C_p	Molar heat capacity / J/K mol
D	Distillate molar flow rate / mol/s
D	Reactor tube diameter / m
D_p	Catalyst pellet diameter / m
F	Molar flow rate / mol/s
f	Fraction of vapor exiting partial condenser
FR	Fractional recovery in distillation column
$\Delta_\mathrm{r}G$	Gibbs energy of reaction / J/mol
$\Delta_\mathrm{r}H$	Enthalpy of reaction / J/mol
$\Delta_\mathrm{vap}H$	Enthalpy of vaporization / J/mol
h	Molar enthalpy / J/mol
J	Mass flux / mol/m^2s
J_e	Energy flux / J/m^2s
J_S	Flux of entropy / J/Ks
J'_q	Sensible heat flux / J/m^2s
K	Equilibrium constant
K	Relative volatility
k	Parameter in reaction rate expression
L	Liquid molar flow rate / mol/s
L	Reactor length / m
L_{ij}	Phenomenological coefficient
$\mathcal{L}$	Lagrange function
l	Transfer coefficient
N	Number of trays in distillation column
N_F	Feed tray number in distillation column
n	Tray number in distillation column
P	Pressure / Pa (or atm)
Q	Heat flow / J/s
q	Fraction of liquid fed to distillation column
q	Fraction of liquid exiting expansion valve
q^*	Heat of transfer / J/mol
R	Universal gas constant / J/K mol

RR	Reflux ratio
r	Reaction rate / mol/kg cat. s
r_{ij}	Resistance coefficient
$(\frac{dS}{dt})^{\mathrm{irr}}$	Entropy production / J/Ks
s	Molar entropy / J/mol
T	Temperature / K
T_{a}	Ambient temperature of reactor / K
U	Overall heat transfer coefficient / J/Km^{2}s
UA_{total}	Total rate of heat transfer per Kelvin / J/Ks
u	Flow velocity / m/s
V	Vapor molar flow rate / mol/s
W	Work / J/s
X	Driving force
x	Liquid mole fraction
y	Vapor mole fraction
z	Mole fraction (vapor or liquid)

Greek letters:

α	Lagrange multiplier
δ	Film thickness / m
η	Energy efficiency
ϵ	Void of catalyst bed
ϕ	Fugacity coefficient
ξ	Reaction conversion
λ	Thermal conductivity / J/Kms
λ_T, λ_P and λ_{ki}	Lagrange multipliers
μ	Chemical potential / J/mol
μ	Viscosity / kg/m s
Ω	Reactor tube cross-sectional area / m^2
ρ	Density / kg/m^3
σ	Local entropy production / J/Km^{3}s

Contents

Chapter 1

Introduction

1.1 Motivation

Since ancient times Man has tried to explain the phenomena of Nature and use knowledge derived from this to his benefit. From the first use of fire, to the latest development in medical technology, we have put to use a vast number of discoveries. These scientific achievements form the basis on which our modern way of life is built. It seems that the search for new knowledge and its application is an everlasting quest.

In many regions of the World, the technological development has lead to an increased sense of welfare among most people. New medical equipment and treatments give many people better and longer lives while many services and appliances make our daily lives more comfortable. To some extent, the scientific development is driven by each individual's wish for higher welfare.

According to the famous hierarchy of needs created by Maslow (see e.g. Maslow (1970)), a human being has needs that fall onto five different levels, where the ones at the lower levels have to be satisfied before those on the higher levels. In societies where the basic needs (like food, water, security etc.) are met, further increase in the welfare is closely related to what Maslow called self-actualization. For many people today, self-actualization is linked to the availability of a wide range of commodities and services. In Norway, for instance, people expect to find hot water and electricity in their house, numerous electrical appliances, as well as one or several cars. Some services and commodities makes our life more comfortable, while others help us to pursue ways

of self-actualization. If basic needs are met, the production of commodities and services in the society as a whole, is related to the welfare experienced among the people. A schematic illustration of this relation is shown in Fig. 1.1. At a

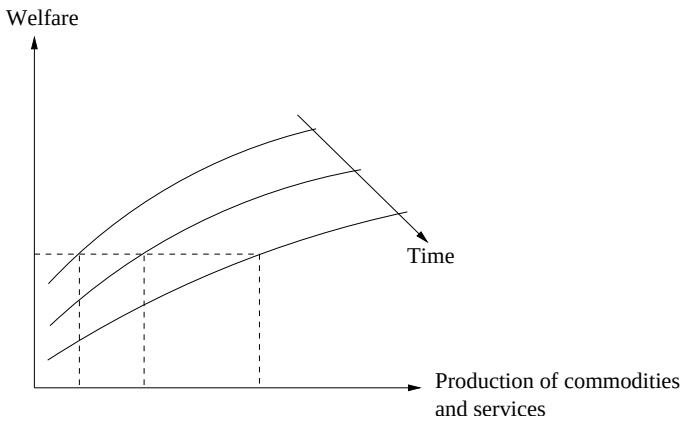

Figure 1.1. Welfare as a function of production of commodities and services at different times (especially in a free market economic system).

certain time, increased production results in higher welfare, but as time passes the production must also increase to maintain the same level of welfare. The underlying force for this development is the economical growth of the society. In a free market economic system, economic growth is a necessity for the system to function. In a command economic system, growth might occur, but it is not an absolute necessity (Amdam et al. 2002). The economic growth is causing us to produce more and more commodities and services, even if this gives us no higher welfare. This time-dependent behavior leads us to make the following two observations of human activities:

1. As humans, we have needs and wishes for commodities and services to give us as high a quality of life as possible. There seems to be *no limitation* to the these needs for humans as a group as time passes.
2. There are *limited* possibilities to satisfy these needs.

In the list below are some very visible limitations and problems we face when trying to increase the welfare of *all* regions of the World:

- Shortage or lack of clean water.

- Limited reservoirs of fossil fuels.
- Decreasing availability of materials (i.e copper).
- High levels and increasing emissions of greenhouse gases.

Many types of limitations are coupled directly to energy availability. For instance, most materials can be brought back to a useful state through recycling, and clean water can be produced from seawater, provided enough energy is available. In this sense, the availability of energy is a more fundamental limitation than other limitations.

Actually, we do not lack energy in itself; the problem is that we lack *useful* energy. This is explained well through two of the most fundamental laws of Nature, namely the First and Second Law of Thermodynamics. In short, the first law states that energy is conserved, while the second law states that when energy changes form, its ability to do work is reduced (Atkins 1998). The production of the commodities and services that we have grown accustomed to, often involve transfer of energy from a state of high quality (high ability to do work) to a state of low quality. For instance, when we drive a car, petrol (high quality) is converted into heat and exhaust (low quality). Currently, we are reducing the quality of the energy we use in a fast pace. Most of our high quality energy is found in the form of fossil fuels and radioactive materials, and these sources are not renewable.

A very important concept in this respect is sustainable development. Perhaps the most rigorous definition so far has been given by Dr. Angela Merkel while she was a German Minister of the Environment, Nature Conservation and Nuclear Safety: "Sustainable development seeks to reconcile environmental protection and development; it means nothing more than using resources no faster than they can regenerate themselves, and releasing pollutants to no greater extent than natural resources can assimilate them" (Merkel 1998). This also applies to the use of high quality energy. As long as most of our energy is supplied from fossil fuels, the production of for instance carbon dioxide will be linked to the global energy conversion. At the moment, many scientists are concerned about the Earth's ability to assimilate the emitted carbon dioxide. It may be impossible to arrive at a development that is sustainable, but it is our obligation to try. In terms of Fig. 1.1, there is then a limit for production of for instance carbon dioxide that cannot be crossed. Another issue is that what we today regard as an energy source may have optional uses in the future.

It is therefore important to use as little as possible of resources that are not renewable.

To reach a level of development that can be called as sustainable as possible, we have to follow two approaches, both of equal importance:

- We must develop ways to obtain high quality energy other than through fossil fuels (renewable energy sources).
- We must reduce the rate at which we lower the quality of the energy we transform and thus make it be useful longer.

Even if more high quality energy were supplied from renewable sources like biomass, the conversion of energy would not necessarily become friendly toward the environment. Most energy carriers contain species that will react to form environmentally harmful products upon combustion (like NOx). Better technology is clearly needed to put alternative energy sources into use.

It is nevertheless important to try to make the most out of the sources we already have (and will find in the future). We therefore focus our attention accordingly in this thesis by developing a methodology for increasing the *energy efficiency* of processes where energy is transformed.

1.2 The second law efficiency and the entropy production

The thermodynamic meaning of a process is a change of state (such as expansion), a change in physical state (such as melting or freezing), or a chemical change in which new substances are produced from old. A process that does *work* is one that can be used to change the height of a weight somewhere in the surroundings. If the height of this weight is decreased, work is done *on* the system and we define this work as positive (for instance a turbine). If the work is negative, the height of the weight will increase and work is done *by* the system (for instance an engine).

Several definitions of energy efficiency exist, but they can broadly be divided into two categories, based on the first and second law of thermodynamics (Smith and Van Ness 1987). Popularly speaking, the first law efficiencies are ratios between that we want and what we have to pay energy-wise to get it. The second law efficiencies are ratios between what we get and what we could have gotten if the process was done reversibly (the theoretically best

possible way). The major difference between the two types is that second law efficiencies say something about the quality of the energy and its ability to do useful work, while first law efficiencies do not.

For a process where work is done on the system, W, the second law efficiency, η_{II}, is defined as (Smith and Van Ness 1987):

$$\eta_{\text{II}} = \frac{W_{\text{rev}}}{W} \tag{1.1}$$

where W_{rev} is the reversible work needed to carry out the process.

To evaluate the second law energy efficiency, we need to know the minimum (or maximum) work that can be used (or produced) by the system while performing its tasks, cf. Eq. (1.1). Compared to the actual work that is used (or produced) by the system, the difference is called the *lost work*. A review of this term is given by Nevers and Seader (1984). The lost work is caused by irreversibilities (friction) in transport of for instance heat, mass and momentum in the system, which lowers the ability to obtain work from energy. When a process occurs reversibly, there are no such losses, and the entropy increase in the universe is zero. However, no real process is reversible, and the entropy in the universe will always increase because of any process occurring. The increase in entropy per unit of time is called the *entropy production* or sometimes the *entropy production rate* or *entropy generation*.

The following example shows the nature of an irreversible process: A car driving along the road has a certain mechanical or kinetic energy due to its velocity and mass. When the driver is bringing the car to a complete halt, all this energy is transformed into thermal energy that is heating the brakes, tires and road. After a while, the thermal energy has been completely transferred to the environment. In a reversible world, the car should be able to regain its speed just by absorbing the heat from the environment again and transform it into kinetic energy. Due to the irreversibilities in the system, this cannot be done; the quality of the energy input to the car has sunken, permanently.

The irreversibilities in a process, represented by the entropy production, is related to the lost work through the Gouy-Stodola theorem (Bejan 1996b):

$$W_{\text{lost}} = T_0 \left(\frac{dS}{dt} \right)^{\text{irr}} \tag{1.2}$$

where W_{lost} is the lost work, T_0 is the temperature of the environment and $(\frac{dS}{dt})^{\text{irr}}$ is the entropy production. Introduced in Eq. (1.1), we obtain a final

expression for the efficiency:

$$\eta_{\mathrm{II}} = \frac{W_{\mathrm{rev}}}{W_{\mathrm{rev}} + W_{\mathrm{lost}}} = \frac{W_{\mathrm{rev}}}{W_{\mathrm{rev}} + T_0(\frac{dS}{dt})^{\mathrm{irr}}} \tag{1.3}$$

If the material input and output, as well as their thermodynamical states are fixed, the maximum second law efficiency is found by minimizing the entropy production. However, fixing the material input and output will in many systems lead to an undesired reduction in the degrees of freedom associated with the optimization. If the material input and output are not fixed, the reversible work will not be constant either. In such cases, minimum entropy production is not equivalent with maximum second law efficiency. We will study the entropy production rather than the efficiency. There are two reasons for this. Firstly, the entropy production is directly related to physical phenomena like fluxes and forces in the system. This can allow for interesting characterization of the system in the state of minimum entropy production. The energy efficiency has no such physical interpretation. Secondly, the energy efficiency is a property that depends on factors that are not related to the irreversibilities in the system (like T_0). The entropy production, on the other hand, is an absolute property. We consider this an advantage since the resulting analysis will be more general.

The aim of this work is to increase the energy efficiency by analysis and minimization of the entropy production. From the theory of nonequilibrium thermodynamics, it is possible to relate the entropy production to fluxes and forces in any system in a systematic manner. A brief overview of nonequilibrium thermodynamics and its potential use in industrial applications is given in Chapter 2.

1.3 Unit and process optimization

Until this point, we have only dealt with the energy efficiency of processes in general terms and we now narrow our scope to treat the energy efficiency and irreversibilities of chemical industrial units and processes. The purpose of industrial processes is to transform raw materials into desired products. To move from raw materials to products through the process state space, requires the use of appropriate process units and it also involves transfer and transformation of energy. On a worldwide scale, the chemical industry is responsible for a large share of the total consumption of high quality energy. In the United States, the production of chemicals is the second largest industrial user of energy (Chemical Manufacturers Association 1998).

To improve the performance of each process unit and how they work together to achieve their designated goal, it is common to perform some kind of optimization. According to Edgar et al. (2001) two key elements characterize any optimization problem:

- Objective function.
- Constraints and variables.

These elements determine largely what kind of methods and tools that can be used to perform the optimization.

1.3.1 Objective function

The objective function is a mathematical relation between the parameters and variables describing the system and the chosen performance criteria. It does not depend on whether the optimization is carried out on a single process unit or on a process. A broad separation can be made between three kind of objective functions: Economy-, energy-, and material-based functions (Peters and Timmerhaus 1991). The list below contains some common optimization tasks, divided into the three kinds of objective:

Economy: Minimum payback period, maximum net present value, maximum internal rate of return, minimum cost of operation, and minimum cost of operation and equipment cost (Edgar et al. 2001).

Energy: Maximum/minimum work or energy output/input, maximum first law energy efficiency, maximum second law efficiency, minimum loss of exergy, and minimum entropy production.

Material: Maximum production, minimum use of raw materials, and minimum waste production.

Chapters 3 to 7 are all dealing with the entropy production as the objective function for all our optimizations. A substantial amount of work has already been done to minimize the entropy production in selected process units. We shall continue this effort. Heat exchangers (Johannessen et al. 2002), plug-flow reactors (Kjelstrup et al. 2000, Johannessen and Kjelstrup 2002, Nummedal et al. 2003, 2004), and binary tray distillations, (De Koeijer and Kjelstrup 2000, De Koeijer et al. 2002), are units that have been optimized. Several pieces of

process equipment central in mechanical engineering contexts have also been optimized by Bejan and Vargas (1995), Bejan (1996a), Bejan et al. (1996).

The entropy production in several units in connection has until now only been minimized by De Koeijer et al. (2004b) in a study of four fixed-bed reactors and five heat exchangers in series.

A concept identical to the entropy production is the loss of exergy (Szargut et al. 1988). Several authors have been dealing with ways to minimize the loss of exergy in process units and processes (Kotas 1995, Hinderink et al. 1996, Budiman and Ishida 1998, Graveland and Gislof 1998, Sorin et al. 2000, Cornelissen and Boerema 2001). Such optimizations are equivalent to minimization of entropy production. However, it is a tendency in the literature to use the word 'optimization' when in fact no detailed mathematical optimization has been performed. The term 'exergy analysis' is often a more precise term, as this involves identification of the major losses of exergy without any actual optimization.

1.3.2 Constraints and variables

Almost all optimization problems related to physical systems are formulated with constraints. The constraints can be classified as equality constraints and/or inequality constraints. In principle, an equality constraint allows for the elimination of one variable from the mathematical description of the problem. This leads in general to a more complex objective function, but with fewer decision variables. The inequality constraints do in general not affect the number of variables. Examples of equality constraints are the equations that make up the physical model of the system, while inequality constraints often act as upper and lower bounds on the variables.

The variables and the constraints can be either *continuous* or *discrete*. It is important to separate between continuous and discrete variables since they demand a completely different treatment in optimizations. The appearance of discrete variables and constraints are usually found in optimizations where optimal location and number of feed points and interconnection of units are sought. The process units that make up a process and how they are interconnected is called the *superstructure*. In general, optimizations where the superstructure is included among the variables are extremely demanding, computationally speaking.

Ideally, a process optimization problem, regardless of objective function, should

contain a large initial superstructure to ensure that all possible process alternatives are evaluated. The combinatorial complexity is extremely large for process flow sheets of even moderate sizes, so it is not practically possible to optimize large superstructures. Many authors have devised numerical strategies to reduce the combinatorial complexity (Grossmann and Daichendt 1996, Heyen and Kalitventzeff 1997, Wilkendorf et al. 1998, Zamora and Grossmann 1998b,a, Papalexandri and Pistikopoulos 1998, Bauer and Stichlmair 1998).

We shall reduce the combinatorial complexity to its minimum by fixing the superstructure of the process in Chapter 7. This eliminates all discrete variables from the optimization problem, thus bringing the focus entirely to operating conditions and to some extent unit designs. The drawback is that no new superstructures may be found directly from the optimization.

1.3.3 Optimization strategies

After having classified the optimization problem, the appropriate solution procedure is selected. Optimization is the act of obtaining the best result under given circumstances. The optimum seeking methods are also known as *mathematical programming techniques*. Some of the most widely used methods are listed below (Rao 1996):

- Calculus methods
- Calculus of variations
- Nonlinear programming
- Linear programming
- Dynamic programming
- Mixed integer programming (MILP/MINLP)
- Genetic/Evolutionary algorithms

These methods are all well known and described in most books on optimization theory (Rao 1996, Edgar et al. 2001, Nocedal and Wright 1999). No single technique can solve every optimization problem and it is the nature of objective function, variables and possible constraints that determine which technique to use. It is possible to solve simple optimization problems analytically (typically with the aid of calculus methods or calculus of variations), but

for most problems associated with chemical process equipment it is efficient to solve the optimization problem numerically on computers. Since the success of mathematical programming is largely dependent upon efficient and stable numerical routines, new methods are constantly being developed. New algorithms may solve problems related to inversion of Hessians (matrix with second derivatives), slow convergence due to flat minimums, parallel optimization or non-convex optimization (Van der Lee et al. 2001, Rodriguez-Toral et al. 2001, High and Roche 1995, Lucia et al. 1996).

In many cases, however, it is a time consuming affair to find even a local optimum on modern computers. This has led to the development special kinds of optimization strategies, called *heuristic methods* (Edgar et al. 2001) (the meaning of heuristic methods in design and optimization of chemical processes has a more specific meaning than in the field of numerical optimizations in general). Such methods aim to solve the optimization problems with simple-to-use rules, often based on physical/chemical knowledge, providing estimates for the optimum. This requires much less computational effort, but does only provide an approximated solution to the optimization problem. The most famous method is the pinch technology developed by Umeda et al. (1978) and Linnhoff (1979). Other methods aim to reduce the combinatorial complexity of the initial superstructures in MILP/MINLP problems (Marechal and Kalitventzeff 1997, Kravanja and Glavic 1997, Hostrup et al. 2001).

Heuristic methods are in general approximate and largely qualitative methods, while we seek to find the optimum more accurately. We will therefore use several mathematical programming techniques for the optimization problems in Chapter 3 to 7. Only very recently have commercial flow sheet simulators like ASPEN Plus and PRO/II been equipped with optimization tools with limited possibilities. Consequently, we choose to model and optimize process units, both single and connected, through other means. To have highly efficient optimization tools available we will use the Matlab programming environment provided by MathWorks Inc. A drawback is that we have to implement the physical models for the different process units by ourselves. However, this also allows us to use less common, but still interesting degrees of freedom in unit design (for instance the diabatic distillation column in Chapter 3 and the heat-integrated column in Chapters 4 and 5).

1.4 Aim and outline of thesis

The aim of this thesis is to develop a methodology and tools that can be used to increase the second law energy efficiency of single and connected *chemical* process units. To the best of our knowledge, this has not been done for connected units before. The methodology concerns analysis and minimization of the entropy production in the systems under consideration. To find the state of minimum entropy production, we shall use mathematical programming techniques. For development and application purposes a varying number of units from the propane dehydrogenation process based on Lindes design (Rytter and Bölt 2000) shall be used in the different chapters.

The entropy production is uniquely defined from nonequilibrium thermodynamics and can be calculated from the local transport processes in any system. Results found by minimizing the entropy production are best understood in light of the fluxes and forces in the system. In Chapter 2 we give a brief introduction to these concepts and how they can be used for industrial purposes. This gives a perspective for the other Chapters 3-7.

Optimization of single units may often produce results that are optimal for that unit, but not for the process as a whole (assuming they are part of one). Nonetheless, they are well suited for studies that find what impact unit design and geometry, as well as some operating variables have on the entropy production of the unit. In Chapter 3 we minimize the entropy production of a diabatic binary tray distillation column, separating propane and propylene. To find the optimum, we apply a nonlinear programming technique (least-square regression) with inequality constraints. This technique takes in a very efficient way advantage of fact that the entropy production is the sum of only positive terms. Large reductions in the entropy production can be obtained by distributing the heat exchange area among the trays in an optimal way. Furthermore, the total heat transfer area and the number of trays have a large impact on the minimum entropy production of a distillation column.

An advanced distillation technology is the internal heat-integrated distillation column (HIDiC) where heat is transferred from the top section to the bottom section of the column through direct thermal contact. In Chapter 4 and 5 we study how the entropy production in this kind of column is affected by some crucial operating parameters and how the optimal distribution of rates of heat transfer should be. In Chapter 5 we use a nonlinear programming technique (sequential quadratic programming) with both equality and inequality constraints to find the optimum. The binary mixture of benzene and toluene is

studied to enable comparison with other works. The method thus established is easily converted to a form that makes it suitable to use in the optimization of the propane dehydrogenation process.

The heart of most processes is the reactor(s) around which the rest of the process is usually designed. For fixed inlet conditions, we minimize the entropy production of a heat exchanger, a plug-flow reactor, and a heat exchanger in series in Chapter 6. This configuration of units lets us find the optimal way to heat/cool the propane dehydrogenation reactor by taking into account the entropy produced in heat exchangers up-stream and down-stream. The state of minimum entropy production is found through a combination of calculus of variations and nonlinear programming with constraints.

In the final chapter in the thesis, Chapter 7, we minimize the entropy production of a simplified version of the propane dehydrogenation process. A reactor with very similar properties as the one in Chapter 6 is used. This gives the optimal operating conditions of all the process units, as well as some design parameters. This information can be important in itself, but it is our goal to answer some particularly interesting questions about the way this process should be operated. A very simplified schematic picture of a chemical process is given in Fig. 1.2. After the feed is mixed with a recycle stream, it enters

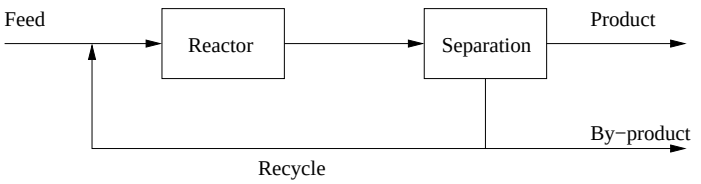

Figure 1.2. The general configuration of a chemical process.

one or more reactors. The reactor(s) can be operated and designed to give a high or low degree of conversion, and this will often influence the selectivity in the reactions. To produce a product of a given purity, by-products must be separated from the product in a separation section. This general layout of a chemical process leads us to ask the following questions:

- Where in the process are the greatest losses of exergy?
- What is the optimal recycle flow compared to feed flow?
- What is the optimal conversion and selectivity in the reactor(s)?

- What other parameters are important for obtaining an efficient process?
- Which premises and assumptions are necessary to make in order for our methodology to work on a process?

In Chapter 7 we try to answer these questions by minimizing the combined entropy production of all the units in a process that converts propane into propylene. To find the state of minimum entropy production, we employ the same optimization technique as in Chapter 5; a sequential quadratic programming technique with both equality and inequality constraints.

Each chapter has been written as independent parts and are published in or submitted to international journals/conferences with review systems.

Chapter 2

Nonequilibrium thermodynamics for industry

Signe Kjelstrup, Audun Røsjorde
and Eivind Johannessen

Department of Chemistry
Norwegian University of Science and Technology
N-7491 Trondheim, Norway

This chapter was published as Chapter 1 in
Chemical Thermodynamics for Industry , T. Letcher editor, 2004

2.1 What can nonequilibrium thermodynamics offer?

Nonequilibrium thermodynamics (NET) offers a systematic way to derive the local entropy production rate, σ, of a system. The total entropy production rate is the integral of the local entropy production rate over the volume, V, of the system, but, in a stationary state, it is also equal to the entropy flux out, $J_{\mathrm{S}}^{\mathrm{o}}$, minus the entropy flux into the system, $J_{\mathrm{S}}^{\mathrm{i}}$:

$$\left(\frac{dS}{dt}\right)^{\mathrm{irr}} = \int_V \sigma dV = J_{\mathrm{S}}^{\mathrm{o}} - J_{\mathrm{S}}^{\mathrm{i}} > 0 \tag{2.1}$$

The entropy flux difference, and the integral over σ, can be calculated independently, and must give the same answer. The entropy production rate governs the transport processes that take place in the system. We have:

$$\sigma = \sum_i J_i X_i > 0 \tag{2.2}$$

where J_i and X_i are conjugate flux-force pairs. Each flux is a linear combination of all forces:

$$J_i = \sum_j L_{ij} X_j \tag{2.3}$$

This means that NET gives flux equations in agreement with the second law of thermodynamics, and that the theory offer a possibility through Eq. (2.1) to check for consistency in the the models that are used.

The usefulness of NET to describe industrial problems has been questioned, because these problems are frequently non-linear. It is then important to know that the flux-force relations in Eq. (2.3) describe also non-linear phenomena. The phenomenological coefficients L_{ij} can for instance be functions of the state variables. By including internal variables in the thermodynamic description, one can extend the application of NET to activated processes. For these reasons, NET appears today as a non-linear and versatile theory that applies to many practical conditions (Hafskjold and Ratkje 1995, Røsjorde et al. 2000, Kjelstrup and Bedeaux 2001, Bedeaux 1986, Bedeaux and Mazur 2001, Reguera and Rubi 2001, Perez-Madrid et al. 1994, Vilar and Rubi 2001, Røsjorde et al. 2001). It is a misunderstanding that the flux equations need be linear on the global level (Demirel 2002).

The total entropy production rate times the temperature of the environment is equal to the exergy destruction rate in a process. Processes with small losses in exergy, have a high second law efficiency. A high second law efficiency, or exergy

efficiency, is seldom a specific aim in process design. An increasing worldwide concern for CO_2 emission may change this. Multi-objective optimization, with small entropy production as one target, may then be interesting in chemical engineering design.

2.2 Developments and status of NET

Nonequilibrium thermodynamics was founded by Onsager (1931a,b). The theory was further elaborated by De Groot and Mazur (1984) and Prigogine (1955). The theory is based on the hypothesis of local equilibrium: A volume element in a nonequilibrium system is in local equilibrium, when the normal thermodynamic relations apply to the element. Evidence is emerging that many systems of interest to the process industry, are in local equilibrium by this criterion (Hafskjold and Ratkje 1995, Røsjorde et al. 2000). Onsager prescribed that each flux be connected to its conjugate force via the extensive variable that defines the flux (Onsager 1931a,b, Coleman and Truesdell 1960).

Onsager assumed that the variables and the rate laws were the same on the macroscopic and the microscopic level; this is the so-called regression hypothesis. Using also the assumption of microscopic reversibility, he proved the reciprocal relations

$$L_{ij} = L_{ji} \tag{2.4}$$

These assumptions restrict the validity of NET, but as stated above, they have a wide range of validity. It has long been known that the Navier-Stokes equations are contained in NET (De Groot and Mazur 1984). NET has more recently been extended to deal with transport across surfaces (Bedeaux 1986), to quantum mechanical systems (Bedeaux and Mazur 2001), and to mesoscopic systems (Reguera and Rubi 2001, Perez-Madrid et al. 1994, Vilar and Rubi 2001). We have chosen to illustrate NET with cases of transport through surfaces in the following sections.

2.3 NET applied to phase transitions

Phase transitions are central in many industrial problems, for instance in distillation, absorption, condensation, manufacture of liquid natural gas, and multiphase flow. We shall use the liquid/vapor transition to illustrate the basic hypotheses and usefulness of NET for surfaces, a relatively new application. For applications to homogeneous phases it is referred to the basic literature, see Section 2.2.

Røsjorde et al. (2001) studied the phase transition in a pure fluid, using nonequilibrium molecular dynamics simulations (NEMD). The NEMD method solves Newton's equations of motion for several thousand particles in an imaginary box, see Hafskjold (2002) for a review. The particles interacted with a Lennard-Jones type pair potential. The phase diagram and the surface tension as a function of temperature of the system was first determined (Røsjorde et al. 2000). The ends of the box were then thermostatted to give an enormous temperature gradient: For argon-like particles the gradient was 10^8K/m. The temperatures of the ends were also chosen so that a liquid-vapor interface established itself. The position of the surface was then determined, according to Fig.2.1. The surface started where the equation of state for the vapor was no longer valid, and ended where the density in the liquid phase started to vary in a linear way.

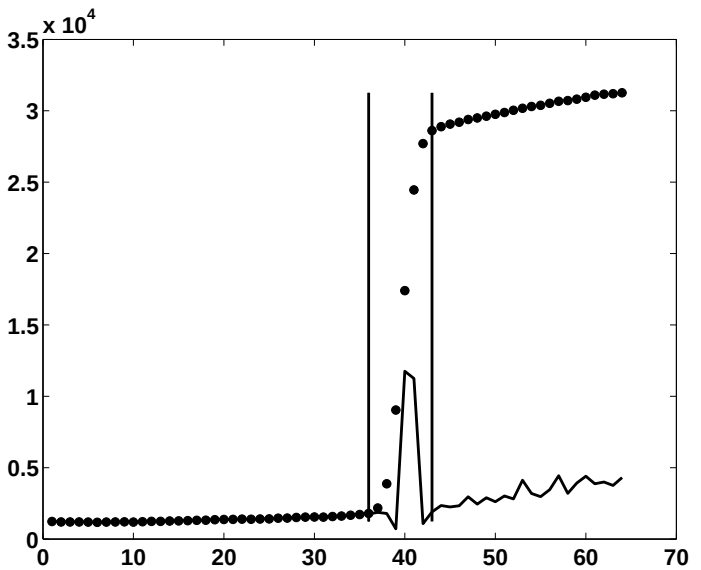

Figure 2.1. Density variation across a non-isothermal NEMD cell with Lennard-Jones spline particles. The extension of the surface is indicated with vertical bars.

It was established that the surface was in local equilibrium: The surface tension calculated for the system with a gradient, was indeed the same as for the system in global equilibrium at a given temperature, see Fig. 2.2. The fluxes for heat

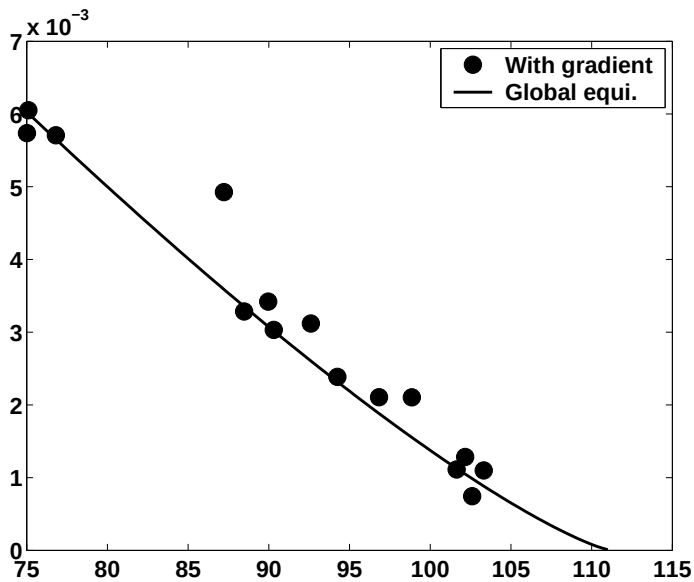

Figure 2.2. Surface tension as function of surface temperature in equilibrium (whole line) and in a temperature gradient (points) for Lennard-Jones spline particles.

and mass across the surface can be written:

$$J'_{\mathrm{q}} = -l_{\mathrm{qq}}\Delta(\frac{1}{T}) - l_{\mathrm{q}\mu}R\ln\frac{P}{P^*(T^{\mathrm{l}})} \tag{2.5}$$

$$J = -l_{\mu\mathrm{q}}\Delta(\frac{1}{T}) - l_{\mu\mu}R\ln\frac{P}{P^*(T^{\mathrm{l}})} \tag{2.6}$$

with the surface transfer coefficients l_{ik}. The coefficients obey Eq. (2.4). The last equation says that evaporation or condensation takes place, when there is a thermal force (a difference in inverse temperature), and/or when there is a chemical potential difference (the pressure of the vapor differs from the saturation pressure at the temperature of the liquid). The first equation can be recast into

$$J'_{\mathrm{q}} = -\lambda\Delta T + q^*J \tag{2.7}$$

Here λ is the stationary state thermal conductivity, and q^* is the heat of transfer. The results of the simulations for λ and q^* are shown as a function of surface tension in Figs. 2.3(a) and 2.3(b). The transfer coefficients decrease in magnitude as we move from the critical point in the phase diagram (zero surface tension) to the triple point (maximum surface tension). It is reasonable that the surface becomes more resistive at high surface tensions. The results are compared to computations from kinetic theory in the same figures. Kinetic theory predicts properties for hard spheres and dilute gases. Indeed, we see from the figures, that the closer one comes to the triple point, the closer is the agreement between theory and simulations. The heat of transfer can be significant, its minimum value here is 20 % of the heat of evaporation. The last term is frequently neglected in thermal modeling of interface transport. In this case, it was found that the flux equations were linear in the forces, even for large gradients. It was thus not necessary to invoke a non-linear dependence on the forces, like it is done in statistical rate theory (Fang and Ward 1999).

Little systematic information is known about surface transfer coefficients. There are indications that the surface transfer coefficients may depend on the range of particle interaction (Kjelstrup et al. 2003). The entropy production rate per m^2 of area, can be high for the surface, meaning that the surface conductivity per m is smaller than the conductivity of the homogeneous phases. But, since the homogeneous phases are thicker than the surface, these phases will still give the dominating total contribution to the entropy production of the system (Kjelstrup and De Koeijer 2003).

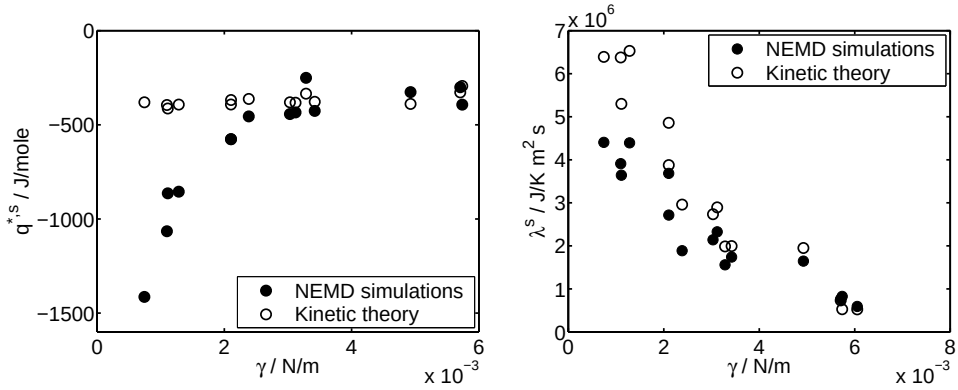

(a) Heat of transfer

(b) Thermal conductivity

Figure 2.3. Properties from the Lennard-Jones spline surface and from kinetic theory (Røsjorde et al. 2001)

2.4 NET equations for distillation columns

Distillation columns are made to separate at least two different components. There are several different types of columns. The assumption of equilibrium between the liquid and vapor that leave each tray, is still in common use to model tray distillation. The work of Krishna and Wesselingh (1997) shows, however, that nonequilibrium models give results that are very different from those obtained with the equilibrium assumption.

A description consistent with NET, is the Maxwell-Stefan equations (Krishna and Wesselingh 1997). In the application of Maxwell-Stefans equations, one frequently neglects the heat of transfer, q^*. This assumption may be good for gases. It is less good for liquid mixtures (Hafskjold 2002). According to Section 3, it is likely that the heat of transfer plays an important role in flux equations for interface transport. Olivier (2003) showed that failure to include the heat of transfer leads to an error up to 20 % in the heat flux calculated for some typical phase transition conditions.

The entropy production rate, and the complete set of equations that follows, can be most conveniently written for the liquid film, the interface and the vapor film in series (Bedeaux and Kjelstrup 2003). Film layers of thicknesses

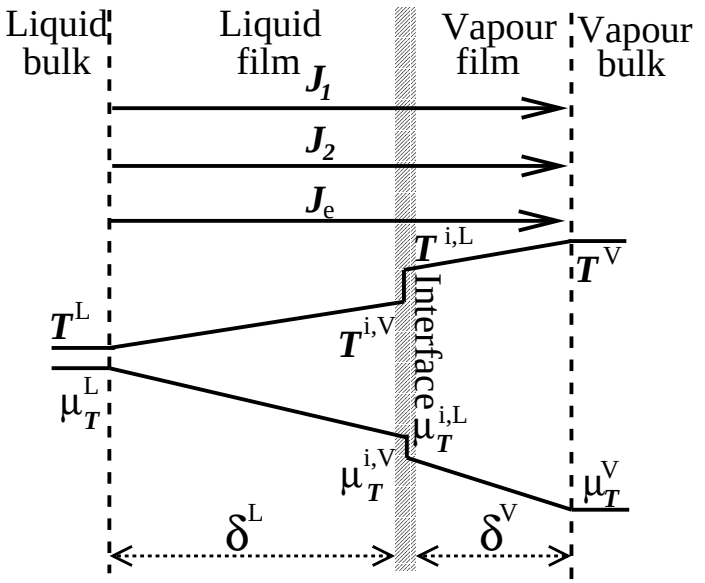

Figure 2.4. Variation in chemical potential and temperature across the liquid layer, the interface and the vapor layer during evaporation/ condensation in a two-component system.

δ^{L} and δ^{V} in the liquid and the vapor are illustrated in Fig. 2.4. With constant fluxes (in stationary states) the integration is easy. The approach was called the integrated interface approach (Bedeaux and Kjelstrup 2003). For the three layers the integrated overall force is the sum of the integrated force across each layer:

$$\begin{aligned}\Delta\left(\frac{1}{T}\right) &\equiv \Delta_{\mathrm{f}}^{\mathrm{i}}\left(\frac{1}{T}\right)+\Delta_{\mathrm{i,o}}\left(\frac{1}{T}\right)+\Delta_{\mathrm{f}}^{\mathrm{o}}\left(\frac{1}{T}\right)\\ \Delta\left(\frac{\mu_j}{T}\right) &\equiv \Delta_{\mathrm{f}}^{\mathrm{i}}\left(\frac{\mu_j}{T}\right)+\Delta_{\mathrm{i,o}}\left(\frac{\mu_j}{T}\right)+\Delta_{\mathrm{f}}^{\mathrm{o}}\left(\frac{\mu_j}{T}\right)\end{aligned} \tag{2.8}$$

With constant fluxes of energy and mass through the interface and adjacent films, the overall resistance coefficients were defined through the parenthesis in the following equations:

$$\begin{aligned}\Delta\left(\frac{1}{T}\right) &= \left(r_{\mathrm{ee}}^{\mathrm{f,i}}+r_{\mathrm{ee}}^{\mathrm{s}}+r_{\mathrm{ee}}^{\mathrm{f,o}}\right)J_{\mathrm{e}}+\sum_{k=1}^{n}\left(r_{\mathrm{e}k}^{\mathrm{f,i}}+r_{\mathrm{e}k}^{\mathrm{s}}+r_{\mathrm{e}k}^{\mathrm{f,o}}\right)J_k\\ -\Delta\left(\frac{\mu_j}{T}\right) &= \left(r_{j\mathrm{e}}^{\mathrm{f,i}}+r_{j\mathrm{e}}^{\mathrm{s}}+r_{j\mathrm{e}}^{\mathrm{f,o}}\right)J_{\mathrm{e}}+\sum_{k=1}^{n}\left(r_{jk}^{\mathrm{f,i,e}}+r_{jk}^{\mathrm{s,e}}+r_{jk}^{\mathrm{f,o,e}}\right)J_k\end{aligned} \tag{2.9}$$

With these relations, the combined films and interface is regarded as an "effective interface". There is no need to assume phase equilibrium between liquid and vapor. The entropy production rate can alternatively be expressed by the measurable heat flux in the vapor and fluxes of mass (Kjelstrup et al. 2003, Bedeaux and Kjelstrup 2003). This set of flux equations was used to explain the entropy production in tray distillation columns. It has not yet been used for predictive purposes, however. Much work remains to include these equations in a software that is useful for industrial purposes.

2.5 The Second law optimal path of operation

A process, natural or industrial, follows a path between states. In the industry this is called "the path of operation". Prigogine (1955) investigated the dissipation of energy in a system out of equilibrium, and found that the entropy production rate was at a minimum in the stationary state close to global equilibrium. Also Schechter (1967) gave a variational formulation of the problem by solving the partial differential equations which resulted from substituting the flux equations into the conservation equations, and confirmed that the entropy production was minimum in the stationary state, provided that the phenomenological coefficients were constant. This may have strengthened a

belief that processes need be globally linear (Bedeaux 1986), in order for NET to be useful, an assumption which would limit the applicability of the theory seriously.

Rather than asking for the general nature of a system that dissipates energy at stationary state, like Prigogine and Schechter did, we find it more appropriate, at least for industrial purposes, to ask about the nature of the operating path, given certain constraints. A typical example would be: How can we minimize the entropy production of a system while we maintain a given production (or heat exchange)? The solution to this minimization problem can be found for conditions far from global equilibrium, and is is different from the solution found by Prigogine (1955) or Schechter (1967).

The question of constrained optimization is standardly answered by Euler-Lagrange optimizations. By formulating the problem with optimal control theory, Johannessen and Kjelstrup (2002) explained that the "Hamiltonian" of the problem was constant, in a study of chemical reactors. The total entropy production for a plug flow reactor was written as a function of a position dependent state variable vector $\mathbf{x}(z)$, and the control variable $\mathbf{u}(z)$

$$\left(\frac{dS}{dt}\right)^{\text{irr}} = \int_0^L \sigma(\mathbf{x}(z), \mathbf{u}(z))dz \tag{2.10}$$

The Hamiltonian for the problem was constructed

$$H(\mathbf{x}(z), u(z)) = \sigma + \lambda_T \left(\frac{dT}{dz}\right) + \lambda_P \left(\frac{dP}{dz}\right) + \sum_i^m \lambda_{k_i}(\frac{dk_i}{dz}) \tag{2.11}$$

The solution to the problem is given by $2(m+2)$ differential equations for the temperature, pressure, degrees of conversion, and of the Lagrange multipliers, (T, P, k_i, λ_T, λ_P and λ_{k_i}), with partial derivatives of H, where m is the number of reactions between the components (Johannessen and Kjelstrup 2002). The constant Hamiltonian of the this problem was reduced to a solution with *constant entropy production*, σ, in the case of a heat exchange process. Using NET, it was also found that that this solution was approximated by a solution with constant driving force, X_i (Johannessen et al. 2002). How to realize this in practice, remains to be solved.

2.6 Second law optimal distillation columns

For an adiabatic distillation column separating a binary mixture, the path of operation is shown through a McCabe-Thiele diagram in Fig. 2.5(a). The com-

positions in the liquid and vapor streams at different trays are shown. Linear operating lines result when the heats of vaporisation of the two components are equal. For a *diabatic* distillation column (Rivero 2001), however, the operating lines are curved and tend to follow the equilibrium line, as shown in Fig. 2.5(b). This kind of operation is possible if heat is added or withdrawn on each tray. As a consequence, the entropy production rate in the column plus heat exchangers decreases.

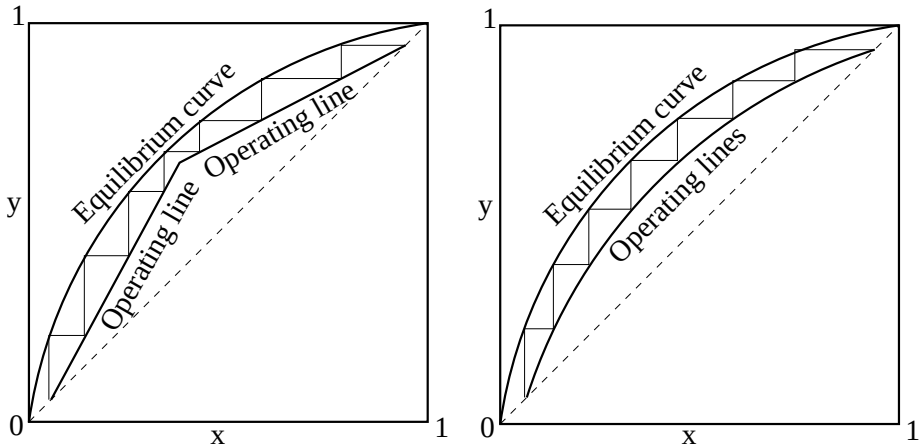

(a) Adiabatic (b) Diabatic

Figure 2.5. Examples of operating lines of an adiabatic and a diabatic column

A reduction of 38% in the entropy production rate was obtained, for a binary separation of benzene and toluene in a equimolar mixture. The heat added on each tray in the optimal diabatic column and the corresponding vapor flows are shown in Fig. 2.6. The results for the corresponding adiabatic column are also shown for comparison. The most important trays for distributed heating were the trays closest to the reboiler and condenser.

A new design that takes the varying vapor flows into account was proposed (De Koeijer et al. 2004b). The effect of the changing hydrodynamic conditions was not yet explored. It is still too early to conclude on the precise outcome of these optimization studies, since also the assumption of equilibrium on each tray was used in the model. Progress in the methods of Section 2.4 may lead

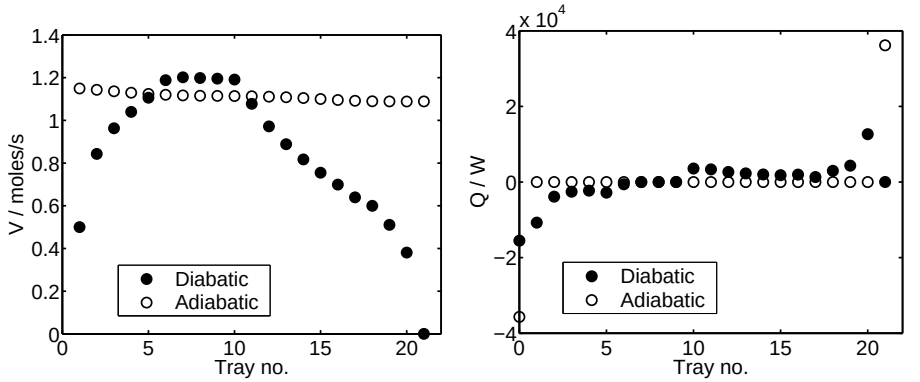

(a) The vapor flow (mol/s) (b) The heat exchanger load (kW)

Figure 2.6. Properties of an optimized diabatic column and an adiabatic column. Both columns separate an equimolar mixture of toluene and benzene.

to improvements in the future. It is documented that the lost work can be reduced, but the increased investment costs are yet not clarified. It is nevertheless important to understand the thermodynamic conditions for optimal performance, independent of technical-economic considerations.

2.7 Second law optimal chemical reactors

The entropy production of a sulfur dioxide oxidation (exothermic) reactor with heat exchangers was minimized in two different cases (De Koeijer et al. 2004a, Johannessen and Kjelstrup 2004b). Case 1 was a four bed reactor with intermediate heat exchangers of a given total area (De Koeijer et al. 2004a), see Fig.2.7. The entropy production rate was calculated from the entropy balance over the system. All inlet and outlet flow conditions were kept constant, except the pressure at the outlet. The problem was to find the inlet and outlet temperatures of the intermediate heat exchangers. Such were found, and shown to give a saving of 16.7% in the lost exergy.

Case 2 was a typical plug flow reactor with temperature profiles as shown in Fig.2.8(a) (Johannessen and Kjelstrup 2004b). The entropy production rate was calculated from NET. The coolant temperature profile that gave minimum entropy production rate was determined. Inlet and outlet conditions were kept

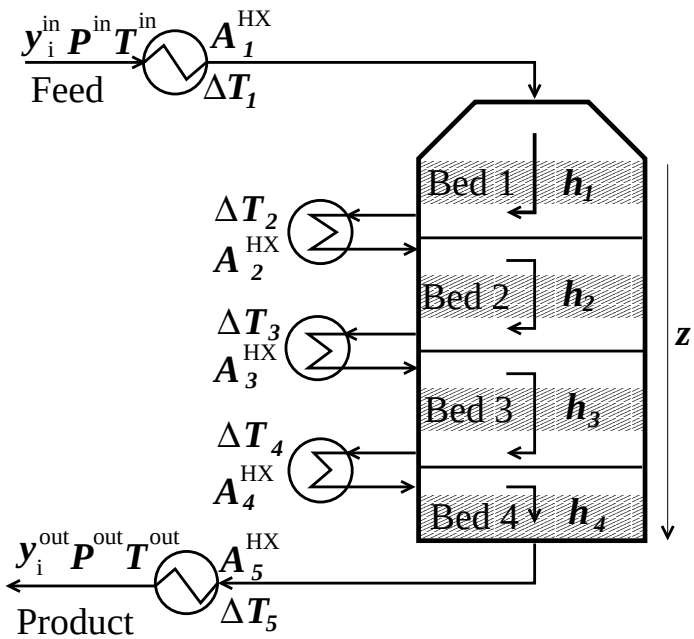

Figure 2.7. The four bed reactor with five intermediate heat exchangers according to De Koeijer et al. (2004a)

constant, and so was the area of heat exchange. The bold lines in Fig. 2.8(b) represent a case with 11% smaller exergy loss. In the next case three constant boiling liquids were used as coolant. The length and temperature of the heat exchangers were set free to vary. The result is shown by the gray lines in Fig. 2.8(b). The length of the coolers are given by the vertical lines in the figure, and their temperature is shown on the ordinate axis. The lost work was now reduced by about 7% (Johannessen and Kjelstrup 2004b).

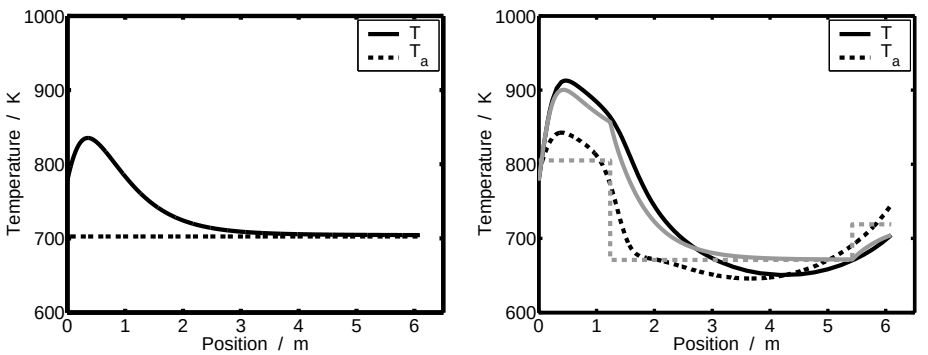

(a) Normal reactor

(b) Second law optimal reactor

Figure 2.8. The temperature of the reaction mixture, T, and of the coolant, T_a in the plug flow reactor for sulfur dioxide oxidation according to Johannessen and Kjelstrup (2004b).

2.8 Conclusion

We have discussed in this chapter, by referring to a few selected examples, that

- The entropy production is important for a proper definition of fluxes and forces in nonequilibrium systems that are relevant to the industry. A higher accuracy in the fluxes can be obtained using NET.
- NET can be used to describe transport of heat and mass in the presence of substantial gradients in systems far from global equilibrium.
- Transport of heat and mass across interfaces can be described without using assumptions of equilibrium at the phase boundary.

- Expressions for the entropy production rate can serve as meaningful object functions in optimizations. NET offers insight into the nature of the solution by characterizing the system's H, σ or X_i.

These properties of NET may prove useful for modeling and design of more energy efficient chemical processes in the future.

Acknowledgment

The Research Council of Norway and the Statoil Vista Program are thanked for financial support.

Chapter 3

The second law optimal state of a diabatic binary tray distillation column

Audun Røsjorde and Signe Kjelstrup

Department of Chemistry
Norwegian University of Science and Technology
N-7491 Trondheim, Norway

This paper has been accepted by
Chem. Eng. Sci. 2004

Abstract

A new numerical procedure to minimize the entropy production in diabatic tray distillation columns has been developed. The method was based on a least square regression of the entropy production at each tray. A diabatic column is a column with heat exchangers on all trays. The method was demonstrated on a distillation column separating propylene from propane. The entropy production included contributions from the heat transfer in the heat exchangers and the mass and heat transfer between liquid and vapor inside the distillation column. It was minimized for a number of binary tray distillation columns with fixed heat transfer area, number of trays, and feed stream temperature and composition. For the first time, the areas of heat exchange were used as variables in the optimization. An analytical result is that the entropy production due to heat transfer is proportional to the area of each heat exchanger in the optimal state. For many distillation columns, this is equivalent to a constant driving force for heat transfer. The entropy production was reduced with up to 30% in the cases with large heat transfer area and many trays. In large process facilities, this reduction would ideally lead to 1-2 GWh of saved exergy per year. The most important variable in obtaining these reductions was the total heat transfer area. The investigation was done with a perspective to later include the column as a part in an optimization of a larger process. We found that the entropy production of the column behaved almost as a quadratic function when the composition of the feed stream changed. This means that the feed composition is a natural, easy variable for a second law optimization when the distillation column is a part of a process. The entropy production was insensitive to variations in the feed temperature.

3.1 Introduction

Distillation is a widely used separation method that requires large inputs of energy (King 1980). Research is therefore being done to find methods that can replace distillation, e.g. membranes (Baker 2002). A lot of effort has also been put into the search for improved designs and operation of the conventional distillation columns. One such design is the *heat-integrated distillation column* (HIDIC) (Nakaiwa et al. 2001), while another is the *diabatic* distillation column, where heat is added or withdrawn by heat exchangers on each tray (Rivero 1993, 2001). We will focus on the efficiency of the latter concept. It has been known for long that this kind of distillation columns have better second law efficiencies (Fonyo 1974a,b). Previous work have shown that potentially large savings could be obtained in the use of high quality energy (Sauar et al. 1997, Kauchali et al. 2000, De Koeijer et al. 2004b).

The aim of this work is to contribute to a better energy economy of distillation

by increasing the energy efficiency. Maximum efficiency is found by minimizing the entropy production in diabatic columns. We continue the work by De Koeijer et al. (2004b), who minimized the entropy production in diabatic distillation columns. We shall add to earlier work and show how we can determine, by theory and calculation, the optimal area of heat exchange at each tray. A new numerical solution procedure shall also be reported. We will not yet include aspects related to the practical implementation (like controllability and cost) in this study. The ultimate goal is to include such aspects in the optimization, but there are still unanswered questions as of how the operating conditions affect the efficiency: How does the composition and temperature of the feed affect the entropy production of diabatic columns operating at minimum entropy production? What effect does the total heat transfer area and number of trays have? When the kind of optimization we study here, is included in a larger process optimization, the effect of these operating conditions must be known.

More specifically, we shall theoretically study the separation of different mixtures of propane and propene at 15 bar. The mixtures are separated into two product streams with mole fractions of propene equal to 0.95 and 0.05 for the top and bottom stream, respectively. Since the product purities are fixed, the thermodynamical state of the material outputs from the columns are also fixed. For a given separation task, the adiabatic and diabatic column have thus the same net energy requirement. The diabatic column is more efficient in terms of the second law. In the present context second law optimization, means to find the amounts of heat transferred locally. Given a certain allowed total heat transfer area, we shall find the distribution of this area, and of the transferred heat, that produces the least entropy. We assume that any kind of cooling or heating medium is available at any temperature. The separation task, number of trays, and total heat transfer area are fixed in the optimization. This problem has not been solved before.

The separation of propene (or propylene) and propane is present in many different chemical plants, especially those producing higher olefins. Olefins are the basic compounds in the making of a large variety of polymers. An additional complication with this separation is that the boiling points are close, which means that the separation must be carried out in columns with many trays and large heat transfer in both the stripping and rectifying sections. Studies so far have mostly been concerned with shorter columns and less heat transfer.

3.2 Diabatic distillation

We have chosen to study the separation of propylene (C_3H_6) and propane (C_3H_8). This is done in a sieve-plate distillation column (McCabe et al. 1993) with N plates (or trays). A sieve plate is designed to bring a rising stream of vapor into intimate contact with a descending stream of liquid. In lack of rate expressions describing the transfer of heat and mass between vapor and liquid, we assume that the liquid and vapor leaving each tray are in equilibrium (see however Wesselingh (1997), Kjelstrup and De Koeijer (2003)). We further assume that the sieve-plate column has no pressure drop. The input of new material is done through a feed stream, F, entering at a certain tray number, N_F. Distillate, D, is removed above the top tray, and bottom flow, B, is removed below the bottom tray. Both product streams are liquids at their boiling points. Figure 3.1 shows the layout of a distillation column. Traditionally,

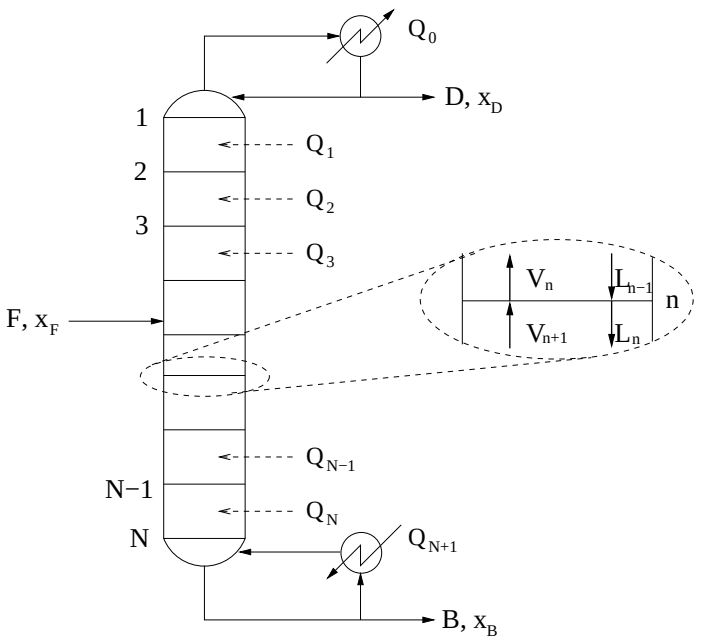

Figure 3.1. A diabatic distillation column.

distillation is done adiabatically, which means that heat is added or withdrawn only in a condenser and a reboiler. No mass transfer is assumed to occur here. In our model, this corresponds to tray number 0 and $N + 1$, respectively. To increase the second law efficiency, heat exchangers may be introduced on each

tray in the distillation column, making the column *diabatic* . This allows heat, Q_n, to be transferred at tray number n. The heat transferred will change the liquid and vapor streams:

$$Q_n = V_n h_n^{\mathrm{V}} + L_n h_n^{\mathrm{L}} - V_{n+1} h_{n+1}^{\mathrm{V}} - L_{n-1} h_{n-1}^{\mathrm{L}} \tag{3.1}$$

where V and L is the vapor and liquid streams, respectively and h is the enthalpy of the streams. At the feed tray ($n = N_{\mathrm{F}}$) and the tray above ($n = N_{\mathrm{F}}$ - 1), the above equation has an additional term on the right-hand-side that includes the heat carried with the vapor and/or liquid part of the feed stream:

$$\text{extra terms} = \begin{cases} -(1-q)F h_{\mathrm{F}}^{\mathrm{V}} & n = N_{\mathrm{F}} - 1 \\ -qF h_{\mathrm{F}}^{\mathrm{L}} & n = N_{\mathrm{F}} \end{cases} \tag{3.2}$$

where q is the fraction of liquid in the feed stream. The symbol Q_n shall for the reminder of this article be referred to as the "duty".

In the modeling of adiabatic distillation columns, the energy balance, Eq. (3.1), is used with $Q_n = 0$ for $n \in [1, N]$. The material balances, on the other hand, are identical for adiabatic and diabatic columns. Rather than considering *one* tray, these balances are constructed by considering the transport of mass in and out of a control surface covering the top of the column. A total mass balance gives:

$$V_{n+1} - L_n = \begin{cases} D & n \in [0, N_{\mathrm{F}} - 2] \\ D - (1-q)F & n = N_{\mathrm{F}} - 1 \\ D - F & n \in [N_{\mathrm{F}}, N+1] \end{cases} \tag{3.3}$$

A similar balance exists for the mass of the light component.

3.3 The entropy production

The objective function for the minimization is the entropy production of the column plus heat exchangers. In the column, there is entropy production due to heat and mass transfer between the fluid streams (De Koeijer et al. 2004b, Ray and Sengupta 1996). In the heat exchanger, there is entropy production due to heat transfer only.

The details of the heat and mass transfer in the column are not well known, so we describe the entropy production on a tray in the column by the entropy flows out minus in on each tray:

$$\left(\frac{dS}{dt}\right)_{\mathrm{col},n}^{\mathrm{irr}} = V_n s_n^{\mathrm{V}} + L_n s_n^{\mathrm{L}} - V_{n+1} s_{n+1}^{\mathrm{V}} - L_{n-1} s_{n-1}^{\mathrm{L}} - \frac{Q_n}{T_n} \tag{3.4}$$

The first four terms to the right represent the entropy carried in and out with the mass flow, while the last term is the entropy change due to flow of heat through the heat exchanger.

The heat transfer in the heat exchangers can be modeled in more detail by the product of an average heat flux from the heat exchangers to each tray, and its driving force (De Koeijer and Rivero 2003).

$$\left(\frac{dS}{dt}\right)^{\text{irr}}_{\text{hx},n} = Q_n X_n \tag{3.5}$$

The average heat flux is Q_n, and the average driving force is X_n. The following simple model was used before (De Koeijer et al. 2004b):

$$X_n = \frac{\delta}{\lambda_n T_n^2}\frac{Q_n}{A_n} \tag{3.6}$$

Here δ and λ_n are the thickness and thermal conductivity of the liquid film covering the heat exchangers, respectively, and A_n is the area of heat exchange at tray n.

The objective function is now the sum of Eqs. (3.4) and (3.5) over n:

$$\begin{aligned}\left(\frac{dS}{dt}\right)^{\text{irr}} &= \sum_{n=0}^{N+1}\left(\frac{dS}{dt}\right)^{\text{irr}}_{\text{col},n} + \left(\frac{dS}{dt}\right)^{\text{irr}}_{\text{hx},n} \\ &= Bs^{\text{B}} + Ds^{\text{D}} - Fs^{\text{F}} + \sum_{n=0}^{N+1}\left(-\frac{Q_n}{T_n} + Q_n X_n\right)\end{aligned} \tag{3.7}$$

Equation (3.7) does not require knowledge of the heating/cooling medium in the heat exchangers.

3.3.1 An analytical formulation of the minimization problem

The optimization task is to minimize the objective function, Eq. (3.7), while keeping the total heat transfer area constant. However, it has proved to be difficult to perform this minimization with ordinary constrained optimization tools. An analytical formulation of the problem, provides an alternative route to obtaining the minimum.

A complete problem formulation is given in the appendix, while a short version of the most important part of the derivation is given here. The parts of the

objective function and constraints that contain A_n, constitutes a Lagrangian function:

$$\mathcal{L} = \left(\frac{dS}{dt}\right)^{\text{irr}} - \alpha\left(\sum_{n=0}^{N+1} A_n - A_{\text{total}}\right) \tag{3.8}$$

where $\mathcal{L}$ is the Lagrangian function and α is a Lagrange multiplier. Other constraints are required for a complete description, but they do not include A_n. Differentiation of Eq. (3.8) with respect to A_n, produces a set of relations that must be fulfilled in the optimal state. Since the objective function has a term containing X_n, which is a function of A_n by Eq. (3.6), we get the following expression:

$$\frac{\partial \mathcal{L}}{\partial A_n} = \frac{\partial}{\partial A_n} Q_n X_n - \alpha = -\frac{Q_n X_n}{A_n} - \alpha \equiv 0 \tag{3.9}$$

This relation states that the entropy production in all the exchangers must be proportional by the same factor to their heat transfer area. Equation (3.9) is valid as long as the model of the heat exchangers, Eq. (3.6), are on the general form:

$$X = \frac{f}{A} \quad \text{and} \quad \frac{\partial f}{\partial A} = 0 \tag{3.10}$$

Even though we do not know the value of α, Eq. (3.9) allows us to use less variables in the numerical optimization of Eq. (3.7). This greatly enhances the speed and stability of the numerical algorithms. At the same time, it explains some observations done by De Koeijer et al. (2004b). They found that the lowest entropy production in a binary separation of benzene and toluene, was obtained by setting $|X_n|$ equal on all trays. If we eliminate Q_n and A_n from Eq. (3.9), we obtain:

$$X_n^2 = -\alpha \frac{\delta}{\lambda_n T_n^2} \tag{3.11}$$

When the variations in λ_n and T_n are small from top to bottom of the column, $|X_n|$ is close to constant. With the numbers from De Koeijer et al. (2004b), the relative variation of $|X_n|$, calculated from the above equation, was in the order of 1%.

3.4 Calculations

3.4.1 Numerical solution procedure

The minimization problem is a nonlinear constrained optimization problem. The most straightforward way to do the optimization, is to minimize the ob-

jective function as it is given in Eq. (3.7), by varying the independent variables. Unfortunately, this method converges only for a small set of initial conditions, and then very slowly. Another way, is to solve the analytically derived equations in the appendix, which we tried without success.

Due to the nature of the function, it was possible to adopt a different approach. The objective function is, through our formulation, the sum of many contributions. Each contribution may or may not be affected by the different variables. However, the *sum* of them will always depend on all of the variables. The sum of the terms in Eq. (3.7), is hiding the structure of the objective function. Rather than minimizing the sum, we shall perform a least square regression including each of the terms in the sum. More specifically, there are $N+2$ terms due to the internal entropy production and $N+2$ terms due to the entropy production of heat transfer. A general formulation of the sum in Eq. (3.7) is:

$$F(x) = [f_1(x)]^2 + [f_2(x)]^2 + ... + [f_{2(N+2)}(x)]^2 \tag{3.12}$$

where $F(x)$ is the objective function, and $f_i(x)$ is the *square root* of each contribution to the total entropy production. The square root is always a real number since the local entropy production is positive by nature. Experience has shown that least square regression converges much faster and are more stable than other optimization methods.

In our description of diabatic distillation, we have N independent degrees of freedom. This number is found by subtracting the number of relations from the number of variables. To arrive at this number we also made use of relation (3.9). The independent variables were the temperatures, T_n (from tray 2 until tray $N-1$). The temperatures T_0, T_1, T_N and T_{N+1} are given, once the product amount and purity are specified. Through the equilibrium relation and the energy, mass and component balances, the duties of all trays, except in the condenser and reboiler, are determined. The optimal values of Q_0 and Q_{N+1} are determined from the optimal vapor flows, $V_1 = D$ and $V_{N+1} = 0$ (see the appendix).

By combining Eq. (3.6) with Eq. (3.9), we obtain A_n as function of α and Q_n, independent of X_n:

$$A_n = \frac{1}{\sqrt{-\alpha}} \sqrt{\frac{\delta Q_n^2}{\lambda_n T_n^2}} \tag{3.13}$$

Through this equation, we ensured that $\sum_{n=0}^{N+1} A_n = A_{\text{total}}$, by adjusting α in each iteration.

To solve this regression problem, we used a nonlinear least squares function called *lsqnonlin* from the Optimization Toolbox in Matlab R13, MathWorks Inc. This algorithm uses a Gauss-Newton method (Dennis 1977) with line search.

Before the actual optimization studies were started, we calculated adiabatic distillation columns as reference columns. The heat exchange area was equally divided between the condenser and reboiler only. For a given feed tray position, we found the set of independent variables (i.e the tray temperatures and duty of condenser and reboiler) that satisfied the energy balances, Eq. (3.1). This was done with a non-linear equation solver in Matlab called *fsolve*. Through repeated calculations, we found the position of the feed tray that gave the lowest entropy production (or equivalently, the lowest reflux ratio $\mathrm{D/L_0}$). The results were used as a fair basis for measuring reductions in the entropy productions.

The optimizations of the diabatic columns were then carried out. As initial guesses for the temperatures on each tray, we used the values from the adiabatic distillation columns. The optimal location of feed trays was found by repeated minimizations with different guesses for N_{F}.

3.4.2 Case studies

The numerical procedure described above was used to find the state of minimum entropy production for a set of diabatic distillation columns. Each column had fixed total heat transfer area, A_{total}, total number of trays, N, feed temperature, T_{F}, and overall feed composition, z_{F}. The two first variables are related to the geometry of the column, while the two last are related to the operating conditions. Each of the two sets of variables was kept constant, while the other was varied systematically:

Case I. Changing operating variables: The geometric variables of the column (total heat transfer area and number of trays) were fixed at $A_{\mathrm{total}} = 15\ \mathrm{m}^2$ and $N = 90$. The properties of the feed stream were changed systematically in 156 optimizations, with $z_{\mathrm{F}} \in [0.2, 0.8]$ and $T_{\mathrm{F}} \in\ [300\ \mathrm{K}, 325\ \mathrm{K}]$. This covered feed conditions ranging from super-cooled liquid to super-heated vapor of different composition.

Case II. Changing geometric variables: The properties of the feed stream were kept at $z_{\mathrm{F}} = 0.5$ and $T_F = 312.35\mathrm{K}$ (liquid at the bubble point, $q = 1$). 70 optimizations were performed with changing geometry, $A_{total} \in [5\ \mathrm{m}^2, 100\ \mathrm{m}^2]$ and $N \in [60, 120]$.

The feed stream to the column was always 1.0 mol/s, while the operating pressure was 15 bar. At this pressure, the boiling points of the pure components were 308.03 K and 317.05 K for propylene and propane, respectively. In all optimizations, the product streams, D and B, had compositions 0.95 and 0.05, respectively. We used data from Daubert and Danner (1992), to calculate the thermal conductivity of the liquid films covering the heat exchangers, $\lambda(T)$. The thicknesses of these films were assumed to be 10^{-5} m, and constant (Taylor and Krishna 1993).

The enthalpy, entropy and equilibrium relations as functions of temperature and composition, were found from the equation of state, see e.g. Prausnitz et al. (1999). We used a cubic equation of state for mixtures of propylene and propane as reported by Ishikawa et al. (1980).

3.5 Results

We present first some optimal properties of an adiabatic and a diabatic column with a particular geometry and operation. We then proceed with results that show the response of the entropy production to changes in the feed properties (Case I). Finally, we present results for the entropy production for changing heat transfer area and number of trays (Case II).

3.5.1 Optimal properties, fixed geometry and operating conditions

The properties of the adiabatic and diabatic column with geometric and operating variables $z_{\mathrm{F}} = 0.5$, $T_{\mathrm{F}} = 312.35$ K, $A_{\mathrm{total}} = 15$ m^2 and $N = 90$ are shown in Figs. 3.2 to 3.4. Fig. 3.2 shows the vapor flows through both columns, while Fig. 3.3 shows the corresponding distributions of heat transfer areas. In Fig. 3.4, the duties at the trays are shown. The profiles are represented by continuous lines rather than discrete points to enhance the clarity. In the case of the adiabatic column, the reflux ratio was 17.0, while it was reduced to 0 in the diabatic column.

The total entropy production as well as the magnitude of its two contributions are given in Tab. 3.1, for the two columns. The entropy produced by the internal mass and heat transfer increased somewhat by making the column diabatic. However, the entropy produced by heat transfer, decreased more, giving a net decrease of 0.45 W/K.

In the adiabatic column, the feed tray was at tray 54, while the optimal position in the diabatic column, was at tray 52.

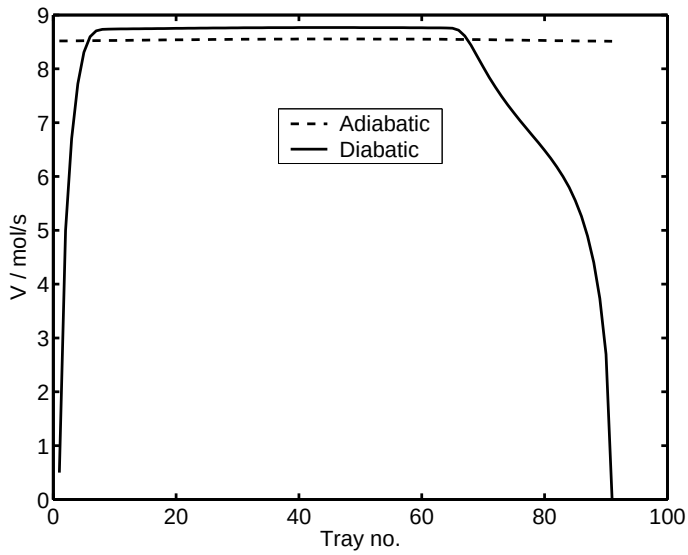

Figure 3.2. The vapor flow (mol/s) in two columns with $z_{\mathrm{F}} = 0.5$, $T_{\mathrm{F}} = 312.35\ K$, $A_{\mathrm{total}} = 15\ m^2$ *and* $N = 90$.

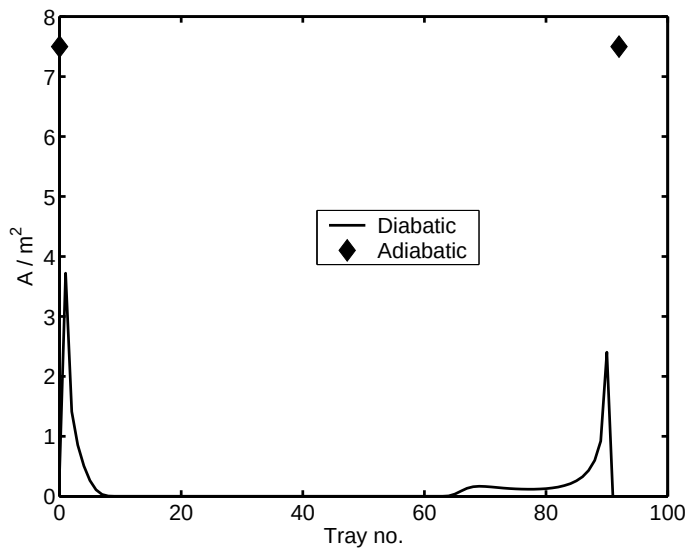

Figure 3.3. The distribution of heat exchanger area (m^2) *in two columns with* $z_{\mathrm{F}} = 0.5$, $T_{\mathrm{F}} = 312.35\ K$, $A_{\mathrm{total}} = 15\ m^2$ *and* $N = 90$.

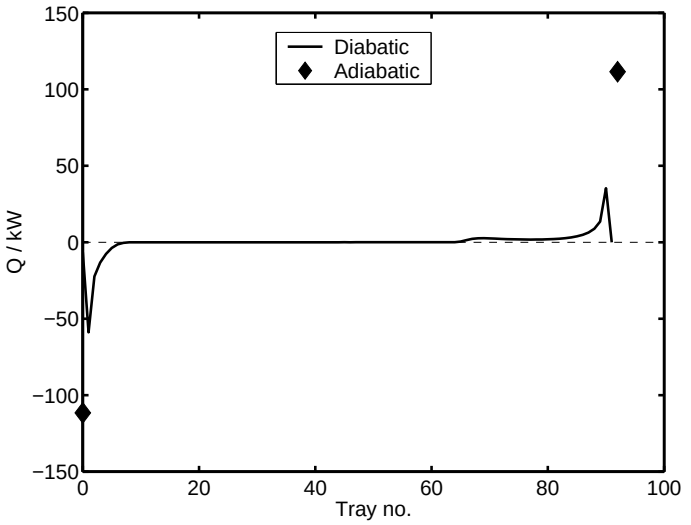

Figure 3.4. The duties (kW) along the diabatic column and the adiabatic column with $z_{\mathrm{F}} = 0.5$, $T_{\mathrm{F}} = 312.35\ K$, $A_{\mathrm{total}} = 15\ m^2$ *and* $N = 90$.

Table 3.1. Entropy productions (W/K) in an adiabatic and diabatic column.

	$(\frac{dS}{dt})^{\mathrm{irr}}_{\mathrm{col}}$	$(\frac{dS}{dt})^{\mathrm{irr}}_{\mathrm{hx}}$	$(\frac{dS}{dt})^{\mathrm{irr}}$
Adiabatic	3.83	4.34	8.17
Diabatic	4.01	3.71	7.72
Change	4.59 %	-14.56 %	-5.58 %

3.5.2 Case I: Changing operating variables

At fixed geometry $A_{\text{total}} = 15\ \text{m}^2$ and $N = 90$, the feed properties were varied. The total entropy production for the different optimizations are plotted in Fig. 3.5. A parabolic behavior was observed, with changing feed composition.

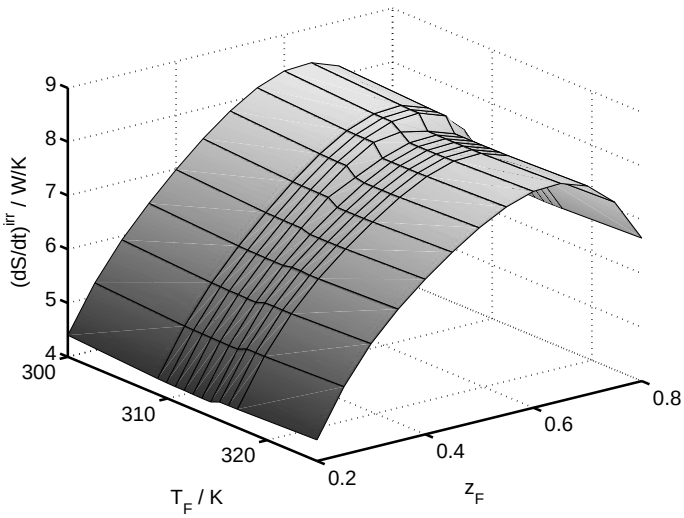

Figure 3.5. Optimal total entropy production with changing operating variables.

As the mole fraction of propene in the feed approached high and low values, the entropy production approached low values. A change in the feed temperature had little effect on the entropy production.

3.5.3 Case II: Changing geometric variables

When we kept the feed properties fixed while changing total heat transfer area and column length, we found optimal diabatic columns with total entropy production as shown in Fig. 3.6. Clearly, the entropy production was highest for short columns with small heat exchanger area. By increasing either the number of trays, or available heat exchanger area, the total entropy production was reduced. This is expected, since both these variables made the mass and heat transfer more reversible when they increased. The two contributions to the total entropy production were plotted separately as function of the total

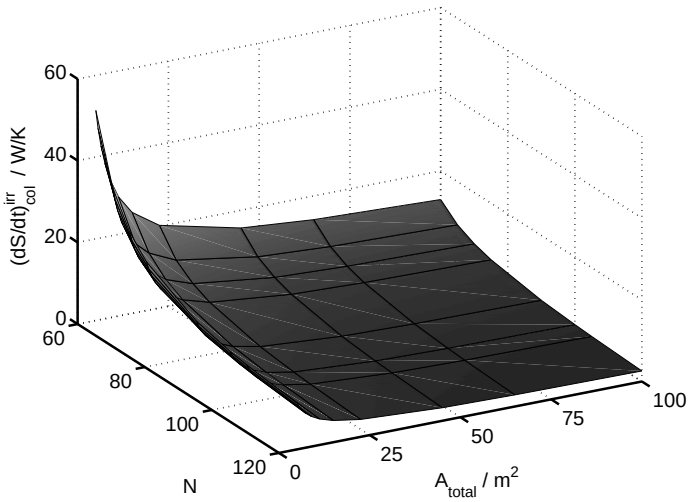

Figure 3.6. Total entropy production vs. total heat transfer area and number of trays in the optimizations with changing geometric variables.

heat transfer area and number of trays in Figs. 3.7 and 3.8. The entropy production due to the heat transfer showed the same behavior as the total entropy production. It did, however, approach zero at large heat transfer areas and number of trays. The internal entropy production dropped as the number of trays was increased. Fig. 3.8 shows that changes in the heat transfer area had little effect on this term.

Compared to adiabatic columns with the same geometric and operating variables, the diabatic columns had lower total entropy production. Fig. 3.9 shows the obtained reduction. At low tray numbers and heat exchanger area, the possible saving was very small. Larger number of trays and higher heat exchanger area, gave much larger savings in the entropy production. This also corresponded to the greatest relative reductions, of approximately 30%.

3.6 Discussion

3.6.1 The model

The first law of thermodynamics does not rank the performance of distillation columns with respect to their ability to use energy for the purpose of separation. This information is only obtained from a second law analysis, which

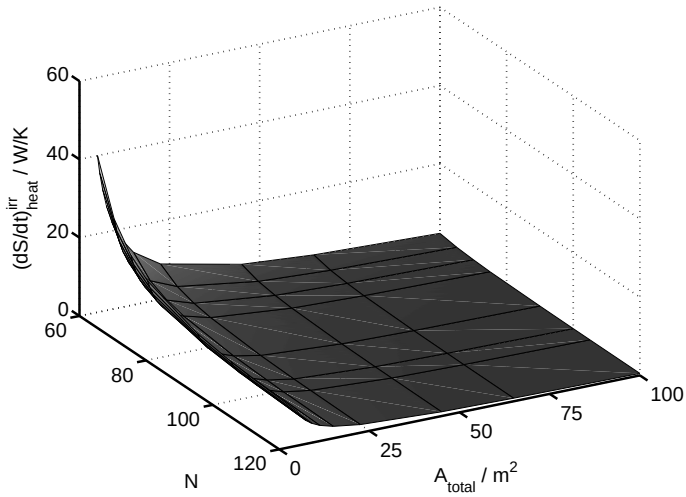

Figure 3.7. Entropy production due to heat transfer in the optimizations with changing geometric variables.

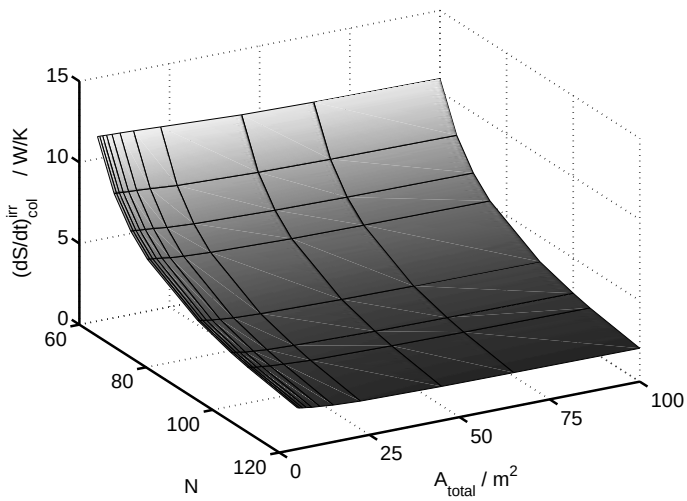

Figure 3.8. Entropy production due to internal heat and mass transfer in the optimizations with changing geometric variables.

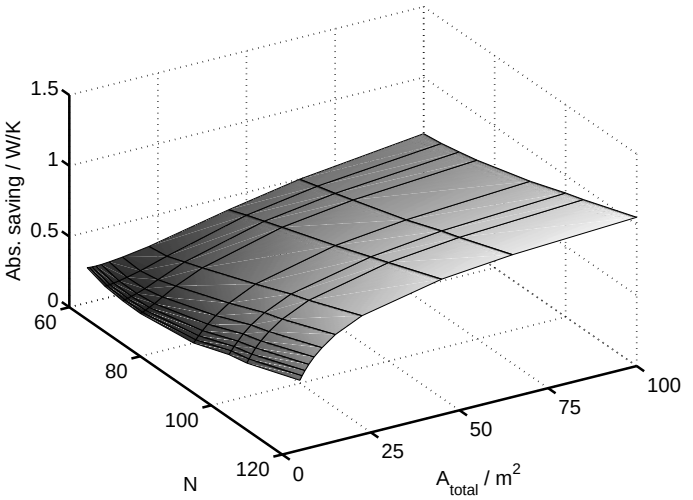

Figure 3.9. Absolute savings in entropy production in the optimizations with changing geometric variables.

computes the entropy production. In our distillation model, the net energy input/output is completely specified by the difference between the enthalpy flow of products and feed. A first law optimization of the *net* energy requirement of the column has therefore little meaning. The second law optimization, however, has predicted columns that all produce heat at higher temperatures and consume heat at lower temperatures than conventional columns. There are some flaws in the model we have used, however. We shall first discuss these, to give a perspective on the validity of the results.

We have done two crucial assumptions in order to model the column: Equilibrium between the vapor and liquid leaving each tray and constant pressure through the column. It is justifiable to ask how well our model of the distillation column predicts reality.

Results for the entropy production in a diabatic column have to some extent been compared and verified with experiments, and it is known that the assumption of equilibrium between the fluids at the outlet on each tray is not good (De Koeijer and Rivero 2003, Wesselingh 1997). By allowing the mixture of vapor and liquid on each tray to reach equilibrium, we end up with a column that is more efficient than it should be. It is not known in what direction a nonequilibrium model will change the potential reduction in the entropy production.

Nonequilibrium models are available (De Koeijer and Kjelstrup 2002, Taylor and Krishna 1993, Krishna and Wesselingh 1997), but have not been used in optimization studies. Clearly, there is a potential for further improvements, by using nonequilibrium models in the optimization.

The pressure changes in a column with frictional flows. Relatively large pressure drops at small absolute pressures, may give a significant contribution to the entropy production. In the present case with a pressure of 15 bar, this direct effect is probably small. We expect further that the entropy production due to heat transfer is not affected by a pressure change. The entropy produced by the internal heat and mass transfer may be influenced to a larger degree since the internal flow rates changes a lot as a consequence of the changing heat transfer along the column.

3.6.2 Properties of an optimal column

The results from the optimization of a particular set of operating and geometric variables give characteristics of a representative optimal diabatic column. The variables $z_{\mathrm{F}} = 0.5$, $T_{\mathrm{F}} = 312.35$ K, $A_{\mathrm{total}} = 15$ m^2 and $N = 90$ are typical for industrial purposes.

In an adiabatic distillation column, there are only small variations in the vapor flow along the column, since the enthalpies of the vapor and liquid streams are relatively constant. This is not so in the diabatic column: From the energy balance, (3.1), we see that a nonzero Q_n allows for large variations in vapor (and liquid) flows. The reflux ratio is furthermore zero in the diabatic column; most of the condensation that was done in the condenser of the adiabatic column, has been shifted down in the column. The optimal vapor flow profile, Fig. 3.2, was similar to the one reported by De Koeijer et al. (2004b). As they point out, this profile may have implications for design of diabatic columns.

The optimal distribution of the heat transfer area, Fig. 3.3, is a new interesting finding. In the top and bottom of the column, the areas of heat exchange on many trays became relatively large. From tray 10 to 65, the area was approximately zero, which in practice means that these heat exchangers can be removed. It was the redistribution of the area of the condenser and reboiler that gave a lower entropy production, compared to the adiabatic column. It was surprising that only about one third of the heat exchangers were active. One explanation for this is that the total heat transfer area (15 m^2) was small. We observed a slight increase in the fraction of active heat exchangers with a

larger area.

The optimal duty profile, Fig. 3.4, was similar (except the sign in the rectifying section) to that of the heat transfer area profile, Fig. 3.3. This is explained by Eq. (3.11). Since X_n varied little through the column, the relation $Q_n X_n / A_n = -\alpha$ made Q_n proportional to A_n.

To summarize, we have found that all optimal columns had non-constant material flows, contrary to the adiabatic column, a fact that may have a bearing on the design of such columns. An interesting and useful outcome of the optimization was a large fraction of inactive heat exchangers. A redistribution of the entropy production took place over the trays, with a reduction in entropy production due to a change in the heat transfer in the reboiler and condenser (see Tab. 3.1).

3.6.3 Effects of changing operating conditions

One of the aims of the present investigation was to find how sensitive the results for the optimal column were to changes in operating conditions. Operating conditions can normally not be varied freely; they are given by upstream process units. It is thus important to understand how the surrounding process influences an optimal diabatic column. Consider the results in Fig. 3.5 from this perspective.

The optimal entropy production varied in a parabolic-like manner as the feed composition was changed. This is expected. When the feed composition was equal to the distillate composition, x_{D}, or the bottom composition, x_{B}, no separation was needed and the entropy production was zero. The curve therefore approached zero for these conditions. The large variation between these two values followed z_{F}, in agreement with Agrawal and Herron (1997).

The temperature of the feed, however, had only a very small effect on the entropy production. This is surprising, considering that a phase transition can take place. Evidently, the heat transfer required to change the temperature and phase of the feed, produced little entropy. The small irregularity in the entropy production with changing temperature, was caused by a phase transition of the feed phase. Below $z_{\mathrm{F}} \approx 0.36$, the entropy production was highest when the feed was in the vapor phase. Above $z_{\mathrm{F}} \approx 0.36$, the entropy production was highest when the feed was in liquid phase. The feed composition governed the ratio between D and B, and through the energy balance, this affected which part of the column had the largest heat transfer.

To summarize, we have observed from Fig. 3.5 the following interesting features: If the feed composition changed, the entropy production of the column behaved almost as a quadratic function. This means that z_F is a natural variable to use in a process optimization. On the other hand, the entropy production was insensitive to variations in the feed temperature. This means that the feed temperature can be determined by the optimization of an upstream unit, i.e. a reactor, without need for heat exchange up-front to adjust the temperature.

3.6.4 Effects of changing geometry

Large variations in the entropy production by changing the geometry were expected. Interesting here was to see how a variation in A_{total} could be traded by a variation in N.

The total entropy production in Fig. 3.6, can be understood through its two contributions. The entropy production due to heat transfer, Fig. 3.7, varied in a hyperbolic manner with respect to the variables, A_{total} and N. Independently of N, the entropy production due to heat transfer approached zero when A_{total} increased. Increasing N to infinity, in order to make the column operate reversibly, did not eliminate the entropy produced in the heat exchangers. As long as the total heat transfer area was finite, the heat that was transferred inevitably produced some entropy. The entropy produced in the heat transfer was equal to $\sum \frac{Q_n^2}{A_n}(\frac{\delta}{\kappa_n T_n^2})$, which will only be zero if Q_n is zero or A_n is infinitely large for all n. According to Schaller et al. (2002), $\sum Q_n$ approached zero in the limit of infinitely many trays. This cannot be correct, since $\sum Q_n$ was independent of the number of trays, and only dependent on the state of the feed and product streams.

When N decreased toward the minimum number of trays, fewer trays were available for heat transfer. With fewer degrees of freedom, the minimum entropy production increased.

The entropy production due to the internal heat and mass transfer, Fig. 3.8, varied little with the total heat transfer area. This suggests that properties of optimal columns with different A_{total} are the same, except that heat is transferred more reversibly for larger A_{total}. With increasing N, the internal entropy production approached zero, as the separation was done reversibly.

The results in Fig. 3.6 was the sum of the results in Figs. 3.7 and 3.8. The

two contributions to the total entropy production dominated different regions of Fig. 3.6, depending on the total heat transfer area. We see that A_{total} was a number that weighed the relative importance of the two contributions to the entropy production. High available area meant that $\sum XQ$ was small, effectively reducing the objective function to $\sum -\frac{Q}{T}$. For small heat transfer areas, the opposite occurred when $\sum XQ$ became exceedingly large compared to $\sum -\frac{Q}{T}$.

Figure 3.9 shows that the largest reductions in entropy production could be obtained if the total heat transfer area and number of trays were large. It was interesting that the *relative* reductions in entropy production, although not shown in this paper, behaved in the same way as the *absolute* reductions shown in Fig. 3.9 (maximum saving equal 30%). As both N and A_{total} increased, the reduction in entropy production strictly increased. This reduction was solely due to the decrease in entropy produced by heat transfer. Second law analysis and optimizations are always valid, but the gain in entropy production may not necessarily be large enough to be of practical interest. The absolute reductions in entropy production showed clearly that for combinations of low tray numbers and low heat transfer area, little was gained by making an diabatic column.

The result of this study was therefore that a larger N made the internal heat and mass transfer more reversible and gave more degrees of freedom in the optimization. This resulted in a lower minimum for the entropy production. A larger A_{total} allowed more heat exchangers to be used, thereby enabling large reductions. The largest reductions found for the entropy production was approximately 1.0 W/K. Initially, this might seem a small number, but our feed stream was also small. For larger throughput than 1 mol/s, this saving could be substantial. At BASF's propane dehydrogenation plant in Tarragona, Spain, a typical production of propylene is 350,000 ton/year (Net Resources International Limited 2002) (or an equimolar feed of 500 mol/s). If we assume that all propylene could be separated from propane in an optimal diabatic distillation column, the saved exergy during the course of one year would ideally amount to approximately 1.3 GWh.

3.6.5 Practical considerations

We have seen above that a relative reduction up to 30% was obtainable in the entropy production for the given system. This was surprising considering that T_0 and T_{N+1} differed by only 9 K. Intuitively, one may expect a small potential for second law improvements in distillations of components with close boiling

points. However, the close boiling points are not the only consideration to take into account. Our system is also characterized by the relatively large amounts of heat to be transferred, and this property makes the particular distribution of heat along the column a target for improvements.

A number of hot and cold utility streams are required to realize the optimal distribution of heat exchangers. The optimal solution gives the local targets for design of X_n, Q_n and A_n. It is a rather practical finding that more than half of the heat exchangers were not needed in the optimal solution, cf. Fig. 3.3. The right Q_n, X_n and A_n are realized by finding the right flow rate and temperature of each utility stream. If we are allowed to tailor the heat capacity of the utility fluids, the number of different ways to operate the heat exchangers grows.

To assist in the design of diabatic columns, a contour plot of the surface in Fig. 3.10 may be helpful, see Fig. 3.6. From the contour plot, it is easy to iden-

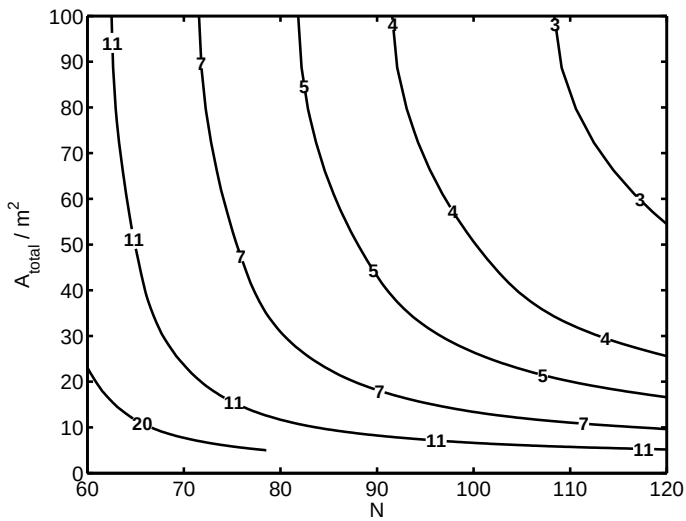

Figure 3.10. A contour plot of the total entropy production at different total heat transfer areas and number of trays.

tify the preferred direction for further changes, given that the variables A_{total} and N are available. For instance, when N is already high, it is meaningless to increase N further, unless A_{total} is also very high. If the heat transfer area is 100 m^2, the only reasonable thing to do is to increase N. By following a path that is always orthogonal to the level curves, a design engineer can identify

the path with the best improvement of the second law efficiency. Furthermore, since A_{total} and N are central in a calculation of investment cost, the information contained in Fig. 3.10, can also assist in identifying the cost optimal diabatic distillation column.

The numerical procedure that has been documented in this work, is an improvement of earlier procedures because it is more robust and simpler. This makes it also a suitable tool for more practical problem formulations than the ones we report here. The number of heat exchangers is normally limited in a plant, and this number and other boundaries for the heat exchangers must be included as constraints to make the optimization a practical one. A particular heat exchanger network, like for instance the one given by Rivero (1993, 2001) and Jimenez et al. (2003), where the heat exchangers in the rectifying and stripping section are connected in series, is a more practical form of column. Such columns may easily be studied with our numerical tool by adding a model for the heat exchanger medium and some new constraints. The introduction of additional constraints, will lead to solutions with higher entropy productions than what we have found here, but the economical barrier to practical implementations may be smaller.

3.7 Conclusion

We have developed further the method for minimizing the entropy production of a diabatic tray distillation column. A new numerical procedure has been used, based on a least square regression of the entropy production at each tray. The method was demonstrated on a distillation column separating propylene from propane. The numerical procedure gives a basis for further theoretical and practical studies.

The entropy production included contributions from the heat transfer in the heat exchangers and the heat and mass transfer between liquid and vapor inside the distillation column. No pressure drops were accounted for and equilibrium was assumed between vapor and liquid leaving each tray. The entropy production was minimized for a number of binary tray distillation columns with fixed heat transfer area, number of trays, and feed stream temperature and composition.

For the first time, the areas of heat exchange were used as variables in the optimization. An analytically derived result is that the entropy production due to heat transfer is proportional to the area of each heat exchanger in the

optimal state. This is for many distillation columns equivalent with a constant driving force for heat transfer, and explained previous findings. Numerical results give the most important positions for heat exchange in the column. Surprisingly, less than half the positions are needed.

Compared to the state of adiabatic columns, the optimal state was characterized by varying fluid flows and varying heat exchanger areas and corresponding duties along the column. The entropy production was reduced with up to 30% in the cases with large heat transfer area and many trays. In large process facilities, this reduction would ideally lead to 1-2 GWh of saved exergy per year. The most important variable in obtaining this reduction is the total heat transfer area.

We observed that the entropy production of the column behaved almost as a quadratic function when the composition of the feed stream changed. This means that the feed composition easily can be used as variable when a distillation column is part of a process optimization. Surprisingly, the entropy production was almost independent of the feed temperature. This reduces the sensitivity of the entropy production toward changes in the column feed temperature in a process optimization.

Acknowledgments

Statoil's VISTA program is thanked for the financial support to Audun Røsjorde.

Appendix

Variables and constraints

We use the tray temperatures as one set of free variables. From a given set of temperatures, the equilibrium relations give the compositions of the vapor and liquid streams. With known compositions, we can find the vapor and liquid streams from the mass balances, (3.3), and the component balances. Using the energy balances, Eq. (3.1), the duty on each tray can be calculated. However, in the condenser and reboiler, we cannot calculate the vapor and liquid flows, and thus not the duties. In the condenser and reboiler, the component balances are reduced to the mass balances, since we have assumed total condensation/evaporation. This means that V_1 and V_{N+1} are free variables, independent of any tray temperature, T_n.

The driving force for heat transfer can be eliminated by introducing the heat

transfer area through Eq. (3.6). Since A_n is not related to the tray temperatures or to the vapor flows in the condenser or reboiler, the heat transfer areas are also considered as independent variables.

To avoid trivial or unphysical solutions, the minimization of Eq. (3.7), must be done subject to one equality constraint and two inequality constraints:

1. The total heat transfer area must add up to a certain fixed value: $\sum A_n = A_{\text{total}}$.

2. The vapor flow leaving tray 1 must be equal to or greater than the distillate flow: $V_1 \geq D$.

3. The liquid flow leaving tray N must be equal to or greater than the bottom product flow: $L_N \geq B$ or equivalently, $V_{N+1} \geq 0$.

The Lagrangian function

Based on the three constraints we formulate a Lagrangian function, $\mathcal{L}$:

$$\mathcal{L} = \left(\frac{dS}{dt}\right)^{\text{irr}} - \alpha\left(\sum_{n=0}^{N+1} A_n - A_{\text{total}}\right) + \beta(V_1 - D) + \gamma(V_{N+1} - 0) \tag{3.14}$$

where α, β and γ are Lagrange multipliers. The necessary condition for a minimum is that the derivatives of $\mathcal{L}$ with respect to the different variables are equal to zero:

$$0 \begin{cases} \frac{\partial \mathcal{L}}{\partial T_n} & n \in [2, N-1] \\ \frac{\partial \mathcal{L}}{\partial A_n} & \text{all n} \\ \frac{\partial \mathcal{L}}{\partial V_n} & n = 1 \text{ or } N+1 \end{cases} \tag{3.15}$$

The duty of one heat exchanger depends on the temperature on the tray above and below, as well as the current one. The partial derivative of $\mathcal{L}$ with respect to the temperature is then:

$$\begin{aligned} \frac{\partial \mathcal{L}}{\partial T_n} =& \frac{\partial}{\partial T_n}\left(\frac{dS}{dt}\right)^{\text{irr}} = \frac{\partial}{\partial T_n} \sum_{i=n-1}^{n+1} \left(- \frac{Q_i}{T_i} + \frac{Q_i^2 \delta}{A_i \kappa_i T_i^2} \right) \\ =& \frac{Q_n}{T_n^2} - Q_n X_n \left(\frac{2}{T_n} + \frac{1}{\kappa_n} \frac{\partial \kappa_n}{\partial T_n} \right) + \sum_{i=n-1}^{n+1} \left(- \frac{1}{T_i} + 2X_i \right) \frac{\partial Q_i}{\partial T_n} = 0 \end{aligned} \tag{3.16}$$

In the last transformation we have re-introduced X_n into the equations to simplify the final result. The differentiations of the duties, $\frac{\partial Q_{n-1}}{\partial T_n}$, $\frac{\partial Q_n}{\partial T_n}$ and $\frac{\partial Q_{n+1}}{\partial T_n}$, in Eq. (3.16), are trivial and are not given.

The partial derivative of $\mathcal{L}$ with respect to the heat transfer area is:

$$\frac{\partial \mathcal{L}}{\partial A_n} = \frac{\partial}{\partial A_n}\left(\frac{dS}{dt}\right)^{\text{irr}} - \alpha = -\frac{Q_n^2 \delta}{A_n^2 \kappa_n T_n^2} - \alpha = -\frac{Q_n X_n}{A_n} - \alpha = 0 \qquad (3.17)$$

Since the constraints on the vapor flows in the condenser and reboiler are inequality constraints, we must find out whether the constraints are active or not, in the minimum state. An active constraint means that the inequality operator is replaced by an equality operator. If the objective function is a convex function in the dimension of the constrained variable, it is sufficient to evaluate the sign of the derivative at the point where the constraint becomes active. Depending on the sign, the optimal value of the constrained variable will be in the interior or at the border of the constraint.

From the energy balance, Eq. (3.1), we find that the duty is a linear function of the vapor flows. The entropy production is a quadratic function of the duties, and hence also of the vapor flows. It is therefore easy to see from the sign of the derivative at the border of the constraint, whether the unconstrained minimum will fall within the constraint or not.

In a series of test trials, the derivatives of the entropy production with respect to V_1 and V_{N+1} were estimated numerically. The sign of the derivative was positive in both cases, which means that the vapor flow must be decreased beyond the constraints to decrease the entropy production further. Both inequality constraints were in other words active: $V_1 = D$ and $V_{N+1} = 0$. This result has a somewhat intuitive meaning: The heat transferred in the condenser and reboiler becomes as small as physically possible when the constraints on the vapor flows are active. This means that less heat is produced at low temperature and less heat is consumed at high temperature. The net effect is a decrease in the entropy production.

Chapter 4

Second law analysis of an internal heat-integrated distillation column

Audun Røsjorde, Masaru Nakaiwa[#], Kejin Huang[#],
Koichi Iwakabe[#] and Signe Kjelstrup

Department of Chemistry
Norwegian University of Science and Technology
N-7491 Trondheim, Norway

#: Energy-efficient Chemical Systems Group
National Institute of Advanced Industrial Science and Technology
(AIST) Tsukuba, Ibaraki 305-8565, Japan

This paper was published in
Proceedings of ECOS 2004, Guanajuato, Mexico.

Abstract

The principal objective of this work was to study the effect of different operating conditions and designs on the thermodynamic efficiency of an internal heat-integrated distillation column. A second law analysis was performed by calculating under various conditions, the entropy production of a column that separates a mixture of equi-molar benzene and toluene into products of fixed composition. The HIDiC is designed and operated so that heat can be transferred directly from the rectifying to the stripping section. To make this possible, the pressure in the rectifying section must be high. Important conditions are thus the pressure ratio between the two sections and the type of heat integration. For pressure ratios and total rates of heat transfer ranging from 1.5 to 3.0 and 0 to 2000 kW/K, we calculated numerically the entropy production of the system. These numbers were compared to the entropy production of a corresponding conventional distillation column. It was clear that only for limited conditions did the heat-integrated distillation column have a better thermodynamic efficiency than the conventional distillation column. A minimum was found in the entropy production at a pressure ratio of 2.14 and a total rate of heat transfer per Kelvin of 1745 kW/K. The entropy production was 2.01 kW/K in this column, which compared to the conventional distillation column at 3.19 kW/K, was 37% lower. This was equal to a reduction in the lost exergy of 351.5 kW, which is a substantial amount.

4.1 Introduction

A big part of the energy used in the chemical industry is used for separation and purification of chemicals. Especially for large throughputs, distillation seems to be the only real choice when it comes to separation technologies. At the same time, it is well known that the energy efficiency of most distillation equipment is low (Fonyo 1974a,b). Both out of concern for the economy of a chemical plant and the necessary development toward a sustainable society it is important to find ways to improve the energy efficiency of distillation.

Several improvements have been developed to increase the energy efficiency of distillation, of which some are: Diabatic distillation (Rivero et al. 1994, De Koeijer et al. 2004b), heat pump assisted distillation (Null 1976) and heat-integrated distillation (Nakaiwa et al. 1986). In this work, we concentrate on the latter concept.

In conventional distillation, energy is supplied in the bottom at high temperature and withdrawn at the top at a lower temperature. In the heat-integrated distillation column (HIDiC) on the other hand, some or all of the heat released in the top part (rectifying section) is transferred directly to the bottom

part (stripping section) where heat is needed. This reduces the heat consumed/produced in the reboiler/condenser. However, this direct heat transfer is only possible if the pressure of the rectifying section is higher than that of the stripping section. In other words: By adding electrical or mechanical work through a compressor, the heat consumed in the reboiler will decrease. An excellent review of the concept is given by (Nakaiwa et al. 2003).

In this work, we focus on the following central questions: Does the HIDiC always have a higher energy efficiency compared to its conventional counterpart, independent of design and operating conditions? With operating conditions, we mean the pressure ratio between the pressure in the two sections and with design, we mean the effective rate of heat transfer per Kelvin. The latter is strongly dependent on the choice of construction materials and the effective heat transfer area. Intuitively, one might guess that the best thermodynamic performance of the HIDiC is found when the rate of heat transfer per Kelvin becomes infinitely large (reversible heat transfer). Is this the case or do there exist a set of optimal operating conditions and design? Finally, we will quantify how much better in terms of energy efficiency the HIDiC is compared to the conventional column.

We will try to answer these questions at least partially by performing a set of numerical simulations based on commonly accepted models of binary tray distillation. As a concrete case, we have chosen the separation of a benzene-toluene mixture.

4.2 The system

Our system is an internal HIDiC with N trays, surrounded by compressors, expanders, and heat exchangers, as shown in Fig. 4.1. Internal heat integration means that the rectifying and stripping sections are in direct thermal contact. Feed, F, of a certain quality, temperature and average composition enters at tray N_{F}. The vapor leaving the top of the rectifying section is fully condensed in the condenser, and a certain amount D, is withdrawn as liquid product. The rest is fed back into the column at tray number 1, thereby creating a reflux.

At the bottom of the stripping section, a certain amount of liquid product B, is removed from the column. The rest part is evaporated (brought to the dew point) in the reboiler and fed back into the stripping section just below tray N.

The rectifying section is operated at elevated pressures, P_{R}, so a compressor

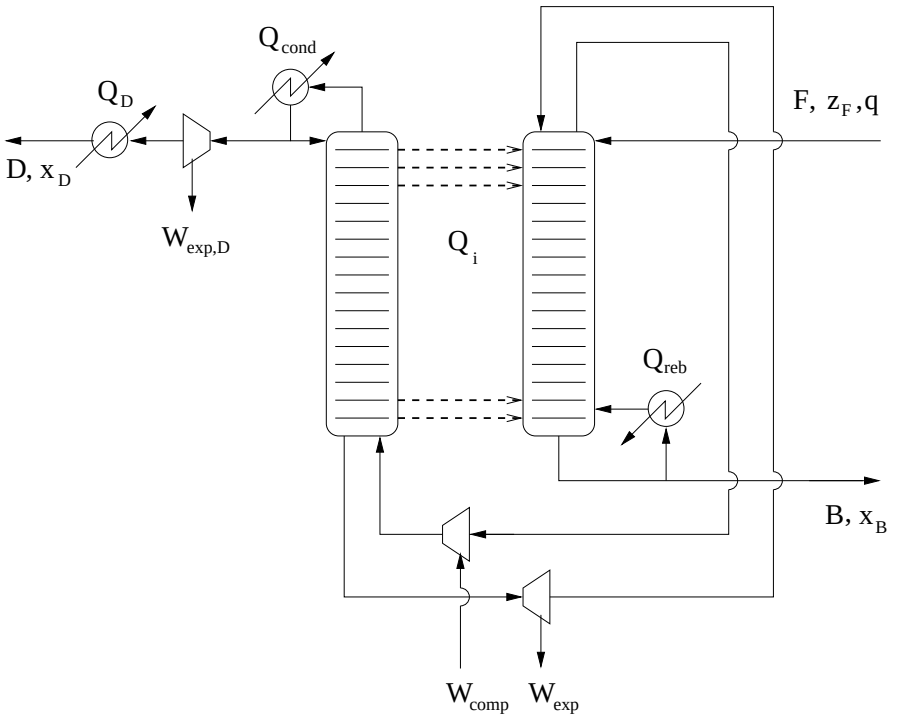

Figure 4.1. Schematic illustration of the HIDiC. For symbols explanation, see text. The trays are counted, starting from the top in the rectifying section (to the left).

and an expander operates on the material streams between the bottom of the rectifying section and the top of the stripping section.

The thermodynamical states of all material streams entering and exiting the system are fixed in our analysis, see Tab. 4.1. To bring the distillate from higher pressure and temperatures to a fixed state, we have introduced an expander and a heat exchanger working on the distillate stream.

Table 4.1. Operating conditions for the HIDiC.

Property	Value
Pressure in stripping section, P_S	1.013 bar
Total number of trays, N	20
Feed flow rate, F	100.0 mol/s
Overall feed composition	0.500
Feed temperature, T_F	365.93 K
Feed quality	0.8293
Overhead product composition	0.995
Overhead product flow rate, D	50.0 mol/s
Bottom product composition	0.005
Bottom product flow rate, B	50.0 mol/s
Temperature difference (pinch) in condenser and reboiler, ΔT	-/+ 30 K

We model the HIDiC using the following four assumptions:

- There is equilibrium between vapor and liquid leaving each tray.
- There are no pressure drops across the trays.
- Expanders, compressors, valves etc. operate reversibly.
- The condenser and reboiler have no mass transfer.
- The column is perfectly insulated against the environment.

Tray distillation is commonly modeled by the so-called MESH-equations, which are the material and energy balances across each tray as well as an equilibrium relation. By giving the rectifying and stripping section the same number of trays, we can easily formulate the equation for heat transfer. Heat transfer occurs between pairs of trays (Nakaiwa et al. 2003):

$$Q_i = -Q_{i+\frac{N}{2}} = UA_i(T_{i+\frac{N}{2}} - T_i) \qquad i \in [1, \frac{N}{2}] \tag{4.1}$$

where U is the overall heat transfer number and A_i is the effective area of heat transfer at tray i. We call the product UA_i the *rate of heat transfer per Kelvin* between tray i and $i + \frac{N}{2}$.

4.3 The entropy production

For a work consuming process (work positive when added to the system), the energy efficiency based on the second law of thermodynamics is defined as (Smith and Van Ness 1987):

$$\eta^{\mathrm{II}} = \frac{W_{\mathrm{rev}}}{W} = \frac{W_{\mathrm{rev}}}{W_{\mathrm{rev}} + T_0(\frac{dS}{dt})^{\mathrm{irr}}} \tag{4.2}$$

The actual work put into the process is equal to the work we would have to add if the process was reversible, W_{rev}, plus a part that is lost due to irreversibilities. The work that is lost equals, according to exergy analysis, the product of the entropy production of the system, $(\frac{dS}{dt})^{\mathrm{irr}}$, and the temperature of the surroundings T_0. The reversible work is equal to the change in exergy in the material streams entering and leaving the system.

The irreversibilities occur at different places in the system, and we broadly divide the entropy production into two parts:

$$\left(\frac{dS}{dt}\right)^{\mathrm{irr}} = \left(\frac{dS}{dt}\right)^{\mathrm{irr}}_{\mathrm{int}} + \left(\frac{dS}{dt}\right)^{\mathrm{irr}}_{\mathrm{ext}} \tag{4.3}$$

where we have split the total entropy production into *internal* and *external* contributions. The entropy production caused by phenomena inside the rectifying and stripping section (including the heat transfer between them) are the internal contributions. The entropy production in the reboiler and condenser, external to the column, are counted as external contributions (cf. Eq. (4.5)).

The internal entropy production is found from the entropy balance over the total column, expressed as the difference in entropy carried with the material streams that leave and enter:

$$\left(\frac{dS}{dt}\right)^{\mathrm{irr}}_{\mathrm{int}} = V_1 s_1^{\mathrm{V}} + L_N s_N^{\mathrm{L}} - V_{N+1} s_{N+1}^{\mathrm{V}} - L_0 s_0^{\mathrm{L}} - F s^{\mathrm{F}} \tag{4.4}$$

where s_i is the molar entropy of stream i and superscript V and L represent vapor and liquid phase, respectively. The reboiler and condenser have the approximate entropy production (Kjelstrup and Bedeaux 2001):

$$\left(\frac{dS}{dt}\right)^{\mathrm{irr}}_{\mathrm{ext}} = \int_V J'_{\mathrm{q}} X_{\mathrm{q}} dV \approx \int_V J'_{\mathrm{q}} dV \int_V X_{\mathrm{q}} dV \approx Q(\frac{1}{\overline{\overline{T}}} - \frac{1}{\overline{\overline{T}} + \Delta T}) \tag{4.5}$$

where J'_{q} and X_{q} is the local heat flux and its conjugated driving force, respectively. Q is the total amount of heat transferred, and $\overline{T}$ is the average temperature in the unit. The temperature difference between the process stream and the utility stream is ΔT. We have then assumed that no mass transfer occurs in the two units. We have also specified a pinch for the heat transfer, instead of introducing the heat transfer area and rates.

4.4 Calculations

Thermodynamical properties; enthalpy, entropy and equilibrium relations, were found from the Soave-Redlich-Kwong (SRK) equation of state (Prausnitz et al. 1999). For a fixed number of trays we numerically solved the MESH-equations and Eq. (4.1) according to the following scheme:

1. The rate of heat transfer per Kelvin between each pair of trays $[UA_1,...,UA_{\frac{N}{2}}]$ and the ratio between the pressure in the rectifying and stripping section $P_{\mathrm{R}}/P_{\mathrm{S}}$ were fixed.
2. The liquid composition on each tray was guessed. The equilibrium relation gave then the corresponding temperature and vapor composition.
3. The heat transfers between the stripping and rectifying section were found from Eq. (4.1).
4. The reflux ratio was guessed and the heat released in the condenser was calculated.
5. From the heat transfer on each tray, we calculated the vapor and liquid molar flow rates from the energy balance across each tray.
6. Finally, the vapor and liquid flows were checked for agreement with the component and mass balances on each tray.

This procedure ensured that the feed and product states were constant, at varying reflux ratios and internal flows. By repeating point 2 to 6, using the function *fsolve* from the Optimization Toolbox in Matlab R13, MathWorks Inc., we found the solution to the system of nonlinear equations. We used the liquid mole fractions and reflux rate as variables to fulfill the component balances. The rate of transfer per Kelvin between each pair of trays was the same on all trays and equal to $UA_{\mathrm{total}}/\frac{N}{2}$ kW/K. This choice for the distribution of UA was motivated by simple geometric design.

The entropy production of a conventional distillation column with $UA_{\text{total}} = 0$ and $P_{\text{R}}/P_{\text{S}} = 1.0$ was first determined to have a reference for the calculations. In the next calculations, $P_{\text{R}}/P_{\text{S}}$ and UA_{total} were systematically set to values varying from 1.5 to 3.0 and 0 to 2000 kW/K, respectively. For each set, we evaluated the entropy production of the HIDiC from Eq. (4.3). By repeated calculations we found for each combination of $P_{\text{R}}/P_{\text{S}}$ and UA_{total} the location of the feed tray giving the lowest entropy production.

4.5 Results and discussion

The chosen inlet and outlet states gave a very low and varying efficiency for temperatures T_0 around 280-300 K. We continue with a discussion of the entropy production, which is absolute.

In all calculations the optimal feed tray location was at tray 11 (the topmost tray in the stripping section). Also in the conventional column this feed location was the best, giving an entropy production of 3.19 kW/K.

Figure 4.2 shows a surface plot and a corresponding contour plot, Fig. 4.3, of the entropy production of the HIDiC with different rates of heat transfer and pressure ratio. The 3-D representation of these results is very similar to a valley with the bottom slowly descending as one moves from left to right in the figure. For relatively high and low pressure ratios, we are high in the sides of the valley, while the bottom follows a slightly curved path around $P_{\text{R}}/P_{\text{S}}$=2.3 (marked with a dashed curve).

An area covering the upper right-hand quarter of the figure (marked with 'x') represents combinations of UA_{total} and $P_{\text{R}}/P_{\text{S}}$ that gave physically impossible columns. Inside this area the heat transfer between the stripping and rectifying section was so big that the topmost vapor flow was smaller than the desired production (V_1 <D). Along the border between this area and the rest of the entropy production landscape we found columns with zero reflux. We call this the line of zero reflux.

The entropy production landscape in Fig. 4.3 has some interesting features. Primarily, it is clear that many combinations of UA_{total} and $P_{\text{R}}/P_{\text{S}}$ resulted in HIDiC's that actually had a higher entropy production than the conventional column had. The thick level curve represents the entropy production of the latter, enclosing the area where the HIDiC's entropy production were the lowest. For UA_{total} >650 kW/K the upper limits to this feasible area is given by the line of zero reflux in Fig. 4.3.

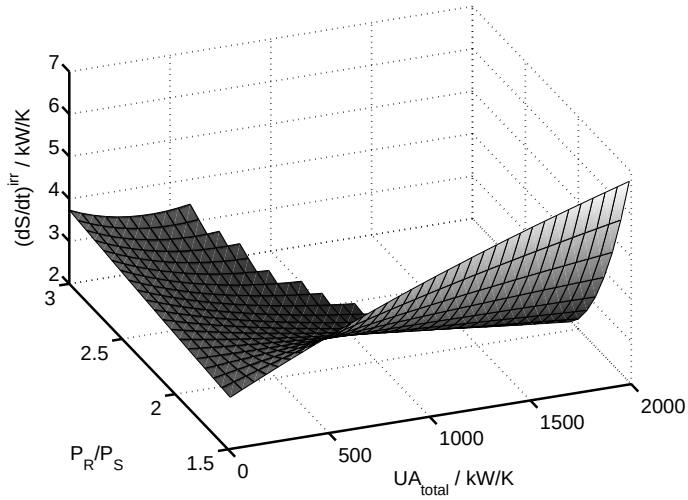

Figure 4.2. Surface of entropy production (in kW/K) of the HIDiCs for combinations of UA_{total} and $P_{\mathrm{R}}/P_{\mathrm{S}}$.

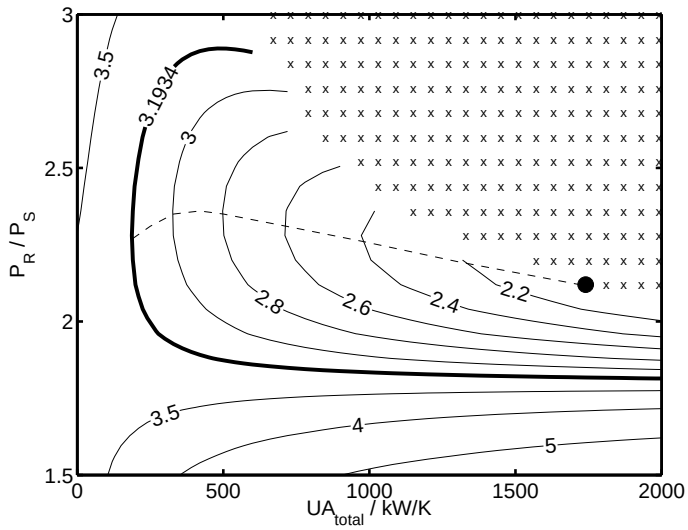

Figure 4.3. Contour plot of the entropy production (in kW/K) of the HIDiCs for combinations of UA_{total} and $P_{\mathrm{R}}/P_{\mathrm{S}}$.

The fact that the entropy production landscape is mainly convex means that for a HIDiC with a given UA_{total} it is possible to find an optimal $P_{\text{R}}/P_{\text{S}}$. In an existing column it is expensive to change UA_{total}, but by increasing/decreasing the pressure ratio it is possible to move toward the dashed line in Fig. 4.3 and thus increase the energy efficiency. At the point where the "bottom of the valley" intersects with the line of zero reflux, we found a minimum in the entropy production. At $UA_{\text{total}} \approx 1745$ kW/K and $P_{\text{R}}/P_{\text{S}} \approx 2.14$ the entropy production was 2.01 kW/K (marked with a black dot). Compared with the conventional distillation column this represented a reduction of 37.0%. The general behavior of the entropy production landscape suggests that this minimum was in fact a global minimum. If so, this means the highest energy efficiency possible is not found for rates of heat transfer approaching infinity, but rather for a finite value.

Finally, to illustrate how the reduction in entropy production translates into changes in utility requirements, we compared the required heat and work in the conventional column and the optimal HIDiC in Tab. 4.2. The temperatures given in the table are calculated from $\tilde{T} = \frac{Q}{\Delta S - XQ}$, which is the temperatures we would have to use in order to ensure consistency between nonequilibrium thermodynamics and the entropy balance (ΔS is the entropy change in the material stream in/out of the heat exchangers). By replacing the conventional

Table 4.2. Required work and heat flows in the conventional distillation column and the optimal HIDiC.

	Conventional column	Optimal HIDiC
Reboiler heat [kW]	5353.5 (at 413.1 K)	376.4 (at 413.1 K)
Condenser heat [kW]	-5840.3 (at 323.9 K)	-1495.6 (at 350.8 K)
Net compressor work [kW]	0	830.7
Extra heat exchange [kW]	0	-198.2 (at 367.2 K)

distillation column with the optimal HIDiC the amount of heat required in the reboiler was greatly reduced, with a factor of 14! In addition, due to the elevated pressure in the stripping section, the heat produced in the condenser held a much higher temperature, almost 30 K more. A small amount of heat at a temperature 14 K higher than the reboiler was also produced in the extra heat exchanger operating on the product stream. The improvements all came at the cost of the addition of a substantial amount of electrical work and reduced amount of heat released in the condenser (with a factor of 4).

In an environment with temperature T_0=298 K the reduced entropy production

means that the lost work was reduced with 351.5 kW. The detailed exergy content in the heat and work flows are given in Tab. 4.3. The exergy of all the material streams entering and leaving the system was constant and is not taken into consideration.

Table 4.3. The exergy content corresponding to the work and heat flows in Tab.4.2 for a conventional column and the HIDiC.

	Conventional column	Optimal HIDiC
Reboiler exergy [kW]	1491.6	104.9
Condenser exergy [kW]	-467.0	-225.1
Net compressor work [kW]	0	830.7
Extra heat exchanger exergy [kW]	0	-37.4
Sum = Lost exergy [kW]	1024.6	673.1

Further reductions in the entropy production of the HIDiC may be obtained by allowing UA to be different from one pair of trays to another. This will increase the number of degrees of freedom the system has to obtain a state of high energy efficiency. Even higher efficiencies can be found by allowing for a more flexible heat integration, i.e. heat transfer not only between tray i and $i + \frac{N}{2}$ but any possible interconnection. It may be necessary to abandon the internal heat integration to realize such an improved heat integration scheme.

4.6 Conclusion

An analysis based on the second law of thermodynamics was performed on a heat-integrated distillation column separating a mixture of benzene and toluene. The HIDiC is successfully operated by increasing the pressure in the rectifying section thus enabling heat transfer directly to the stripping section. For pressure ratios and total rates of heat transfer ranging from 1.5 to 3.0 and 0 to 2000 kW/K, we calculated numerically the entropy production of the system.

By comparing these entropy productions to the one found in the corresponding conventional distillation column it is clear that only for limited conditions did the HIDiC have a lower entropy production than the conventional column. For pressure ratios approaching 1.5 and 3.0, and rates of heat transfer lower than approximately 300 kW/K, the HIDiC had the higher entropy production compared to the conventional column.

A minimum was found in the entropy production at a pressure ratio of 2.14 for given product quality. The total rate of heat transfer per Kelvin was then 1745 kW/K. The entropy production was 2.01 kW/K in this column, which compared to the conventional distillation column at 3.19 kW/K, was 37% lower. This was equal to a reduction in the lost exergy of 351.5 kW. The saving can be realized through a much lower reboiler duty and a higher temperature on condenser cooling fluid. The drawbacks are that mechanical work must be supplied and less heat is released in the condenser.

Acknowledgments

Audun Røsjorde thanks the Energy-efficient Chemical Systems Group at the National Institute of Advanced Industrial Science and Technology (AIST), Tsukuba, for their generous hospitality and support.

Chapter 5

Minimizing the entropy production of an internal heat-integrated distillation column: Optimal heat transfer

Audun Røsjorde, Masaru Nakaiwa[#], Kejin Huang[#],
Koichi Iwakabe[#] and Signe Kjelstrup

Department of Chemistry
Norwegian University of Science and Technology
N-7491 Trondheim, Norway

#: Energy-efficient Chemical Systems Group
National Institute of Advanced Industrial Science and Technology
(AIST) Tsukuba, Ibaraki 305-8565, Japan

This paper is proposed for
The 7th World Congress of Chemical Engineering, Glasgow, 2005

Abstract

The heat-integrated distillation column (HIDiC) improves the conventional adiabatic distillation column by internal heat transfer between the rectifying and stripping section. Potential savings in terms of lost exergy are high, and make the HIDiC an interesting object for optimization. The internal heat transfer requires a higher pressure in the rectifying section than in the stripping section, and this pressure rise costs work. We have studied the optimal performance of the column for a ratio of the pressure in the rectifying and stripping section of 1.5 to 3.0, when a physical solution is possible, keeping the feed and product specifications fixed. In the optimization, we allowed the rates of heat transfer per Kelvin between the pair of trays to vary. Values for the total rate of heat transfer per Kelvin ranged from 0 to 2000 kW/K. The combination of pressure ratio and total rate of heat transfer per Kelvin that gave the lowest entropy production was 1.88 and 2000 kW/K, respectively. This column had an entropy production of 1.66 kW/K, which was 48% lower than the conventional column doing the same separation task, but this result must be regarded on the basis of the assumption of equilibrium between the vapor and liquid at the outlet of each tray. The distribution of the heat transfer showed a systematic behavior, as the total rate of heat transfer per Kelvin and the pressure ratio were changed. In columns with low heat transfer (low total rate of heat transfer per Kelvin and/or low pressure ratio), only the pair of trays closest to the condenser and reboiler were active in transferring heat. As we increased the total rate of heat transfer per Kelvin and the pressure ratio, more heat was transferred and at some point, more pair of trays became active. This sudden transition was due to the reflux ratio becoming zero. Since the column with the lowest entropy production also had a reflux ratio equal to zero, an important result is that large savings in the entropy production can be achieved with heat transfer only on the pair of trays closest to the reboiler and condenser. This may have large implications for the design of highly energy efficient HIDiCs. We proposed a modified design of the HIDiC, in which heat transfer was only allowed between the topmost and bottommost tray in the rectifying and stripping section, respectively. Initial calculations showed that such design enabled an even lower entropy production.

5.1 Introduction

Distillation is the most widely used separation technology for purification of chemicals, but in its simplest form it is a technology with low energy efficiency. For several decades effort has been put into the development of improved distillation concepts, of which one is the internal heat-integrated distillation column (HIDiC), see review by Nakaiwa et al. (2003).

The concept of the HIDiC is to use a higher operating pressure in the rectifying

section than in the stripping section of the column. Since this shifts the phase equilibrium toward higher temperatures, it is possible to obtain a direct heat transfer from the rectifying to the stripping section, thereby lowering the heat transfer in the reboiler and condenser and increasing the exergy efficiency.

Economical and controllability aspects of this column have been studied by Nakaiwa et al. (2001), Engelien et al. (2003), Wendt et al. (2003). Recently we performed a second law analysis of the HIDiC where the entropy production was calculated for different combinations of the operating pressure ratio (P_R/P_S) and the total rate of heat transfer per Kelvin (UA_{total}) between the two sections in the column (Røsjorde et al. 2004), and the state of minimum entropy production was found. In the product UA, U is the overall heat transfer coefficient, and A is the transfer area. The rate of heat transfer per Kelvin was in that case, by choice, the same for each pair of trays along the column. We shall now relax this condition, and ask for the optimal distribution of the product $(UA)_i$ among each pair of trays i, when the entropy production of the total column is minimum and $\sum(UA)_i = UA_{total}$. As before, we shall also find the optimal location of the feed tray. In this manner, we shall seek more knowledge about the nature of the state of minimum entropy production of HIDiC columns. This may contribute to a broader basis for choice of HIDiC column design parameters. The study will also enable us to compare the performance of HIDiC to diabatic and other columns.

A practical column has UA in the reboiler and condenser of a certain finite magnitude. One way to realize such UA is to set a relatively large average temperature difference between heat exchange medium and process stream. We shall here use 30 K for this temperature difference instead of specifying the heat transfer areas in the condenser and reboiler. Apart from this specification, we do not introduce any particular requirements on the column operation. The temperature differences between the corresponding trays in the two sections of the column are not fixed or limited and may attain any values. We shall then see that we can determine a range of P_R/P_S and UA_{total} values where the HIDiC column performs better than an adiabatic column. The range is qualitatively similar to the one determined before for uniform UA-distributions. The value of the minimum is substantially smaller, however, by 17%. Also the physical solution of the optimization problem exists for a broader range in the values of P_R/P_S and the values of UA_{total}: A favorable situation for heat transfer is obtained only when P_R/P_S is in a relatively narrow range, between the lower value (1.5) and an upper value (2.9), and when UA_{total} is greater than a minimum value (150 kW/K).

As before, we have used the binary mixture of benzene and toluene as an example to illustrate the features of the column. The feed and product compositions were the same as used by Røsjorde et al. (2004). This allows us to compare the HIDiCs performance to other work reported in the literature. Much of the system and the governing equations have been described before, but the essential information is repeated to a degree that facilitates reading.

5.2 The system

The internal HIDiC studied here had N trays; half of them in the rectifying and half of them in the stripping section. Figure 5.1 show the schematics of the system. Since we want to compare columns operated at different pressures

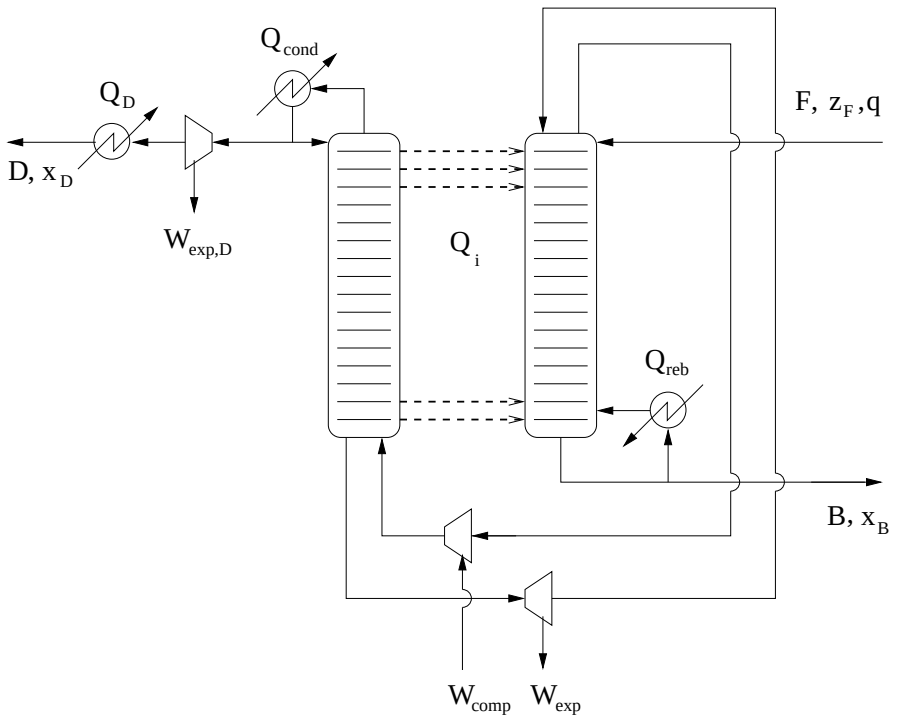

Figure 5.1. Layout of the HIDiC.

we have introduced an expander and heat exchanger bringing the distillate product to the same thermodynamical state as the environment. Assuming that the feed and bottom product both have a pressure of 1 atm, the expander and heat exchanger ensure that the material streams entering and exiting the

system have constant thermodynamical states. When operated in a process, the HIDiC is surrounded by other process units instead. The system was earlier described in Røsjorde et al. (2004).

A liquid distillate (D) primarily composed of the light component was withdrawn at the top of the rectifying section, while a liquid phase (B) of the heavy component was withdrawn at the bottom of the stripping section. The feed stream (F) can be located anywhere between tray 1 and N and the best position shall be found through optimization. To increase the pressure of the vapor leaving the top of the stripping section, a compressor was introduced, operating on this stream. Similarly, an expander (or expansion valve) was placed on the liquid stream flowing from the rectifying section to the stripping section. As in conventional distillation, a condenser and a reboiler were used to create an internal reflux.

The HIDiC is modeled in the same way as conventional distillation (see for instance Chapter 3), except that each tray may have a heat flow in/out according to the following equation (Nakaiwa et al. 2003):

$$Q_i = -Q_{i+\frac{N}{2}} = (UA)_i(T_{i+\frac{N}{2}} - T_i) \qquad i \in [1, \frac{N}{2}] \tag{5.1}$$

where Q is the heat flow, $(UA)_i$ is the rate of heat transfer per Kelvin between a pair of trays, and T is the temperature on the tray. We do not separate $(UA)_i$ into U_i and A_i, thereby making the analysis more general.

We do not have to specify the geometrical aspects of the HIDiC in order to use the above equation for the heat transfer. In reality, the stripping and rectifying sections may be incorporated into different constellations (for instance with a dividing wall, or as two concentric shells). Our analysis will be independent of these practical considerations.

5.3 The entropy production

In this work we are primarily interested in the irreversibilities related to the heat and mass transfer in the HIDiC. The compressor, expanders and heat exchanger are thus assumed to be operated reversibly. Entropy is consequently only produced in the condenser, reboiler, and the distillation column itself. Røsjorde et al. (2004) divided the total entropy production in the HIDiC in two parts; internal and external contributions. We shall in addition separate the entropy production produced internally in the column in two parts: Entropy produced by heat and mass transfer between the liquid and vapor phase,

$(\frac{dS}{dt})^{\text{irr}}_{\text{trans}}$, and entropy produced by heat transfer between the rectifying and stripping section, $(\frac{dS}{dt})^{\text{irr}}_{\text{hx}}$.

An entropy balance across each tray (except at the feed tray and the tray above where the entropy of the feed must be included in addition) gives:

$$\left(\frac{dS}{dt}\right)^{\text{irr}}_{\text{trans},i} = V_i s_i^{\text{V}} + L_i s_i^{\text{L}} - V_{i+1} s_{i+1}^{\text{V}} - L_{i-1} s_{i-1}^{\text{L}} - \frac{Q_i}{T_i} \tag{5.2}$$

where s is the molar entropy of a stream and V and L are the molar flows of vapor and liquid, respectively. The superscripts V and L refer to properties in vapor and liquid phase, respectively. The total entropy produced by the heat and mass transfer between the two phases is:

$$\begin{aligned}\left(\frac{dS}{dt}\right)^{\text{irr}}_{\text{trans}} &= \sum_{i=1}^{N} \left(\frac{dS}{dt}\right)^{\text{irr}}_{\text{trans},i} \\ &= V_1 s_1^{\text{V}} + L_N s_N^{\text{L}} - V_{N+1} s_{N+1}^{\text{V}} - L_0 s_0^{\text{L}} - F s^{\text{F}} - \sum_{i=1}^{N} \frac{Q_i}{T_i} \\ &= V_1 s_1^{\text{V}} + L_N s_N^{\text{L}} - V_{N+1} s_{N+1}^{\text{V}} - L_0 s_0^{\text{L}} - F s^{\text{F}} - \sum_{i=1}^{N/2} Q_i X_i\end{aligned} \tag{5.3}$$

where $X_i = \frac{1}{T_i} - \frac{1}{T_{i+\frac{N}{2}}}$ is the thermodynamic driving force for the heat transfer between each pair of trays.

Expressed as the product of the measurable heat flow and its average conjugate driving force, the total entropy produced by the heat transfer between the rectifying and stripping section is:

$$\left(\frac{dS}{dt}\right)^{\text{irr}}_{\text{hx}} = \sum_{i=1}^{N/2} Q_i X_i \tag{5.4}$$

The above expression is also readily obtained by subtracting Eq. (5.3) from the expression for the internal entropy production given in Røsjorde et al. (2004) (Eq. (4.4)).

We use the same approximated expression for the entropy produced in the condenser and reboiler, $(\frac{dS}{dt})^{\text{irr}}_{\text{ext}}$, as Røsjorde et al. (2004) (referred to as external since this entropy is created outside the column itself):

$$\left(\frac{dS}{dt}\right)^{\text{irr}}_{\text{ext}} \approx Q\left(\frac{1}{\overline{T}} - \frac{1}{\overline{T} + \Delta T}\right) \tag{5.5}$$

where Q is the heat transferred in the reboiler or condenser and $\overline{T}$ is the arithmetic average temperature between inlet and outlet stream temperature. The temperature difference between the distillate/bottom stream and the utility stream is ΔT. We have then assumed that no mass transfer occurs in the two units (total evaporation and condensation). Instead of specifying the heat transfer area and heat transfer coefficient for the condenser and reboiler, we specified the average temperature difference, ΔT, between the hot and cold streams.

The total entropy produced by the HIDiC is the sum of the three above contributions:

$$\left(\frac{dS}{dt}\right)^{\text{irr}} = \left(\frac{dS}{dt}\right)^{\text{irr}}_{\text{trans}} + \left(\frac{dS}{dt}\right)^{\text{irr}}_{\text{hx}} + \left(\frac{dS}{dt}\right)^{\text{irr}}_{\text{ext}} \tag{5.6}$$

The total entropy production is the objective function in our optimization.

5.4 Calculations

Minimizing the entropy production of the HIDiC, can mathematically be stated as:

$$\underset{\mathbf{UA},N_{\text{F}}}{min}\left(\frac{dS}{dt}\right)^{\text{irr}}, \qquad \sum_{i=1}^{N/2} UA_i = UA_{\text{total}} \tag{5.7}$$

where $\mathbf{UA} = [UA_1, ..., UA_{\frac{N}{2}}]$ and N_{F} is the feed tray number. The two crucial parameters in the HIDiC design are the ratio between the pressure in the rectifying and stripping section, $P_{\text{R}}/P_{\text{S}}$, and the total rate of heat transfer per Kelvin, UA_{total}. These parameters were not subject to any variation in each optimization, however many different optimizations were carried out with values for UA_{total} and $P_{\text{R}}/P_{\text{S}}$ systematically selected from the intervals [0, 2000 kW/K] and [1.5, 3.0], respectively. The range of $P_{\text{R}}/P_{\text{S}}$ was motivated by findings from modeling of HIDiCs with equal UA on each tray (Røsjorde et al. 2004). The maximum value of UA_{total} corresponds to 200 m^2 of heat transfer area per tray with a heat transfer number around 1000 W/K. We consider this more than what is practically possible and it thus serves as an upper limit. All other parameters such as product compositions, the number of trays, and the feed properties were fixed to the values given in Tab. 5.1.

A possible way to solve this problem would have been to guess **UA** and then solve the mass, energy and equilibrium equations, before evaluating the entropy production. However, since the equilibrium relations and enthalpies depended on compositions and temperatures inside the column in a non-trivial

Table 5.1. Operating conditions for the HIDiC.

Property	Value
Pressure in stripping section, P_S	1.013 bar
Total number of trays, N	20
Feed flow rate, F	100.0 mol/s
Overall feed composition, z_F	0.500
Feed temperature, T_F	365.93 K
Feed quality, q	0.8293
Overhead product composition, x_D	0.995
Overhead product flow rate, D	50.0 mol/s
Bottom product composition, x_B	0.005
Bottom product flow rate, B	50.0 mol/s
Temperature difference in condenser and reboiler, ΔT	-/+ 30 K

way, we preferred to introduce more variables followed by the same number of equality constraints. Specifically, we introduced $N-1$ additional variables $\mathbf{x}$ $=[x_2, ..., x_{N-1}]$ and RR, and the constraints:

$$V_{i+1}y_{i+1} - L_i x_i = Dx_D - \delta(i = N_F - 1)Fy_F - \delta(i \geq N_F)Fz_F, i \in [1, N-1] \quad (5.8)$$

where δ was the Kronecker delta-function. In addition, we introduced a set of inequality constraints ensuring that the internal mass flows always was positive:

$$\begin{aligned} V_i &\geq 0, \qquad i < \frac{N}{2} + 1 \\ L_i &\geq 0, \qquad i > \frac{N}{2} + 1 \end{aligned} \quad (5.9)$$

The optimization problem could efficiently be solved with nonlinear programming techniques.

We used the function *fmincon* from the Optimization Toolbox in Matlab R13, MathWorks Inc. to solve the optimization problem. Below is a stepwise procedure:

1. *fmincon* guessed $\mathbf{UA}$, $\mathbf{x}$, and RR.
2. From the product specification we knew that x_0 and x_N always were equal to x_D and x_B, respectively. Furthermore, we knew that $y_1 = x_D$, and combined with $\mathbf{x}$ we calculated the temperature on each tray from the equilibrium relations.

3. The heat transfer between the stripping and rectifying section on each tray were then found from Eq. (5.1).

4. The heat released in the condenser was calculated from T_0, T_1 and RR.

5. Using the energy and mass balance on each tray, the molar flow rates were calculated.

6. The entropy production was calculated and the constraints, Eqs. (5.8) and (5.9), were evaluated.

By using a sequential quadratic programming technique, the function *fmincon* found the minimum of the entropy production. The value of N_{F} giving the lowest entropy production was then found by repeated optimizations with different values for N_{F}.

The entropy production of a conventional distillation column ($UA_{\mathrm{total}} = 0$ and $P_{\mathrm{R}}/P_{\mathrm{S}} = 1.0$) was calculated and were used as a benchmark.

Thermodynamical properties (enthalpy, entropy and equilibrium relations), were found from the Soave-Redlich-Kwong (SRK) equation of state (Prausnitz et al. 1999). The binary interaction coefficient was set to 0.005751 and was found by fitting of the equation of state to experimental data taken from Gmehling and Onken (1980). Expressions for the ideal gas heat capacity were taken from Daubert and Danner (1992).

5.5 Results

441 optimizations were carried out and selections of properties from these columns are presented. In all of these optimizations, we found that the optimal location of the feed tray was at the top of the stripping section (tray no. 11). In Fig. 5.2 the total entropy production for these columns is shown as a surface plot. To see the features of this surface more clearly, a contour plot based on the same data is presented in Fig. 5.3. The entropy production of the conventional distillation column, doing the same separation task as the HIDiCs, was 3.19 kW/K. This value is marked in the contour plot by a thicker curve. The shape of the entropy production surface is similar to that of a valley with the lowest point found for increasingly larger values of UA_{total}. The entropy production was higher for columns with low and high pressure ratios, than for columns with pressure ratios in the middle of the range. Especially at high pressure ratios, the entropy production became very large. Fig. 5.3 shows clearly that

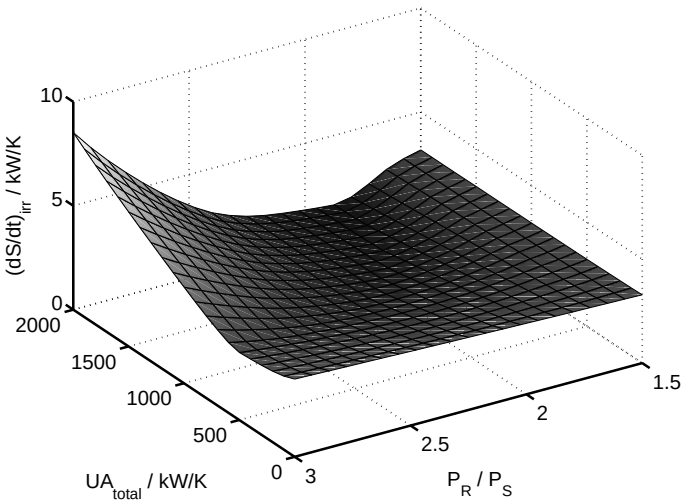

Figure 5.2. The entropy production at different pressure ratios and total rates of heat transfer per Kelvin.

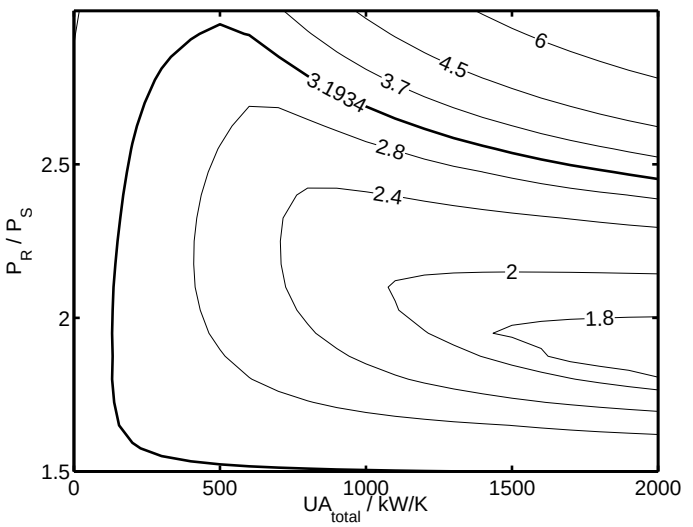

Figure 5.3. The entropy production at different pressure ratios and total rates of heat transfer per Kelvin. The thick level curve equals the entropy production in conventional distillation.

for most combinations of UA_{total} and $P_{\text{R}}/P_{\text{S}}$ the optimized HIDiC obtained a lower entropy production than the conventional distillation column. The lowest value for the entropy production was 1.66 kW/K at UA_{total} = 2000 kW/K and $P_{\text{R}}/P_{\text{S}}$ = 1.88. Compared to the conventional distillation column this represents a reduction of 48%.

Fig. 5.3 further shows that below UA_{total} around 150 kW/K it was not possible to find any pressure ratios that gave the HIDiC a lower entropy production than the conventional column. Similarly, a lower and upper limit on the pressure ratio around 1.5 and 2.9, respectively, was found.

Since the variables in the optimizations were the total rates of heat transfer per Kelvin at 10 trays, it is difficult to present the values of these variables found at all the 441 optimal solutions. However, the UA-distributions did show a typical trend that is especially easy to see from the solutions around pressure ratios of 2.1-2.2. Figure 5.4 shows how UA distributed itself among the 10 pair of trays with increasing UA_{total} at $P_{\text{R}}/P_{\text{S}}$=2.18. At low values of UA_{total} it was

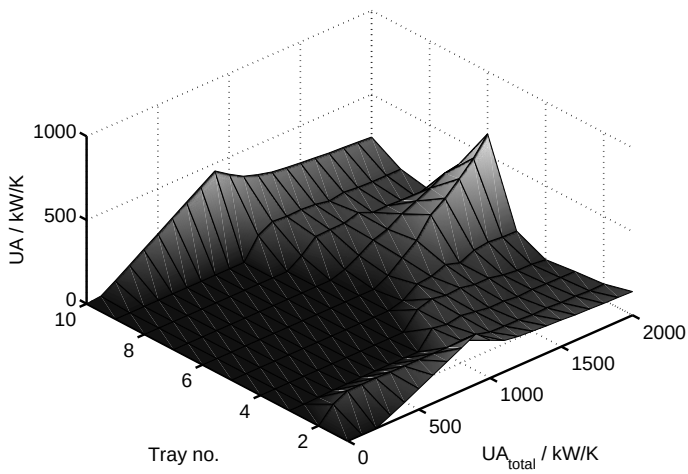

Figure 5.4. Distribution of UA at different UA_{total} and $P_{\text{R}}/P_{\text{S}}$=2.18

only shared between tray pair 1, 2 and 10. No other pairs of trays were active. When reaching a certain value, the rate of heat transfer per Kelvin started to center more and more on tray pair 5 and 6. As UA_{total} continued to increase, these trays were completely dominating the heat transfer in the columns. The same behavior was observed at all pressure ratios; the only difference being the

position where the transition from the end-dominated to the center-dominated UA-distribution took place. For lower pressure ratios, the transition came at high values of UA_{total}, while the opposite was true for higher pressure ratios.

To see the effect this redistribution of UA had on the material streams inside the columns, we have plotted three vapor flow profiles in Fig. 5.5. They are all from the same pressure ratio as the UA-distributions given in Fig. 5.4, $P_{\text{R}}/P_{\text{S}}$=2.18. One profile is from optimization with $UA_{\text{total}} = 0$, one is from optimization with UA_{total}=1000 kW/K and one is from the optimization with UA_{total} = 2000 kW/K. As UA_{total} increased, the vapor flow profile changed

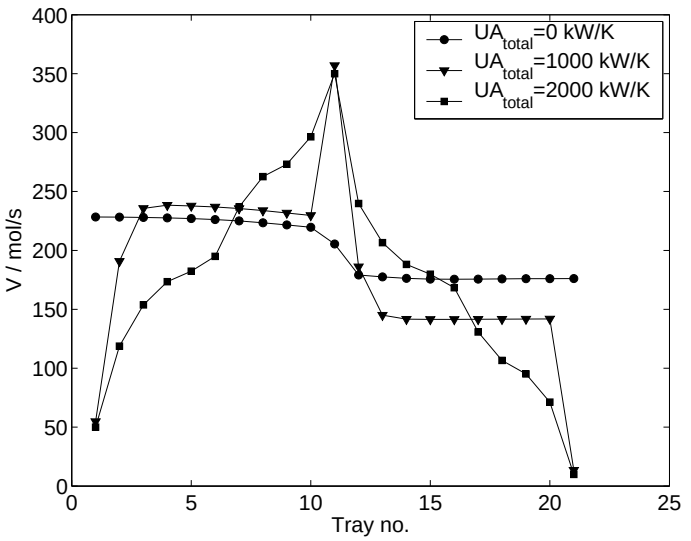

Figure 5.5. Vapor flow profiles in two optimized columns with $UA_{\text{total}} = 0$, 1000 and 2000 kW/K at $P_{\text{R}}/P_{\text{S}}$=2.18.

from almost flat around 200 mol/s, to nearly pyramidal with a max value of 350 mol/s. On the trays where UA was zero the vapor flow changed little.

In Fig. 5.6 the reflux ratio, RR, for all the optimized HIDiCs is plotted. At low values of UA_{total} and/or $P_{\text{R}}/P_{\text{S}}$ the reflux ratio was around 3-4. As either of the two parameters increased, the reflux ratio dropped fast and reached zero. Still increasing values gave a slight increase in the reflux ratio again.

According to the three equations, Eqs. (5.3) to (5.5), the total entropy production can be separated in different contributions. Figures 5.7-5.9 show the contributions from external heat transfer, heat and mass transfer, and internal

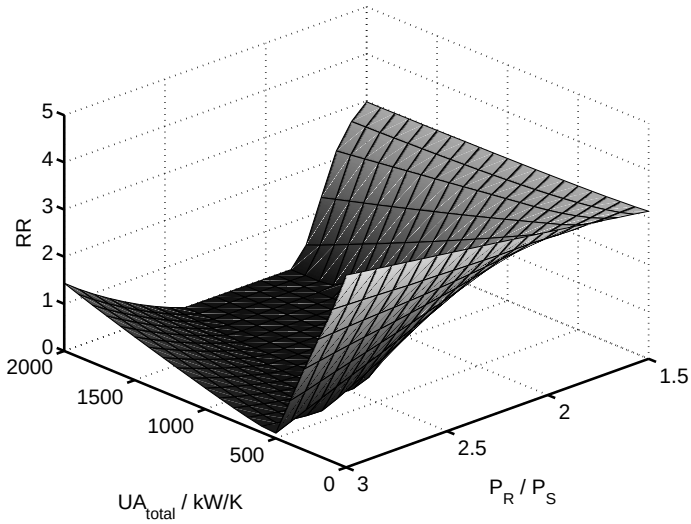

Figure 5.6. Reflux ratio in all optimized columns.

heat transfer, respectively. The surface plot of the entropy produced by heat transfer in the condenser and reboiler in Fig. 5.7 shows a behavior similar to that of the reflux ratio in Fig. 5.6. This is a direct consequence of Eq. (5.5) and the fact that the heat transfer in the condenser and reboiler is directly related to the reflux ratio.

At low values of UA_{total} and $P_{\text{R}}/P_{\text{S}}$ the entropy produced by heat and mass transfer between the liquid and vapor phases was constant around 1 kW/K, accounting for around one third of the total entropy production. However, when the two parameters UA_{total} and $P_{\text{R}}/P_{\text{S}}$ both attained high values, this contribution dominated the total entropy production.

A similar shape was found in Fig. 5.9: At the lowest values of UA_{total} and $P_{\text{R}}/P_{\text{S}}$ the entropy production due to heat transfer between the rectifying and stripping section was small (even zero). As both the parameters increased, the entropy production also increased, before if entered a different region of the surface where it flattened out. For still increasing values of UA_{total} and $P_{\text{R}}/P_{\text{S}}$ the entropy production reached approximately 2 kW/K.

Finally, we make a comparison between the optimized HIDiCs found in this work and the corresponding HIDiCs with uniform UA-distribution found by Røsjorde et al. (2004). The same pressure ratios and total rates of heat transfer

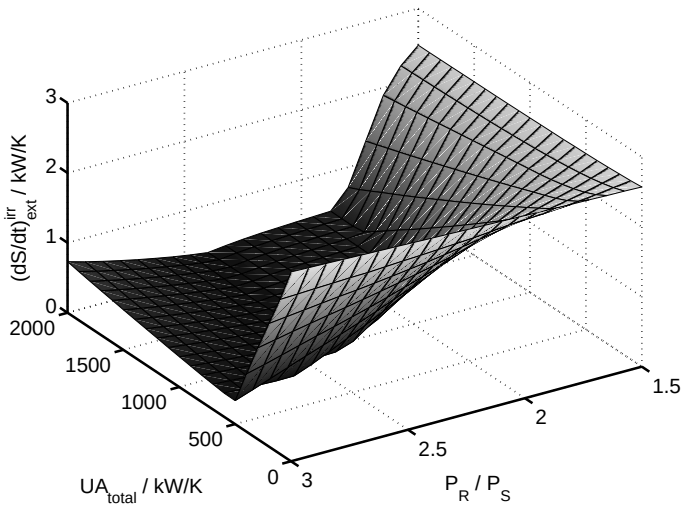

Figure 5.7. The entropy produced by external heat transfer.

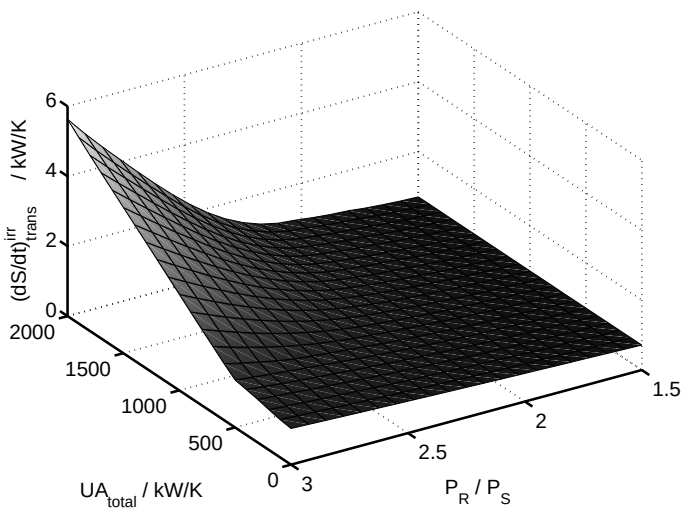

Figure 5.8. The entropy produced by transfer of heat and mass between liquid and vapor phase.

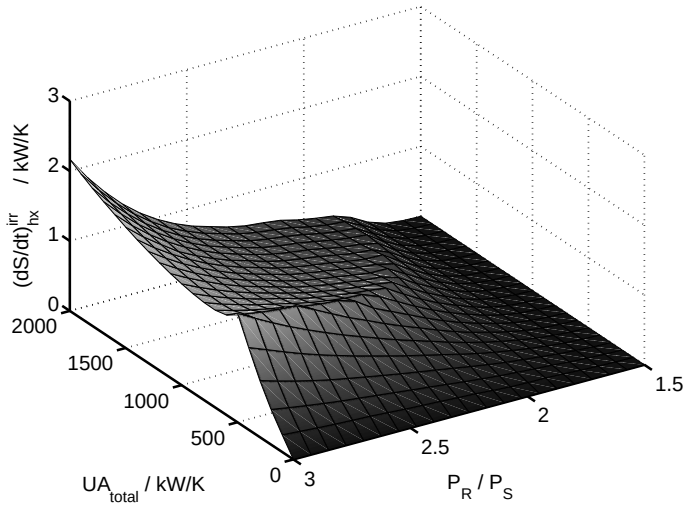

Figure 5.9. The entropy produced by internal heat transfer.

per Kelvin were used in both studies and Fig. 5.10 show the percent-wise reduction obtained by finding the optimal UA-distribution. Since columns with uniform UA-distribution did not exist for UA_{total} and $P_{\text{R}}/P_{\text{S}}$ in a certain region, a comparison could not be made for about one quarter of the calculated columns. When $UA_{\text{total}} = 0$ the two column types are the same, but as more UA_{total} became available, the difference in entropy production between the two column types increased. The largest reduction in entropy production was approximately 50% at the lowest pressure ratio and the highest total rates of heat transfer per Kelvin. Close to the area where the HIDiCs with uniform UA-distribution did not exist, we see that the relative difference in entropy production of the columns was smaller.

5.6 Discussion

5.6.1 The effect of internal heat transfer

To understand the features of the entropy production, distribution of UA, reflux ratio etc., it is advantageous to start with Eq. (5.1). It is the special internal heat transfer that distinguishes the HIDiC from the adiabatic and other columns. Thus, it is this heat transfer that is the key to understand the properties of the HIDiC. According to Eq. (5.1) there are two factors that influence the heat transfer: The rate of heat transfer per Kelvin and the temperature

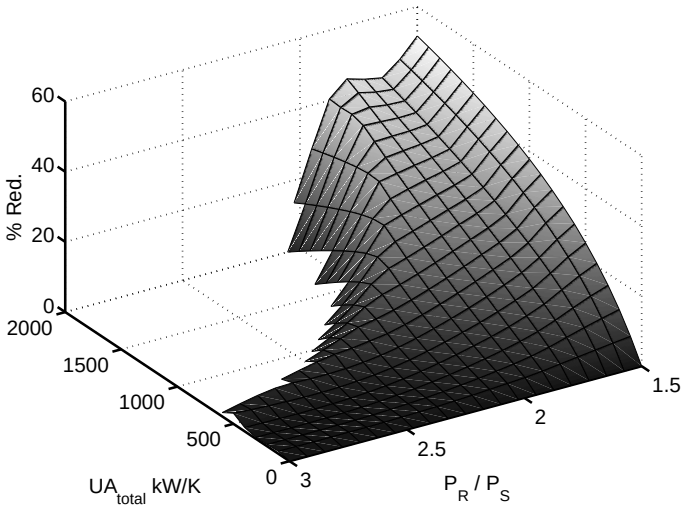

Figure 5.10. The reduction in entropy production obtained by allowing UA-distribution to be non-uniform.

difference between the trays in the rectifying and stripping section. The first is one of the parameters we have specified in each optimization while the latter is highly influenced by the pressure difference between the two sections. Since the pressure in the stripping section was constant, a given $P_{\mathrm{R}}/P_{\mathrm{S}}$ is the same as a specified $P_{\mathrm{R}} - P_{\mathrm{S}}$, and therefore a specified temperature difference between the trays in the two sections. In other words, an increasing UA_{total} as well as an increasing $P_{\mathrm{R}}/P_{\mathrm{S}}$ both lead to higher internal heat transfers.

Internal heat transfer affects the flows of liquid and vapor in the columns in a particular way. In the rectifying section the following energy balance was used on each tray:

$$\begin{aligned} Q_i &= V_i h_i^{\mathrm{V}} + L_i h_i^{\mathrm{L}} - V_{i+1} h_{i+1}^{\mathrm{V}} - L_{i-1} h_{i-1}^{\mathrm{L}} \\ &= V_i (h_i^{\mathrm{V}} - h_{i-1}^{\mathrm{L}}) - V_{i+1} (h_{i+1}^{\mathrm{V}} - h_i^{\mathrm{L}}) - D(h_i^{\mathrm{L}} - h_{i-1}^{\mathrm{L}}) \\ V_{i+1} &= V_i \left(\frac{h_i^{\mathrm{V}} - h_{i-1}^{\mathrm{L}}}{h_{i+1}^{\mathrm{V}} - h_i^{\mathrm{L}}} \right) - \frac{Q_i}{h_{i+1}^{\mathrm{V}} - h_i^{\mathrm{L}}} - D \frac{h_i^{\mathrm{L}} - h_{i-1}^{\mathrm{L}}}{h_{i+1}^{\mathrm{V}} - h_i^{\mathrm{L}}} \end{aligned} \tag{5.10}$$

where h is the molar enthalpy of a material stream. A very similar energy balance was used in the stripping section. The factor behind V_i in the above equation is close to unity if the temperatures and compositions do not change too much. Also, the factor behind D is small and positive. Assuming that

this is true for most of the optimized HIDiCs, it is easy to see that $Q_i < 0$ gives $V_{i+1} > V_i$ ($i < N/2$) and vice versa. This is exactly what is observed in Fig. 5.5 where increased heat transfer gave a vapor flow that increased down the rectifying section ($Q_i < 0$) and decreased down the stripping section ($Q_i > 0$). This behavior is typical for the HIDiC, but also for diabatic columns in general (De Koeijer et al. 2004b). Varying mass flow rates must be considered in their design.

5.6.2 The entropy production in the HIDiC

The best way to explain the shape of the total entropy production surface, Figs. 5.2 and 5.3, is to study each of its three contributions given in Figs. 5.7-5.9. In columns with UA_{total}=0 or $P_{\text{R}}/P_{\text{S}}$=0, most of the entropy was produced by the external heat transfer (in reboiler and condenser). It is not surprising that most of the reduction in the total entropy production at either low values of UA_{total} or $P_{\text{R}}/P_{\text{S}}$ was found in the entropy produced by the reboiler and condenser. This entropy production, shown in Fig. 5.7, was reduced from nearly 2.5 kW/K to 0.5 kW/K when UA_{total} and/or $P_{\text{R}}/P_{\text{S}}$ increased somewhat from their lowest values. Clearly, this is connected to the material flows through the condenser and reboiler. The three vapor flow profiles shown in Fig. 5.5 indicates that the material flows in the top and bottom of the columns decreased, as the heat transfer increased. The reflux ratio in Fig. 5.6 also shows that as the heat transfer between the two sections increased, the reflux ratio dropped to zero. For the highest values of UA_{total} and $P_{\text{R}}/P_{\text{S}}$ the reflux ratio increased again, but in this part the vapor flow through the reboiler became zero instead. It is helpful to divide the $UA_{\text{total}} - P_{\text{R}}/P_{\text{S}}$-space in two: One region where both RR and V_{N+1} are non-zero (low heat transfer), and one region where RR or V_{N+1} are zero (high heat transfer).

As the internal heat transfer increased, the entropy produced by heat and mass transfer between the liquid and vapor phase increased. Especially after crossing into the region where RR or V_{N+1} were zero, this entropy production became dominating (Fig. 5.8). Since Eq. (5.3) is of the same form as the energy balance, Eq. (5.10), this is also what we would expect. Columns with vapor flows that increased toward the middle of the column and then decreased toward the bottom, produced more entropy (in the same way more heat is released or consumed in each section). Note that the increased entropy production due to heat and mass transfer between the two phases was not caused by the increased $\sum QX$ since this term is included in Eq. (5.3) with a minus.

The entropy produced by the internal heat transfer, $\sum QX$, is plotted in Fig. 5.9 and shows that it increased with increasing heat transfer, but as RR became zero a sharp ridge was observed in the entropy production surface. To see what caused this sudden change we can look at the UA-distribution and how it varied with UA_{total} at $P_{\text{R}}/P_{\text{S}}$=2.18 shown in Fig. 5.4. For small values of UA_{total} only one or two pair of trays near the condenser and reboiler were active transferring heat. As UA increased, the same pair of trays were still the only ones active. When UA_{total} reached about 900 kW/K more trays started to become active. This happened at the same UA_{total} as the reflux ratio became zero. An important conclusion emerges: It seems that increasing the heat transfer close to the reboiler and condenser, is the best way to reduce the duty in the reboiler and condenser themselves and thus the best way to reduce their entropy production. Adding to UA_{total} beyond this value required UA to relocate itself slightly away from the top and bottom pair of trays, to avoid the material flows becoming negative at the ends of the column! Consequently, additional heat transfer must then occur in the middle of the rectifying/stripping section. The sudden change from end-dominated to center-dominated heat transfer caused the entropy produced by the internal heat transfer to change its behavior, see Fig. 5.8.

It is now easy to explain the shape of the entropy production surface in Fig. 5.2 through its three contributions. Generally speaking, the entropy produced by the external heat transfer decreased as the internal heat transfer increased, while the other two contributions to the entropy production increased. The minimum in the total entropy production observed in Fig. 5.2 came as a result of a trade-off among the three entropy producing phenomena, and is a general feature of HIDiCs, independent of which binary mixtures are separated. As the total rate of heat transfer increased, the minimum was shifted toward lower pressure ratios. It is probable that the minimum will go asymptotically toward a certain value of $P_{\text{R}}/P_{\text{S}}$ when $UA_{\text{total}} \to \infty$. Furthermore, when comparing the optimized HIDiCs with the corresponding conventional distillation column it is clear that only certain combinations of UA_{total} and $P_{\text{R}}/P_{\text{S}}$ give columns with lower entropy production. This is especially clear in Fig. 5.3 from which we can see that low and high pressure ratios give columns that perform badly. As the total rate of heat transfer increased, the feasible range in pressure ratios became narrower.

To summarize so far, we have found the following characteristics of the optimal HIDiCs. The internal heat transfer in the HIDiC is sensitive to UA_{total} and $P_{\text{R}}/P_{\text{S}}$, and HIDiCs were better than the adiabatic counterparts in terms

of entropy production, only for a range of values of these parameters. In the region where the entropy production was at its lowest, the shape of the UA-distribution changed from end-dominated to center-dominated. However, the minimum of the entropy production, Figs. 5.2 and 5.3 was very flat. This means that a potential reduction in entropy production can be realized with many kinds of UA-distributions, within the appropriate range of allowed values. The simplest realization of the results is then to allow for heat transfer only between the trays closest to the top and bottom. In this manner, one may also better take into account the observation that the vapor flows always increased greatly toward the middle of the column. This is further discussed in the next subsection. The result, that heat should only be transferred close to the reboiler and condenser, was also found for optimum diabatic columns (Schaller et al. 2001, De Koeijer et al. 2004b).

5.6.3 The optimal feed tray and the varying mass flows

In all the optimizations carried out, the optimal feed tray was found at tray number 11, which was the topmost tray in the stripping section. The optimal location of the feed tray depends on the feed and product compositions and should in general be located on trays where the composition of the feed is close to the composition on the tray. Since our product specifications were 0.995 and 0.005 for the top and bottom product, respectively, the composition around the middle of the column should be approximately 0.5, the same as the feed composition. This explains that the optimal feed tray location was constant and in the middle of the column.

The shape of the vapor flow profile in the optimal (and near-optimal) column, shown in Fig. 5.5, indicates that a column with changing diameter is required for optimal performance. We did not include any frictional losses (pressure drop in the two sections of the column) in the current model, but it is clear from the vapor flow profile that frictional losses may represent a substantial addition to the total entropy production of the HIDiCs, especially at high internal heat transfer. This may be counteracted by column design. By choosing a column diameter proportional to the vapor flow, the pressure drop and thus the additional entropy production may be reduced.

An interesting feature of the columns with values of UA_{total} and $P_{\text{R}}/P_{\text{S}}$ close to the optimal values, was that the UA-distribution could equally well be end-dominated or more uniform, without changing the overall performance much. This means again that we can choose a construction with heat transfer in the

bottom and top only, leaving $UA = 0$ in the middle of the column, avoiding the complications of a changing column diameter in the center part of the column, and excess material uses.

5.6.4 Is the optimum HIDiC feasible?

From a purely exergetic point of view, it is possible to conclude that the HIDiC is feasible, more so when the UA-distribution is variable than not. In Tab. 5.2 we have given the work and heat flows in the conventional column and in the optimal HIDiC. Each heat flow is associated with a certain temperature at which the heat was transferred. For the reboiler and condenser these temperatures were taken as the average temperature plus the temperature difference to the heat exchanger fluid (i.e. $(T_0 + T_1)/2 - \Delta T$ for the condenser). The transfer temperature in the extra heat exchanger used to cool the top product was found from the assumption that this unit was reversible ($T = Q/\Delta S_{\text{flow}}$). In an environment with temperature T_0=298 K the reduced entropy production means that the lost work was reduced with 456.1 kW. The detailed exergy content of the heat and work flows are given in Tab. 5.3. The exergy of all the material streams entering and leaving the system was constant and is not shown in the table. A premise for the results is that all heat flows, irrespective of their temperature and amounts, can be used to produce work in a Carnot engine that delivers heat to the surroundings. In some cases, we have obtained flows which differ from T_0 by only 1 K. In such cases one may question, the contribution of the stream's exergy content to Tab. 5.3. The real savings in lost exergy is therefore probably less than predicted by Tab. 5.3.

Table 5.2. Required work and heat flows in the conventional distillation column and the optimal HIDiC.

	Conventional column	Optimal HIDiC
Reboiler heat [kW]	5353.5 (at 413.1 K)	496.1 (at 413.1 K)
Condenser heat [kW]	-5840.3 (at 323.9 K)	-1487.8 (at 345.8 K)
Net compressor work [kW]	0	665.4
Extra heat exchange [kW]	0	-160.4 (at 364.7 K)

We saw above that the results pointed to a HIDiC with heat transfer preferably in the bottom and top of the column. The engineering difficulties in building a column with non-uniform UA-distribution are not greater than those encountered for a HIDiC with uniform UA-distribution. Perhaps the most crucial obstacle in the design and construction of a HIDiC is to have a big enough

Table 5.3. The exergy content corresponding to the work and heat flows in Tab.5.2 for a conventional column and the HIDiC.

	Conventional column	Optimal HIDiC
Reboiler exergy [kW]	1491.6	138.2
Condenser exergy [kW]	-467.0	-205.7
Net compressor work [kW]	0	665.4
Extra heat exchanger exergy [kW]	0	-29.4
Sum = Lost exergy [kW]	1024.6	568.5

total rate of heat transfer per Kelvin. There is a lower limit on UA_{total} of approximately 150 kW/K, below which the conventional column always had a lower entropy production than HIDIC. If we now assume that we share this area equally between the top and bottom pair of trays, each of the pair of trays has approximately 75 kW/K. With a heat transfer number as high as $U = 1000$ W/Km^2, the area of heat transfer must still be 75 m^2! This is a very big number, so even the lower limit value of UA_{total} may prove difficult to realize. Ways to introduce UA between pairs of trays have been proposed (Olujic et al. 2003, Nakaiwa et al. 2003).

According to Nakaiwa (2004) a HIDiC has been constructed and operated successfully with lower UA_{total} than the limit we have identified as the lower limit (approximately 150 kW/K scaled with the internal material flows). The discrepancy between this observation and the results of the present investigation may be sought in the model we have used. Clearly, there are several assumptions that can be changed, to improve the predictive abilities of our model. These are the assumptions of:

- Equilibrium between the liquid and vapor streams leaving each tray.
- No pressure drop through the column.
- No representation of the fluid dynamics on each tray.

Among the three, we consider the first one to be the serious one, see De Koeijer and Kjelstrup (2003). A nonequilibrium model is needed to have a quantitative description of distillation. Our model therefore gives only qualitative information. From the results, we can expect a trade-off in the total entropy production between different phenomena, and that there are upper and lower boundaries

on the feasible pressure ratios as well as a lower boundary on the total rate of heat transfer per Kelvin, but the actual numbers we obtain cannot be trusted.

5.6.5 Earlier results

The major difference between the HIDiCs studied here, and HIDiCs with constant UA on all trays (Røsjorde et al. 2004) is that physical solutions are now obtainable for *all* combinations of UA_{total} and $P_{\text{R}}/P_{\text{S}}$. When UA_{total} was evenly distributed, many combinations of UA_{total} and $P_{\text{R}}/P_{\text{S}}$ gave negative material flows and were thus impossible. By comparing the entropy production of the two types of columns, we observed that the HIDiC optimized with **UA** as variable always had the lowest entropy production (Fig. 5.10). This is a direct consequence of the additional degrees of freedom represented by the non-uniform UA-distribution. For high values of UA_{total} and low $P_{\text{R}}/P_{\text{S}}$ the reduction in entropy production was around 50%. This big difference was due to the HIDiC with uniform UA-distribution being very inefficient (back-transfer of heat). The reduction was closer to 10-20% around the region where the reflux ratio was zero. The entropy production of the optimal HIDiC with non-uniform UA-distribution was 17% lower than the optimal HIDiC with uniform UA-distribution.

It is reasonable that heat-integrated distillation column or diabatic columns with independent heat exchangers on each tray have the best theoretical second law energy efficiency. Diabatic columns with independent heat exchangers require, however, N available cold or hot streams at just the right temperatures. A more realistic column has heat exchangers in the rectifying and stripping section connected in series (Rivero 1993, Jimenez et al. 2003). The degrees of freedom are then reduced, making the column somewhat less efficient. Both these kinds of diabatic columns show, however, that additional heat exchange close to the reboiler and condenser is the most important step one can take to increase efficiency, leaving the central part of the column unchanged. A design which takes the characteristic features of a diabatic column into account, was proposed by De Koeijer et al. (2004b).

5.6.6 An improved design

The results presented for the HIDiC show, as do the earlier results (Røsjorde and Kjelstrup 2004, De Koeijer et al. 2004b), that the reboiler and condenser duties can be reduced by shifting duties to the nearby trays. However, due to HIDiC's construction, heat exchange is now introduced also in the center

of the column, where it is not needed, according to the analysis of diabatic columns! The unfortunate consequence is that HIDiC often will have a higher entropy production than diabatic columns investigated by Røsjorde and Kjelstrup (2004) (see Chapter 3). Mathematically speaking, the HIDiC has fewer degrees of freedom than the ideal diabatic column: The heat transferred internally in the HIDiC is a compromise between the heat ideally released/consumed in the rectifying and stripping section. In the diabatic column this is not so, and this explains their difference.

It seems that the direct thermal coupling in some systems hampers the performance of the HIDiC, and we therefore propose to modify the design by changing the way the rectifying and stripping section are integrated. Since both our present analysis and earlier results show that it is most effective to allow heat exchange close to the top and bottom of the column, a possible design is to integrate only tray 1 and N in the HIDiC. The original plate-to-plate design originally suggested by Nakaiwa et al. (1986) and our proposition for minimum integration are shown in Fig. 5.11.

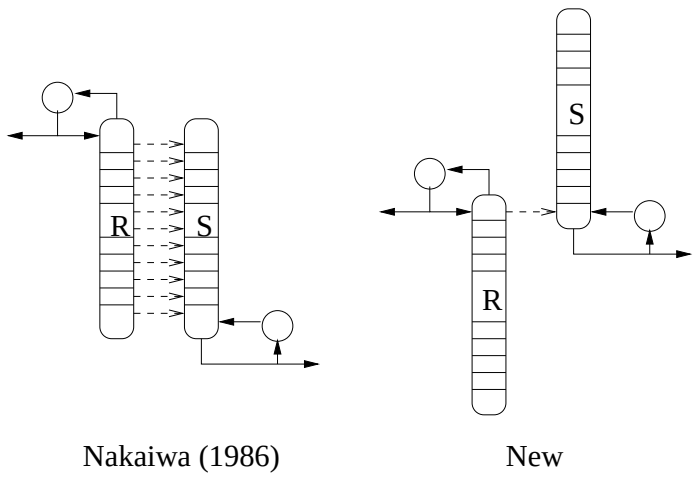

Figure 5.11. The original (Nakaiwa et al. 1986) and new configurations of the HIDiC.

We performed some initial calculations of the entropy production in some HIDiCs with heat integration between tray 1 and N only. For UA_{total}=2000 kW/K we found by trial and error that $P_{\text{R}}/P_{\text{S}}$=2.42 gave the lowest entropy production, equal to 1.42 kW/K. In the original design for heat-integration, the same UA_{total} gave an entropy production of 1.66 kW/K (cf. Section 5.5).

Our calculations also showed that HIDiCs with the new heat-integration did not have any upper bound on the pressure ratio for which the adiabatic column would be better than the HIDiC in terms of entropy production. A side-effect of this was that no lower bound on UA_{total} existed either. By allowing heat transfer between one pair of trays only, the heat transfer, according to Eq. (5.1), may be completely controlled by UA_{total} and $P_{\text{R}}/P_{\text{S}}$. This may be an advantage in practical design and may increase controllability. If more pair of trays are heat-integrated, this one-to-one relationship is lost. Other configurations, where the size of the rectifying and stripping section were different, have been studied in detail by Sun et al. (2003).

5.7 Conclusion

We have shown in this article that HIDiC columns may be constructed for a range of internal rates of heat transfer per Kelvin and pressure ratios, which give a better second law performance than adiabatic columns that produce the same products. For a particular total rate of heat transfer per Kelvin, it was possible to reduce the entropy production of an adiabatic column with 48%, to 1.66 kW/K, assuming that there is equilibrium between vapor and liquid at the outlet of each tray. It remains to see that this heat transfer coefficient and heat transfer area can be realized in practice, however. The results extend earlier results for HIDiCs with constant UA and similar results found for diabatic columns (De Koeijer et al. 2004b, Jimenez et al. 2003).

We conclude that HIDiC may preferably have its internal heat transfer in the bottom and top of the column, thereby minimizing complications given by mass flow rates that vary with internal heat transfer. A lower bound on UA_{total}=150 kW/K was found. Below this value, no pressure ratio gave the HIDiC lower entropy production than the adiabatic column.

The results showed that the direct plate-to-plate heat-integration in the HIDiC leads to internal heat transfer between trays that should have no heat transfer. As a result, the HIDiC might have a lower efficiency than other diabatic distillation columns. In order to improve the energy efficiency of the HIDiC in a simple way, we propose a new design where heat-integration is only allowed between the topmost tray in the rectifying section and the bottommost tray in the stripping section (between tray 1 and N, respectively). Initial calculations show that such columns may obtain even lower entropy production than the plate-to-plate HIDiC.

More work is needed to bridge the gap between the theoretical model and the nonequilibrium performance of distillation columns in general.

Acknowledgments

Audun Røsjorde thanks the Energy-efficient Chemical Systems Group at the National Institute of Advanced Industrial Science and Technology (AIST), Tsukuba, for their generous hospitality and support.

Statoil's VISTA program is thanked for the financial support to Audun Røsjorde.

Chapter 6

Minimizing the entropy production in two heat exchangers and a reactor

Audun Røsjorde, Eivind Johannessen and Signe Kjelstrup

Department of Chemistry
Norwegian University of Science and Technology
N-7491 Trondheim, Norway

This paper was published in
Proceedings of ECOS 2003, Copenhagen 2003, Denmark.

Abstract

A plug-flow reactor for dehydrogenation of propane with a heat exchanger placed before and after was studied. The heating policy and the reactor length that minimized the entropy production of the three units was found. The state of the inlet stream, and the temperature and amount of propylene in the outlet stream, were kept constant during the optimization. The total entropy production rate was reduced with 19.5% compared to a reference case. This reduction may in different ways lead to lower operating costs. A characteristic property of the optimized process was that the reactor should be run almost adiabatically, leaving all the heating and cooling to the heat exchangers. The results also showed that a constant ambient temperature profile in the reactor was equally good as a profile that was allowed to vary along the reactor in an optimal way.

6.1 Introduction

We have over the last years developed procedures to minimize the entropy production of exothermic and endothermic reactors that exchange heat via the reactor walls. The ammonia synthesis (Nummedal et al. 2003) and the steam reforming process (Nummedal et al. 2002) were simulated, and it was shown that substantial savings in lost work was possible. To have heat exchange through the reactor walls, need not be the most favorable way of operation, however. In addition, an ambient temperature profile that changes in a specific way along the reactor may be difficult, if not impossible, to realize. The aim of this work is to analyze practical alternatives to the ideal path of operation presented before (Nummedal et al. 2003, 2002). The results will be important to the way the reactor should be implemented in a bigger process (see Chapter 7).

The first interesting question to ask is whether it pays better to heat the reactants before the reactor inlet, or heat along the reactor. Our studies have all showed that the inlet conditions were important for a reduction in lost work, see e.g. Kjelstrup et al. (2000), but by changing the inlet conditions, one changes the environment such that a new calculation of the lost work should be done to include these changes. So far, we have only optimized single process units. We shall now move one step further and optimize three process units: A heat exchanger, a reactor and a heat exchanger in series. A similar problem was analyzed for distillation (Agrawal and Herron 1997).

Secondly, if one chooses to exchange heat along the reactor wall, what is a the practical way to do this? Should we keep the reactor as one unit, or

divide it into two or more units, each with a constant ambient temperature? Moreover, which length should each unit have? We have found that the length of the reactor is an important variable in the optimization (Johannessen and Kjelstrup 2002).

The problems presented above shall be discussed in this article, using a simplified propane dehydrogenation reactor as example. This reactor is endothermic. We shall see that different paths of operation for a series of three units give significantly different entropy productions, even if the systems produce the same amount of propylene, have the same inlet stream, and the same temperature of the outlet stream. As free variables in the optimization we chose the temperature between the first heat exchanger and the reactor, T_1, the ambient temperature, T_a, along the reactor and the reactor length, L.

6.2 The system

We study the process in Fig. 6.1. The central unit is a fixed bed catalytic reactor where the following reactions take place:

$$C_3H_8 = C_3H_6 + H_2 \quad \text{(I)}$$
$$C_3H_8 = C_2H_4 + CH_4 \quad \text{(II)}$$

Both reactions consume propane. The first reaction is the dehydrogenation of propane to propylene (propene), which is the desired product. The second reaction is a cracking reaction where the unwanted byproducts methane and ethylene (ethene) are produced. The reaction rates of the two reactions are given in the appendix. There is a heat exchanger on each side of the reactor.

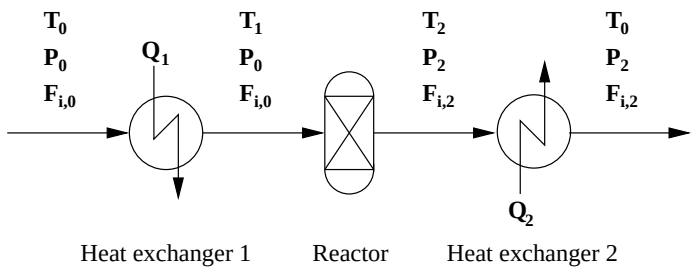

Figure 6.1. Flow sheet of the process.

Heat exchanger 1 heats the reactants and heat exchanger 2 cools the products. Combined, the three units are a small part of a propane dehydrogenation plant.

6.3 Theory

6.3.1 Heat exchanger model

A very simple model for the heat exchangers is adopted. We assume the following:

- Shell-and-tube exchanger with counterflow.
- No pressure drop.
- Constant heat transfer coefficient.
- Constant heat capacity in both hot and cold streams.
- Constant difference in temperature between the hot and cold side.

The last assumption is a simple way to make sure we have a certain pinch for the heat transfer. Based on these assumptions, a total heat balance can be written for the hot side of the heat exchanger:

$$Q = F^{\mathrm{h}} h C_p^{\mathrm{h}} (T_{\mathrm{out}}^{\mathrm{h}} - T_{\mathrm{in}}^{\mathrm{h}}) \tag{6.1}$$

where Q is the heat transferred from the hot to the cold side, F^{h} is the flow rate, C_p^{h} is the heat capacity and T^{h} is the temperature. Superscript 'h' refers to the hot side. Since this heat is transferred to the cold stream, we write a similar balance for that side, only with opposite sign:

$$Q = -F^{\mathrm{c}} C_p^{\mathrm{c}} (T_{\mathrm{out}}^{\mathrm{c}} - T_{\mathrm{in}}^{\mathrm{c}}) \tag{6.2}$$

where superscript 'c' refers to the cold side.

The entropy of a stream depends in general on temperature, pressure and composition. Only the temperature changes in the heat exchangers. It is therefore sufficient to write the entropy in each stream as:

$$s = s_0 + \int_{T_0}^{T} \frac{C_p}{T} dT \tag{6.3}$$

where s_0 is the molar entropy at some reference temperature T_0 and the given pressure and composition. A total entropy balance over the four streams in

and out of the heat exchanger gives the entropy production rate, $(\frac{dS}{dt})^{\mathrm{irr}}_{\mathrm{hx}}$:

$$\begin{aligned}(\frac{dS}{dt})^{\mathrm{irr}}_{\mathrm{hx}} =&(F^{\mathrm{h}}s^{\mathrm{h}} + F^{\mathrm{c}}s^{\mathrm{c}})_{\mathrm{out}} - (F^{\mathrm{h}}s^{\mathrm{h}} + F^{\mathrm{c}}s^{\mathrm{c}})_{\mathrm{in}} \\ =&F^{\mathrm{h}}(s^{\mathrm{h}}_{\mathrm{out}} - s^{\mathrm{h}}_{\mathrm{in}}) + F^{\mathrm{c}}(s^{\mathrm{c}}_{\mathrm{out}} - s^{\mathrm{c}}_{\mathrm{in}}) \\ =&F^{\mathrm{h}}C^{\mathrm{h}}_p \int_{T^{\mathrm{h}}_{\mathrm{in}}}^{T^{\mathrm{h}}_{\mathrm{out}}} \frac{1}{T} dT + F^{\mathrm{c}}C^{\mathrm{c}}_p \int_{T^{\mathrm{c}}_{\mathrm{in}}}^{T^{\mathrm{c}}_{\mathrm{out}}} \frac{1}{T} dT \\ =&F^{\mathrm{h}}C^{\mathrm{h}}_p \ln \frac{T^{\mathrm{h}}_{\mathrm{out}}}{T^{\mathrm{h}}_{\mathrm{in}}} + F^{\mathrm{c}}C^{\mathrm{c}}_p \ln \frac{T^{\mathrm{c}}_{\mathrm{out}}}{T^{\mathrm{c}}_{\mathrm{in}}}\end{aligned} \tag{6.4}$$

We are also interested in the corresponding heat transfer area, which can be found from (McCabe et al. 1993):

$$Q = \int_A U(T^{\mathrm{h}} - T^{\mathrm{c}})dA = UA(T^{\mathrm{h}} - T^{\mathrm{c}}) \tag{6.5}$$

where A is the area and U is the heat transfer coefficient. Here, we have used the assumption of constant U and $(T^{\mathrm{h}} - T^{\mathrm{c}})$. Since we does not include any frictional effects in the model, it does not matter how the area is distributed in the heat exchanger (i.e one large tube or many small tubes). It should be noted that the reactions are frozen in the heat exchangers, due to absence of catalyst.

6.3.2 Reactor model

The reactor is a tube with diameter D and length L. It is filled with catalyst pellets with diameter D_{p} and density ρ_{c}. The fraction of void in the reactor is ϵ, giving an effective density of $\rho^{\mathrm{eff}}_{\mathrm{c}} = \rho_{\mathrm{c}}(1-\epsilon)$.

We use a plug flow reactor (PFR) model (Froment and Bischoff 1990). The conservation equations describing the reactor are the energy, momentum and mass balances.

Energy balance:

$$\frac{dT}{dz} = \frac{\pi D J'_{\mathrm{q}} - \Omega\rho^{\mathrm{eff}}_{\mathrm{c}} \sum_i r_i \Delta_{\mathrm{r}}H_i}{\sum_i F_i C_{p,i}} \tag{6.6}$$

where z is the axial position, Ω is the cross-sectional area, r_i is the reaction rate of reaction i and $\Delta_{\mathrm{r}}H_i$ is the enthalpy of reaction i. The heat flux through the reactor wall is $J'_{\mathrm{q}} = U(T_{\mathrm{a}} - T) \approx UT^2(\frac{1}{T} - \frac{1}{T_{\mathrm{a}}})$ (if T and T_{a} both are high).

Momentum balance (Erguns equation):

$$\frac{dP}{dz} = \frac{u}{D_\mathrm{p}}\frac{(1-\epsilon)}{\epsilon^3}\left(- \frac{150\mu}{D_\mathrm{p}}(1-\epsilon) + 1.75\rho u\right) \tag{6.7}$$

where P is the pressure, u is the flow velocity, μ is the flow viscosity and ρ is the gas density.

Mass balances:

$$\frac{d\xi_i}{dz} = \frac{\Omega\rho_\mathrm{c}^\mathrm{eff}}{F_\mathrm{A}^0} r_i \tag{6.8}$$

where ξ_i is the conversion of the reference species in reaction i and F_A^0 is the inlet flow of the reference species to the reactor.

In accordance with the conservation equations, Eqs. (6.6)-(6.8), the entropy production rate in a PFR have three contributions: The reactions, the heat transfer through the walls and the pressure drop (frictional loss). The entropy produced locally, σ, by these phenomena are described by nonequilibrium thermodynamics (De Groot and Mazur 1984, Kjelstrup and Bedeaux 2001):

$$\sigma_\mathrm{rx} = \Omega\rho_\mathrm{c}^\mathrm{eff}\sum_i r_i\left(- \frac{\Delta_\mathrm{r}G_i}{T}\right) \tag{6.9}$$

$$\sigma_\mathrm{q} = \pi D J_\mathrm{q}'\left(\frac{1}{T} - \frac{1}{T_\mathrm{a}}\right) \tag{6.10}$$

$$\sigma_\mathrm{p} = -\Omega u\frac{1}{T}\frac{dP}{dz} \tag{6.11}$$

where subscripts 'rx', 'q' and 'p', denotes the entropy produced by reaction, heat transfer and pressure drop, respectively. The total entropy production rate is the integral of the sum of the above terms along the reactor:

$$(\frac{dS}{dt})_\mathrm{rx}^\mathrm{irr} = \Omega\int_{z=0}^{L}(\sigma_\mathrm{rx} + \sigma_\mathrm{q} + \sigma_\mathrm{p})dz \tag{6.12}$$

6.4 Calculations

6.4.1 Conservation equations

To solve the conservation equations for the reactor, Eqs. (6.6)-(6.8), we used a standard ordinary differential equation (ODE) solver from Matlab R13, MathWorks Inc. Given a set of initial values for T, P, ξ_1 and ξ_2, the function *ode15s*

integrates the differential equations from one position to another. To solve the reactor equations, we thus had to specify the properties at the reactor inlet and set a wanted reactor length. The ambient temperature is not described by any equation, so it must also be provided. In order to use Eq. (6.8), a reference component must be defined. We used propane as a reference; Both reaction rates and conversions are given in terms of consumption of propane. In the reactor model we used a constant heat transfer coefficient, U=57 W/Km^2 (Fogler 1992), diameter D=0.2 m, catalyst density ρ_c=984.4 kg/m^3, void ϵ=0.45 and catalyst pellet diameter D_p=4.57 mm.

The model of the heat exchanger was trivial to solve compared to that of the reactor. We specified inlet and outlet values of T in the process stream, together with the flow and composition. Depending on whether to add or remove heat, we calculated Q (duty) from Eq. (6.1) or (6.2). Implicitly, the assumptions done in the development of the heat exchanger model, forces the product of flow rate and heat capacity for the hot and cold stream to be equal. Since we know the properties of the process stream, we automatically have the properties of the heat exchanger medium. Knowing the difference in temperature between hot and cold side through the heat exchanger gives us A. For this study, we chose a difference of 30 K (the pinch).

6.4.2 The optimization

As free variables in the optimization we chose the temperature between the first heat exchanger and the reactor, T_1, the ambient temperature, T_a, along the reactor and the reactor length, L. We studied two different kinds of T_a-profiles in the optimizations.

In the first approach, we used *optimal control theory* to identify the optimal value of T_a at every position along the reactor (Bryson and Ho 1975), giving us the T_a-profile. This resulted in continuously varying profiles that could be difficult to implement in practice. In the other approach we divided the reactor into new reactors of varying length coupled in series, each with a constant T_a. In the optimization of such systems, we prescribed a number of reactors, and introduced T_a and L of each as free variables.

Independent of which type of T_a-profile we searched for, the objective function was the total entropy production of the process:

$$(\frac{dS}{dt})^{\text{irr}}_{\text{tot}} = (\frac{dS}{dt})^{\text{irr}}_{\text{hx},1} + (\frac{dS}{dt})^{\text{irr}}_{\text{rx}} + (\frac{dS}{dt})^{\text{irr}}_{\text{hx},2} \tag{6.13}$$

As a benchmark we used the following *reference process*. The first heat exchanger elevated the process stream temperature from 300 K to 900 K. The process stream then entered a 10 m long reactor with a constant ambient temperature of 1000 K. Finally, the products from the reactor were cooled to 300 K again. In all calculations, the input process stream was characterized by T_0 = 300 K, P_0 = 2 bar and $F_{\mathrm{T},0}$ = 1 mol/s. The mole fractions of C_3H_8 was 0.80, while for the other four components, C_3H_6, H_2, C_2H_4 and CH_4, it was 0.05.

We kept the state of the inlet stream to heat exchanger 1 fixed during the optimization. The temperature and the molar flow of propylene out from heat exchanger 2 were also fixed (at the same values as the reference process). The outlet pressure and flow rate of other components out of heat exchanger 2, were not fixed.

The fixed propylene production makes this a constrained nonlinear optimization problem. We used the tool *fmincon* in Matlab to minimize Eq. (6.13).

The following two optimizations were done, to compare with the reference process:

1. The continuous optimal ambient temperature profile was found. This part of the calculation was similar to what we have done before for other reactors (Nummedal et al. 2003, 2002), except that now the results were also combined with those of the two heat exchangers to achieve the optimal state for the three process units.
2. *One* reactor with a constant ambient temperature.

Temperature dependent expressions for C_p of each component were found in Daubert and Danner (1992). Standard values for the enthalpy of formation and absolute entropies were found in Weast and Astle (1982). From these values and the expressions for C_p, we calculated $\Delta_{\mathrm{r}}H$ and $\Delta_{\mathrm{r}}G$.

6.5 Results

The results for the reference process are given in Fig. 6.2. The reaction mixture temperature and the ambient temperature along the reference reactor are shown. The inlet and outlet temperatures of the reference reactor are given in Tab. 6.1, together with the pressure drop. The production of propylene was 0.258 mol/s. Details for the two heat exchangers heating the inlet stream and

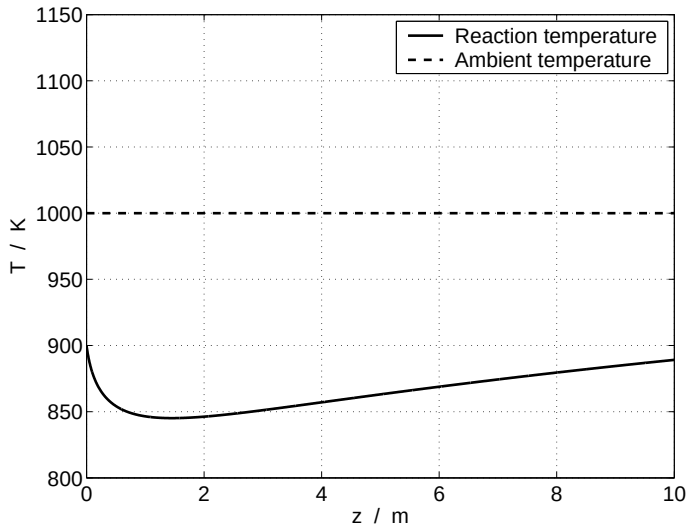

Figure 6.2. Temperatures in the reference reactor.

cooling the outlet stream of the reactor, are given in Tabs. 6.2 and 6.3.

The optimization results for Case 1 are shown in Fig. 6.3, while Fig. 6.4 shows the results for Case 2. The inlet and outlet reactor temperatures for Case 1 and 2 are given in Tab. 6.1. The optimal reactor lengths and corresponding pressure drops are also presented in Tab. 6.1.

Table 6.1. Inlet and outlet temperatures, length and pressure drop in the reactor.

Case	T_1 (K)	T_2 (K)	L (m)	ΔP (bar)
Ref.	900	889	10.0	-0.63
1	1095	883	1.97	-0.12
2	1102	893	1.86	-0.11

Heat exchanger areas times heat transfer coefficient are given in Tab. 6.2. A typical value for U in tubular heat exchange is 100 W/K m^2 (Perry and Green 1997). Since UA for all cases is in proximity of 2000-3500 W/K, we see that A is approximately 20-35m^2.

The heat transferred in the different units of the process, along with the total heat transfer is given in Tab. 6.3. Since the inlet temperature in the reac-

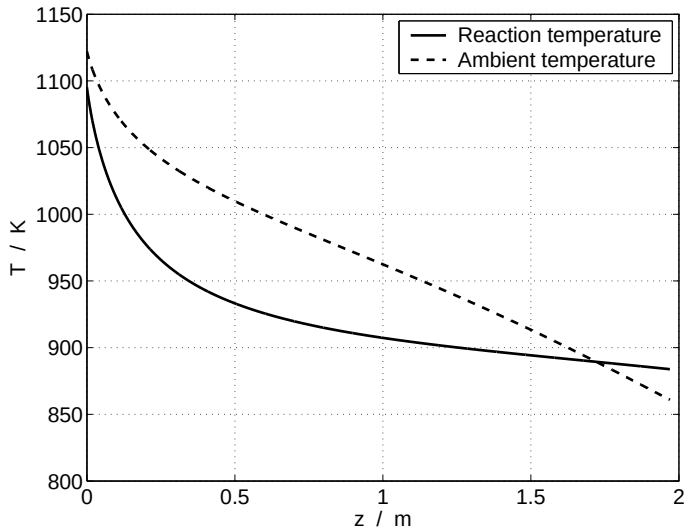

Figure 6.3. Optimal temperature profiles with continuous ambient temperature (Case 1).

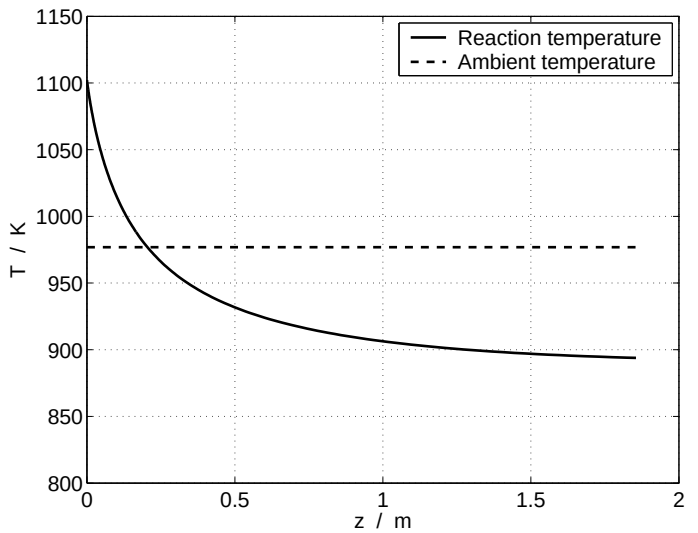

Figure 6.4. Optimal temperature profiles with 1 reactor (Case 2).

Table 6.2. Heat transfer coefficient times area for the two heat exchangers (W/K).

Case	UA_1	UA_2
Ref.	2300	2280
1	3380	2260
2	3430	2310

tor increases in the two optimized cases, the duty of the first heat exchanger increases accordingly. The reactor outlet temperature, on the other hand, is almost identical in the three cases, thus the duty of the second heat exchanger is nearly constant. Due to the increased reactor inlet temperature in Case 1 and 2, the heat supplied along the reactor is much smaller. The net effect of this is a reduced overall need for heating in the process.

Table 6.3. Heat transferred in the different units and in total (kW).

Case	Q_1	Q_{rx}	Q_2	Q_{tot}
Ref.	69.0	41.6	-68.4	42.2
1	101.5	3.1	-67.8	36.8
2	102.7	2.9	-69.3	36.3

The entropy production rate in the heat exchangers and for the different phenomena in the reactor, is presented in Fig. 6.5. The reference process had a total entropy production rate of 33.7 W/K. The case with a non-constant (Case 1) ambient temperature had the lowest value 27.1 W/K, while the case with constant temperature (Case 2) had 27.3 W/K. This gave a reduction in the produced entropy of approximately 19.5%. Cases with the reactor divided into two or more new reactors had, surprisingly enough, practically the same entropy production. The pressure variation (almost linear) and the variation in the conversion of propane through the reactor were not particularly interesting, and are not shown.

6.6 Discussion

6.6.1 The reference process

The temperature profile of the reactor in Fig. 6.2 is as expected, with a constant, relatively low temperature in the furnace chamber. We see a minimum in reaction temperature profile close to the inlet. This can be explained by the relatively large heat consumption in this section, where the reaction rates are

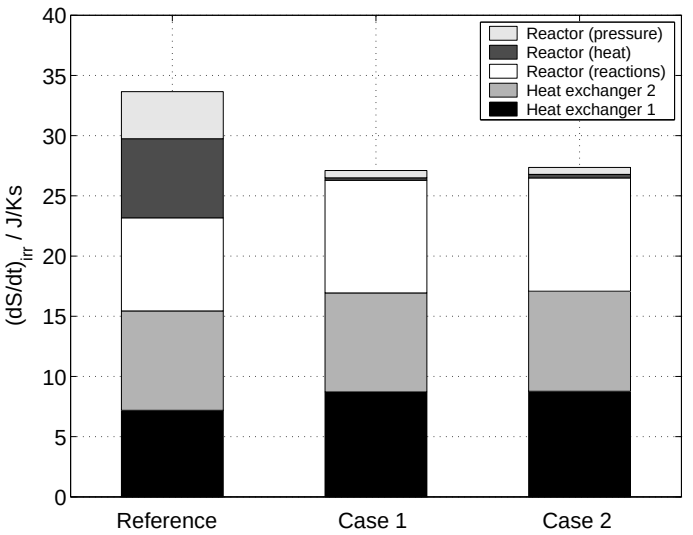

Figure 6.5. The entropy production rates from different phenomena.

high (the feed is far from equilibrium).

Both chemical reactions use propane, but reaction I somewhat more than reaction II. Only reaction I produce propylene, and the production of propylene is quite low. The reaction rate of reaction II is not based on experimental data, since we were not able to find any expressions reported in the literature. Instead, we constructed an expression of the same form as for a first-order, reversible, gas-phase reaction (Froment and Bischoff 1990). This expression was tuned so that the consumption of propane was of the same order of magnitude as the consumption in reaction I. To capture the behavior of the product purification part of a propane dehydrogenation plant, byproducts must be present in the outlet stream from the reactor. As this small process will be part of a plant, reaction II was included.

The pressure drop was low, even though the reactor is 10 m long. This is mainly due to the relatively wide diameter (0.2 m), reducing the flow velocity.

There are significant contributions to the entropy production rate from all relevant phenomena (see Fig. 6.5).

6.6.2 Case 1

The continuous optimal ambient temperature that is shown in Fig. 6.3 starts at a high value (about 1100 K), which is 27 K higher than the reaction mixture. It then sinks almost linearly through the system, and has a crossover with the reaction temperature at 3/4 of the reactor length. At the outlet, the ambient temperature is 23 K lower than the reaction temperature. The reaction temperature behaves somewhat differently, with a strong decrease in the beginning and an almost flat part in the end of the reactor.

Johannessen and Kjelstrup (2002) proved analytically that when a reactor is optimized with no temperature dependent constraints on either inlet or outlet, the reaction and ambient temperature will be equal at the ends. That we in this work find a discrepancy between T and T_{a} at the inlet and outlet, is due to our extended objective function. The difference in temperature mirrors the effects the heat exchangers have on the behavior of the objective function.

The crossing of the ambient and reaction temperature is surprising. This means that heat is added to the reactor the first 3/4 of the reactor length, while it is removed in the last 1/4. This must be seen as a way to minimize the entropy produced by heat transfer, while still maintaining the wanted chemical production.

Compared to the reference case, more entropy is produced in the heat exchangers and by the reaction. There is however, a net reduction due to the nearly vanishing entropy production caused by the heat transfer and pressure drop in the reactor. The reduction in the difference in inverse temperature across the reactor wall, and a large reduction of the reactor length is the source to these improvements.

6.6.3 Case 2

The reaction temperature profile of Case 2, shown in Fig. 6.4, exhibits the exact same behavior as the reaction temperature in Case 1. This is very surprising, considering the different nature of the ambient temperature profile, but can be explained as follows. At such high temperatures, the terms $\frac{1}{T}$ and $\frac{1}{T_{\mathrm{a}}}$ are small, resulting in a small driving force for heat transfer. This greatly reduce the contribution to the total entropy production rate from the heat transfer described by Eq. (6.10). Since this term becomes so small (see Fig. 6.5), the total entropy production rate is rather insensitive to the shape of the T_{a}-profile, as long as the T- and T_{a}-profiles are high enough.

Also in this case, the reactor length is substantially reduced, effectively eliminating the pressure drop and its corresponding entropy production. However, to reduce the length, requires the reaction rate of reaction I to be higher. This is achieved by the increased inlet temperature.

6.6.4 General perspectives

The insensitivity toward the shape of the T_a-profile that we observe in the optimization, means that it is, in this system, little to gain by dividing the reactor into several shorter reactors. This fact is also supported by the almost identical total entropy production rates of Case 1 and 2 (see Fig. 6.5). To back this up further, we did several more optimizations where the reactor was split into an increasing number of reactors with different T_a's. As expected, the entropy production rate of these, lay between those from Case 1 and 2. The case with the most reactors (20 short reactors), had a total length that summed up the reactor length of Case 1, with T_a's approximating the continuous profile of Case 1.

From a process implementation view, but also from a numerical view, it is advantageous to have only one reactor with a constant T_a-profile. However, this scenario is highly dependent on the demands put on the process and the system parameters. Higher U would make it more favorable to transfer heat along the reactor, instead of in the heat exchangers. In the limit of infinitely large U, heat would *only* be transferred along the reactor. If U was 0, *no* heat would be transferred along the reactor, only in the heat exchangers. In a pure reactor optimization done for a different system (Johannessen and Kjelstrup 2002), it was found that at least a couple of reactors in series, was needed to take out the possible reduction in the entropy production rate.

6.7 Conclusion

We have optimized a series of three process units, two heat exchangers and one propylene producing reactor. The units were put together to make possible an answer to the following question: Given that the production of propylene is constant, the inlet streams are the same, and the inlet and outlet temperatures are the same, what is the optimal inlet temperature to the reactor, its cooling conditions and its length?

Compared to the reference process, all optimal processes had shifted the heat transfer from along the reactor to the heat exchangers upstream and down-

stream. In fact, the reactor should preferably be operated nearly adiabatically. In other words: It is optimal to heat the mixture that shall react, before the reactor, and cool it after the reactor, in terms of 2nd law efficiency. The savings in entropy production rate translates in this case into the following three improvements:

- Lower heating requirement for the total process.
- Lower ambient temperature.
- Lower pressure drop (more mechanical work out).

The possible saving that is feasible, about 20 % is substantial. Since the process is running at high temperatures, reduced heating requirements means less fuel spent, while a lower pressure drop in the reactor means that more mechanical work can be taken out (or less work added) later in the process. These things may reduce the operating cost of the process. We also observe that the optimal reactor length is only 1/5 of the reference case. This is clearly an advantage, but it also suggests that the reference reactor is too long for production of only 0.26 mol/s propylene.

Appendix

The reaction rate for reaction I, which is the main reaction for propane dehydrogenation, is (Loc et al. 1996):

$$r_{\mathrm{I}} = k_0 \left(1 - \frac{P_{\mathrm{C_3H_6}} P_{\mathrm{H_2}}}{P_{\mathrm{C_3H_8}} K_{\mathrm{I}}}\right) \frac{P_{\mathrm{C_3H_8}}}{P_{\mathrm{H_2}}^{0.5} + k_1 P_{\mathrm{C_3H_6}}} \tag{6.14}$$

where K_{I} is the equilibrium constant of reaction I and k_0 and k_1 is:

$$k_0 = 0.3874 e^{-\frac{2950}{T}} \tag{6.15}$$

$$k_1 = 3.4785 \cdot 10^{-8} e^{\frac{17200}{T}} \tag{6.16}$$

Based on the standard expression for the reaction rate of a reversible reaction in gas phase, we have chosen the following reaction rate for reaction II:

$$r_{\mathrm{II}} = k_2 \left(1 - \frac{P_{\mathrm{C_2H_4}} P_{\mathrm{CH_4}}}{P_{\mathrm{C_3H_8}} K_{\mathrm{II}}}\right) P_{\mathrm{C_3H_8}} \tag{6.17}$$

where K_{II} is the equilibrium constant of reaction II and k_2 is:

$$k_2 = 6.67 \cdot 10^{-8} e^{-\frac{2000}{T}} \tag{6.18}$$

The value of k_2 and its temperature dependency was chosen to give the observed behavior of the reference reactor. Both equilibrium constants were calculated from the expression derived for $\Delta_r G_0$.

Chapter 7

Minimizing the entropy production in a chemical process

Audun Røsjorde, Signe Kjelstrup,
Eivind Johannessen and Roger Hansen#

Department of Chemistry
Norwegian University of Science and Technology
N-7491 Trondheim, Norway

#: Statoil Research Center
N-7053 Ranheim, Norway

This paper has been proposed for
ECOS 2005, Trondheim

Abstract

We minimize the total entropy production of a process designed for dehydrogenation of propane. The process consists of 21 units, including a plug-flow reactor, a partial condenser, two tray distillation columns and a handful of heat exchangers and compressors. The units were modeled in a manner that made them little sensitive to changes in the molar flow rates, to make the optimization more flexible. The operating conditions, and to some degree the design of selected units, which minimized the total entropy production of the process were found. The most important characteristics were the amount of recycled propane and propylene, conversion and selectivity in the reactor, as well as the number of tubes in the reactor. The optimal conversion, selectivity and recycle flows were results of a very clear trade-off among the entropy produced in the reactor, partial condenser and the two distillation columns. Although several simplifying assumptions were used for computational reasons, this show for the first time that it is also meaningful to use the entropy production as an objective function in chemical engineering process optimization studies.

7.1 Introduction

Large amounts of high quality energy are spent in the chemical process industry to convert raw materials into desired products. Since a large share of this energy is supplied from fossil fuels the use of energy is closely related to emissions of for instance greenhouse gases. At the same time, the amount of energy that is available as fossil fuels, is limited and decreasing. From these perspectives, and from an economical point of view, the art of process design and optimization is continuously being developed (Smith 1995, Edgar et al. 2001). In the present context we shall study the energy efficiency of a chemical process, a topic that so far has received little attention.

We have previously studied the state of minimum entropy production in several process units (Johannessen et al. 2002, Johannessen and Kjelstrup 2004b, Nummedal et al. 2003, De Koeijer et al. 2004a, Røsjorde and Kjelstrup 2004). These studies gave insight in the design of the particular units with more or less fixed boundary conditions. In a process, each unit has few or no boundary conditions; the boundary conditions are placed on the process itself. Optimization of a process, the topic of the present work, may thus likely give very different results from optimization of single units.

In a chemical process, the aim is to convert a feedstock into products of certain purities. Typically, this is done with a reactor(s) that transforms the raw materials, followed by a separation to obtain the desired purity. One particularly important question in such chemical processes is: How does the selectivity and conversion in the reactor affect the downstream separation section? In many systems, the reaction and separation sections are rather energy inefficient. We shall see that the composition and flow rate of the recycle streams, as well as the operation of reactors and separation equipment, will have a large influence on the overall energy efficiency of the process.

We have chosen to study a process in which the goal is to produce propylene of a certain amount and quality from propane. Propylene is mostly used for production of polypropylene, a polymer with numerous applications. Several process alternatives exist for production of propylene, and the two most widely used are based on steam cracking and catalytic cracking of higher alkanes (Kirk-Othmer 1994). An emerging technology is the dehydrogenation of propane, which presently accounts for a small share of the total propylene production in the World. This share is expected to increase due to higher demands for propylene and because the dehydrogenation process uses propane instead of higher alkanes as feed (Kirk-Othmer 1994). Understanding how to further increase the energy efficiency of propane dehydrogenation processes is thus of importance.

We have here chosen to minimize the entropy produced in the propane dehydrogenation process inspired by Lindes design (Rytter and Bölt 2000). The complete process consists of hundreds of units, but we study a simplified version where the main features are preserved. We concentrate our effort on finding the operating conditions of the process that give the least entropy production, without changing the structure of the process. Apart from the reactor and the heat exchangers, the design of the units in the process remains unchanged because of the conditions set for the optimization. Keeping the production of propylene fixed, we can then answer the following questions related to the optimal state:

- What is the conversion and selectivity in the reactor? What is the corresponding recycle of propane and propylene? Given the residence time, what is the number of tubes in the reactor (proportional to the volumetric flow rate)?

- The process includes units where heat must be removed at cryogenic con-

ditions: How much and at which temperatures should heat be transferred in these units?

- What is the optimal feed composition and feed tray location for the distillation column that separates propylene from propane?

The most important result from this study is that there exists a trade-off in the energy efficiency among a handful of units, and that it may be found by minimizing the total entropy production of the process. The exact numerical values for operating conditions are of less importance, because of the assumptions that are used.

7.2 The propane dehydrogenation process

The system we study in this work is a simplified version of the propane dehydrogenation process designed by Linde (Rytter and Bölt 2000). One of the central process units is the dehydrogenation reactor in which the following two reactions are the dominating ones (Sundaram and Froment 1977):

$$C_3H_8 = C_3H_6 + H_2 \quad \text{(I)}$$
$$C_3H_8 = C_2H_4 + CH_4 \quad \text{(II)}$$

The expression for the reaction kinetics of reaction (I) was given by Loc et al. (1996). No expression that included the backward reaction of reaction (II) was found, so we guessed an expression (Røsjorde et al. 2003) (see appendix of Chapter 6).

According to the two reactions, the system contains five components: Hydrogen (H_2), methane (CH_4), ethylene (C_2H_4), propylene (C_3H_6) and propane (C_3H_8). We neglect other species that normally would be present in a real dehydrogenation process, among them water. This is discussed later in Section 7.5.2.

A flow sheet of the dehydrogenation process is shown in Fig. 7.1. The process consists of 21 units and the chosen superstructure is an attempt to keep the main features of a real dehydrogenation process (Bohnet 2003, Rytter and Bölt 2000, Kirk-Othmer 1994, Pujado and Vora 1990). Fresh feed (S1) enters the process and is compressed and heated in the units C-1 and H-1, before it is mixed in M-1 with a recycle stream containing mostly propane and some propylene. The reactor (R-1) is the same reactor as studied by Røsjorde et al. (2003) (see Chapter 6). The reactions (I) and (II) are both endothermic and

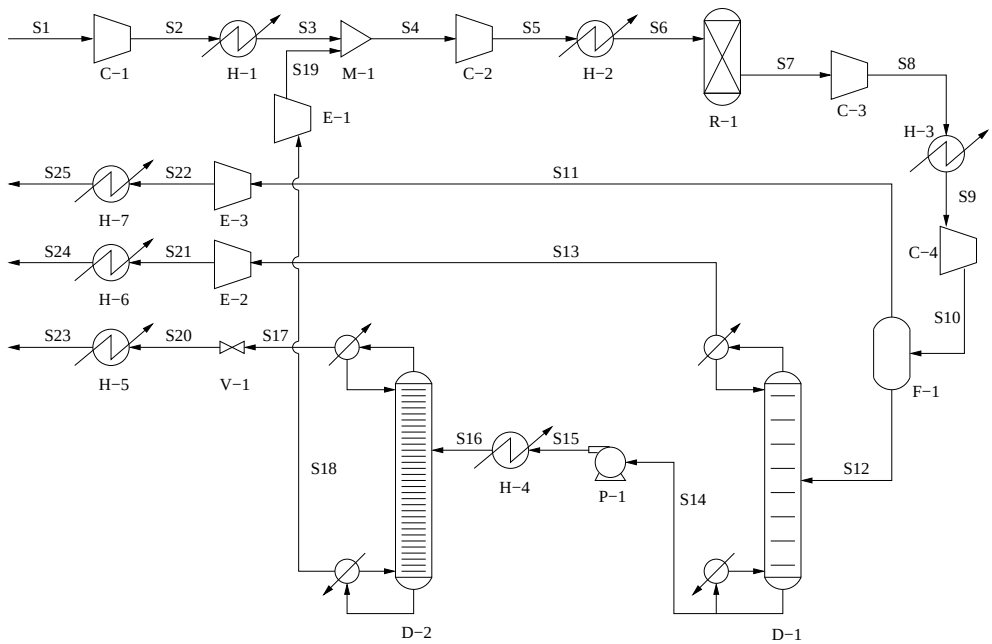

Figure 7.1. Flow sheet showing the propane dehydrogenation process. Symbols are explained in the text.

Røsjorde et al. (2003) found that heat exchange before and after the reactor was advantageous in order to enable significant reductions in the reactor's entropy production. We therefore include heat exchangers up-stream and down-stream of the reactor (H-2 and H-3). According to Resasco and Haller (1994), dehydrogenation reactors must be operated at high temperatures (800-1000 K) and low pressures (1-5 atm) in order to achieve attractive conversion levels. Before and after the reactor, we therefore include compressors/expanders (C-2 and C-3). The reactor is a plug-flow reactor with side firing. In accordance with Røsjorde et al. (2003), we set the ambient temperature constant along the reactor.

Equal amounts of hydrogen and propylene are formed in the reactor, along with some methane and ethylene. To separate the hydrogen from the main process stream, the pressure must be high and the temperature low. The purpose of the units following the reactor is to manipulate the process stream so that hydrogen in vapor phase can be removed from a liquid phase containing the rest of the components. The separation is done in a condenser (F-1). The hydrogen stream, which also contains some methane, is expanded (E-3) and heated (H-7) before leaving the process. The main process stream (S12) is then fed to a tray distillation column (D-1). The bottom products are almost exclusively propylene and propane while the top product consists mainly of ethylene. A second tray distillation column (D-2) is splitting the propylene-propane mixture. The bottom product, propane and some propylene, is used to create a recycle and is mixed with the feed stream in M-1. The top product, propylene of high purity, is expanded and cooled (V-1 and H-5) before leaving the process. The purpose of V-1, E-2, E-3, H-5, H-6 and H-7 is to ensure that all the streams that leave the process has a constant thermodynamic state (a certain pressure and temperature).

In at least three positions, heat exchangers must remove heat at cryogenic conditions (the temperature of the cooling fluid is then lower than the environmental temperature). First, the condenser (F-1) must operate under high pressure, but also at very low temperatures (ca. 230 K) to ensure that a liquid phase of the heaviest components is present. Second, the top condenser in the distillation column separating C_2-components from C_3-components (D-1), must work under quite similar conditions as those of F-1. Third, the required temperature of the cooling medium in the top condenser in D-2, may be below 298 K if the pressure is low. A refrigeration cycle consisting of four units is used to supply these cold heat exchanger fluids (see Appendix B for the detailed models).

7.3 Calculations

We did two kinds of calculations: First, we found a set of initial operating conditions for the process by using a numerical solver (Section 7.3.1 below). Second, we used this information as the initial guess in a minimization of the total entropy production, using a numerical optimization routine (Section 7.3.2 below).

Every unit in the process under consideration had several design parameters that determined how that unit changed the process stream (for instance length of reactor, etc.). We chose to keep most of these parameters fixed during this study and did only allow the *load* or in a few cases other parameters on each unit to vary. With the load, we mean the amount of heat transferred in a heat exchanger, the work input to a compressor, the fractional recovery of a distillation column etc. The values of the fixed unit parameters are given in Tab. 7.1.

Table 7.1. Process unit parameters. Reactor and catalyst parameters taken from Fogler (1992) and compressor efficiency from Perry and Green (1997).

Unit	Parameter	Value	
Reactor	Length	8.0	m
	Diameter	0.2	m
	Heat transfer number	56.784	W/m^2K
	Catalyst density	984.4	kg cat./m^3
	Void of catalyst bed	0.45	
	Catalyst particle diameter	$4.572 \cdot 10^{-3}$	m
	Gas viscosity	$3.7204 \cdot 10^{-5}$	kg/ms
	Residence time	5	s
Heat exchanger	Pinch, ΔT	50	K
Comp./exp.	Efficiency, $\eta_{c/e}$	0.8	
Distillation D-1	Number of trays, N	8	
	Feed tray, N_F	6	
	Light key component, LK	3	
	Heavy key component, HK	4	
Distillation D-2	Number of trays, N	100	
	Distillate composition, $x_{D,LK}$	0.99	

In Appendix B and in previous studies (Røsjorde and Kjelstrup 2004, Johannessen and Kjelstrup 2004b) we have given the equations that were used to model each process unit. In the cases of the heat exchangers, condensers,

compressors and expanders, the thermodynamical state at the outlet of each unit was known, once the load together with the inlet process stream were given. Giving the load of a heat exchanger was thus equivalent to giving the temperature of the process stream at the outlet of that unit. Similarly, the work supplied to a compressor could be translated into a certain pressure at its outlet. By solving the unit models in a serial order, it was possible to easily replace the load with thermodynamical state variables like temperature or pressure at the outlet of many units.

The following properties were chosen for the fresh feed stream to the process (Bohnet 2003): $T_1 = 275$ K, $P_1 = 1$ atm, $F = [1, 1, 1, 1, 96]$ mol/s. The components in this vector are ranged from lightest to heaviest. We use this notation to describe the composition of process stream from now on. The temperature and pressure of the three process streams exiting the process (S23, S24 and S25) were set to 310 K and 1 atm, respectively.

We specified further that each process stream should be either liquid or vapor according to the information given in Tabs. 7.5 and 7.6 in Appendix A. The environmental temperature, T_0, was set to 298 K. All physical and thermodynamical properties were taken from Aylward and Findlay (1994) and Daubert and Danner (1992). The molar enthalpy, entropy and fugacity coefficients were derived from the Soave-Redlich-Kwong equation of state with the binary interaction parameters equal to 0 (Prausnitz et al. 1999).

7.3.1 Modeling the process

For a given temperature, pressure and flow rates of the five components at the inlet of the process (S1), we calculated serially the change each unit did on the process stream. All parameters in Tab. 7.2, except T_{19}, F_{19,C_3H_6} and F_{19,C_3H_8}, were fixed to a set of reasonable values. In the third unit, the mixer (M-1), we did initially not know the state of the second stream entering the mixer (S19, recycle from propane-propylene separation (PP-splitter)). It was therefore necessary to solve the following three equations to find the right values of T_{19}, F_{19,C_3H_6} and F_{19,C_3H_8}:

$$\hat{T}_{19} - T_{19} = 0 \tag{7.1}$$

$$\hat{F}_{19,C_3H_6} - F_{19,C_3H_6} = 0 \tag{7.2}$$

$$\hat{F}_{19,C_3H_8} - F_{19,C_3H_8} = 0 \tag{7.3}$$

where the variables with a hat symbol represent the guessed values and those without represent the values found after calculating through the whole process.

The numerical solver *fsolve* from the Optimization Toolbox in Matlab R13, MathWorks Inc. was used to find the solution to the above nonlinear problem.

With the correct values of the recycle stream (given in Tab. 7.2) we calculated all properties of the process like duties of heat exchangers, work of compressors, entropy production of each unit etc. The set of values for the properties given in Tab. 7.2 were used as initial guess in the optimization problem. We will therefore refer to this process as the *initial* process.

7.3.2 Optimizing the process

To find the state of minimum entropy production of the propane dehydrogenation process, we used the sum of the entropy produced by each of the 21 units as the objective function:

$$\left(\frac{dS}{dt}\right)^{\text{irr}}_{\text{process}} = \sum_{i=1}^{21} \left(\frac{dS}{dt}\right)^{\text{irr}}_{i} \tag{7.4}$$

where $(\frac{dS}{dt})^{\text{irr}}_{i}$ was the entropy production of unit i.

The variables we used in this optimization problem are listed in Tab. 7.2, along with their initial value and upper (UB) and lower boundaries (LB). Table 7.2 gives also the fractional recovery, FR, of the two distillation columns, defined as (McCabe et al. 1993):

$$FR = \frac{Dx_{\text{D,LK}}}{Fx_{\text{F,LK}}} \tag{7.5}$$

where D and F are the molar flow rate of distillate and feed stream, respectively. Furthermore, $x_{\text{D,LK}}$ and $x_{\text{F,LK}}$ are the mole fractions of the light key component in the distillate and feed stream, respectively. The light (LK) and heavy (HK) key components are the components that we wish to separate in distillate and bottom product of the distillation column, respectively.

As equality constraints we used the three Eqs. (7.1)-(7.3) in addition to the following demand on the production of propylene:

$$F^{\text{init}}_{17,\text{C}_3\text{H}_6} - F_{17,\text{C}_3\text{H}_6} = 0 \tag{7.6}$$

where $F^{\text{init}}_{17,\text{C}_3\text{H}_6}$ was the flow of propylene out of the PP-splitter (and thus out of the process) in the initial process. A constant purity of the propylene product was ensured by always enforcing $x_{\text{D,LK}} = 0.99$ from the PP-splitter (D-2).

Table 7.2. Variables in the optimization. LB and UB are abbreviations for the lower and upper bounds put on the variables in the optimization.

Unit	Variable	Initial value	LB	UB
Compressor (C-1)	P_2 / atm	3.0	1.0	25.0
Heat exchanger (H-1)	T_3 / K	500	200	1500
Mixer (M-1)	T_{19} / K	261.1	200	1500
	F_{19,C_3H_6} / mol/s	0.72	0	∞
	F_{19,C_3H_8} / mol/s	99.4	0	∞
Compressor (C-2)	P_5 / atm	5.0	2.0	25.0
Heat exchanger (H-2)	T_6 / K	1100	500	1500
PFR reactor (R-1)	T_a / K	1300	600	2000
Compressor (C-3)	P_8 / atm	10.0	1.0	25.0
Heat exchanger (H-3)	T_9 / K	500	200	1500
Compressor (C-4)	P_{10} / atm	15.0	10.0	18.0
Condenser (F-1)	T_{12} / K	230	200	270
Distillation (D-1)	RR	10.0	0.5	∞
	FR	0.99	0.5	0.999
Pump (P-1)	P_{15} / atm	15.0	13.0	18.0
Heat exchanger (H-4)	T_{16} / K	300	280	340
Distillation (D-2)	FR	0.99	0.9	0.99

To find the minimum of Eq. (7.4) we used the function *fmincon* from the Optimization Toolbox in Matlab. This function solves numerically constrained nonlinear optimization problems by employing a sequential quadratic programming technique. At every iteration the Jacobian and Hessian of the objective function were estimated and actively used in the search for the minimum state. An important requirement for such methods to work satisfactorily, is that the variables, constraints and objective function are all continuous. If not, the information contained in the Jacobian and Hessian will give an extremely bad performance of the overall algorithm.

We formulated the optimization problem, without discrete variables or constraints. The models for the phase equilibrium that were used in several units introduced discontinuities, however: The temperature, pressure and composition are continuous properties, but the number of phases in equilibrium is not! A small change in temperature may result in a transformation from two phases in equilibrium to only one phase. In the condenser (F-1), this transformation results in the disappearance of the liquid output stream, if for instance the temperature at the outlet was guessed too high. If no liquid exits from

the condenser, half of the process will also disappear and no propylene of the desired purity will be produced.

A way to avoid this discontinuous behavior was to enforce the presence of a liquid phase, and at the same time introduce a penalty function that made this an unattractive solution in terms of entropy production. If the thermodynamical state of the condenser was such that no liquid existed at the outlet, we therefore first found the temperature at which liquid would exist (the dew point) and used the entropy production of this hypothetical condenser modified with a penalty term linear in the temperature:

$$\left(\frac{dS}{dt}\right)^{\text{irr}}_{\text{cond},T} = \left(\frac{dS}{dt}\right)^{\text{irr}}_{\text{cond},T_\text{d}} + 10|T_\text{d} - T|F_{10} \tag{7.7}$$

where T_d was the dew point temperature.

To reduce the required computational time needed to find the optimum, we made the additional assumption that the process stream (S16) entering the PP-splitter (D-2) consisted of propylene and propane only. This means that traces of the three lightest components were technically removed from the process entirely. To simulate binary distillation required only 1/10 of the computational time needed to simulate even a ternary distillation. Since any components that are lighter than propylene will almost exclusively end up in the distillate, we added the following inequality constraint on the content of C_2H_4 in the bottom stream from D-1 (and thus inlet stream to D-2):

$$F_{14,\text{C}_2\text{H}_4} - F^{\text{init}}_{14,\text{C}_2\text{H}_4} \leq 0 \tag{7.8}$$

By keeping the amount of ethylene at least as low as in the initial process, we reduced the error associated with the assumption of a binary distillation in D-2.

To further reduce the required computational time, we compiled a table with the entropy production, product temperatures etc., for different combinations of variables in D-2, before we did the process optimization. For four values of the feed mole fraction, fractional recovery, feed temperature and pressure, we carried out 256 simulations of D-2. We used this four-dimensional table instead of solving the distillation model itself when we optimized and modeled the process.

7.4 Results

We first give the results for the initial process, followed by the results for the optimal process. A comparison between the two highlights the most interesting findings. We present here only results for the most important units in the process (the reactor and the three separation units). Complete overviews of the operating conditions for the initial and optimal processes are given in Tab. 7.5 and Tab. 7.6 in Appendix A.

7.4.1 The initial process

The results for the initial process are reasonable. This is discussed in Section 7.5.1, while the facts are reported in this subsection. By solving Eqs. (7.1)-(7.3) we found the properties of the recycle stream that corresponded to the operating conditions chosen as the initial process. The recycle stream had T_{19} = 261.1 K, F_{19,C_3H_6} = 0.72 mol/s and F_{19,C_3H_8} = 99.4 mol/s.

The residence time of 5 seconds was fulfilled with a number of tubes in the reactor equal to 72. The pressure drop in the reactor was 1.7 atm. The amount of heat transferred was 5400 kW and the ambient temperature was 1300 K. This gave a conversion of propane and selectivity toward propylene of 0.47 and 0.82, respectively. The total entropy production in the reactor was divided between the three different phenomena in the following way: The pressure drop, 0.94 kW/K, the heat transfer, 1.63 kW/K, and the reactions, 10.14 kW/K.

The flow rate to the condenser (F-1) was 291.1 mol/s and the composition was [0.26, 0.059, 0.059, 0.26, 0.36]. With an inlet and outlet temperature of 527.5 K and 230.0 K, and a pressure of 15.0 atm the fraction of the material stream still in vapor phase when exiting the condenser was 0.34. This gave a flow of hydrogen (y_{H_2}=0.75) equal to 99.3 mol/s out of the process.

The flow rate to the distillation column separating C_2-components from C_3-components (D-1) was 191.8 mol/s and its composition was [0.009, 0.022, 0.063, 0.38, 0.53]. With a reflux ratio of 10 and a fractional recovery of ethylene in the distillate of 0.99, the distillate flow (exiting the process) became 19.6 mol/s (mostly methane and ethylene).

Finally, in D-2 where the propylene product was purified to a mole fraction of 0.99, the input flow rate was 172.2 mol/s of a composition [0, 0, 0.002, 0.42, 0.58]. A fractional recovery of propylene in the distillate equal to 0.99 gave a propylene flow rate of 71.0 mol/s in the distillate. The optimal location of the

feed tray was at tray 50.

The work and heat input/output to all process units, as well as their entropy production, are given in Tab. 7.3. The temperature at which the heat was transferred (T_u) is also given in the table. The total entropy production of

Table 7.3. The work and heat supplied and entropy produced by each unit in the initial process. The properties of the distillation columns are separated in condenser (c) and reboiler (r). Total entropy production of the columns is located at the entry for the condenser.

Unit	W / kW	Q / kW	T_u / K	$(\frac{dS}{dt})^{irr}$ / kW/K	$(\frac{dS}{dt})^{irr}_{cryo}$ / kW/K
C-1	330	0	-	0.21	0
H-1	0	1690	460.9	0.47	0
M-1	0	0	-	0.91	0
C-2	420	0	-	0.20	0
H-2	0	19900	808.2	2.31	0
R-1	0	5400	1300.0	12.63	0
C-3	3290	0	-	0.64	0
H-3	0	-16030	718.3	1.08	0
C-4	620	0	-	0.24	0
F-1	0	-9030	230.0	21.47	9.68
D-1 (c)	0	-2990	216.3	14.24	4.88
D-1 (r)	0	4770	343.6	-	-
P-1	0	0	-	0	0
H-4	0	-310	300	0.20	0
D-2 (c)	0	-44960	279.1	38.93	7.83
D-2 (r)	0	46600	317.1	-	-
E-1	-260	0	-	0.25	0
V-1	-10	0	-	0	0
E-2	-60	0	-	0.11	0
E-3	-290	0	-	0.60	0
H-5	0	30	358.6	0.01	0
H-6	0	120	277.6	0.12	0
H-7	0	560	271.2	0.59	0
Sum	4040	5750	-	95.21	22.39

the initial process was 95.21 kW/K. Most of this entropy was produced in the reactor (R-1) and the three separation units (F-1, D-1, D-2). In Tab. 7.3 we have also specified how much of the entropy production in each unit was due to heat exchange at cryogenic conditions. The three units F-1, D-1 and D-2

had cryogenic heat exchange and this accounted for 24% of the total entropy production in the initial process. In net, 4040 kW and 5750 kW of work and heat, respectively, were added to the process. The total amount of energy added to the process was thus 9790 kW.

7.4.2 The optimal process

One of the equality constraints, Eq. (7.6), ensured that the optimal process had the same product flow rate as the initial process (S16).

The number of tubes in the reactor in the optimized process was calculated to be 124 and the pressure drop was 0.95 atm. The amount of heat transferred was 9560 kW with a furnace temperature equal to 1343 K. This gave a conversion and a selectivity of 0.74 and 0.92, respectively. The pressure drop, heat transfer and reactions caused 1.11 kW/K, 2.77 kW/K and 9.80 kW/K of entropy production, respectively.

The flow rate to the condenser (F-1) was 230.0 mol/s and the composition was [0.37, 0.037, 0.037, 0.42, 0.14]. With the fraction of vapor exiting the condenser equal to 0.48, the vapor stream was 110.9 mol/s (y_{H_2}=0.75).

From F-1 a liquid stream with composition [0.013, 0.011, 0.036, 0.70, 0.24] and flow rate 119.2 mol/s entered the distillation column D-1. The optimal reflux ratio and fractional recovery of ethylene were 9.82 and 0.986, respectively, giving a distillate flow rate of 8.7 ($y_{C_2H_4}$=0.45).

The input flow rate to D-2 was 110.5 mol/s and the composition was [0.000, 0.000, 0.003, 0.74, 0.26]. With the given input stream, the specified flow rate of propylene in the distillate (72.2 mol/s) was obtained with a fractional recovery of 0.871. The bottom stream from D-2, serving as recycle to the reactor, consisted of propylene and propane with flow rates 10.5 mol/s and 27.9 mol/s, respectively. The optimal location of the feed tray was at tray 76.

The work and heat input/output and entropy production of each unit in the optimal process are given in Tab. 7.4. The optimal process had an entropy production of 44.66 kW/K of which 5.57 kW/K was due to production of cryogenic conditions for heat transfer. The net addition of work to the compressors/expanders was 8230 kW and 2030 kW of heat was added to the process. In total, this gave a net addition of 10260 kW.

Table 7.4. The work and heat supplied and entropy produced by each unit in the optimal process. The properties of the distillation columns are separated in condenser (c) and reboiler (r). Total entropy production of the columns is located at the entry for the condenser.

Unit	W / kW	Q / kW	T_u / K	$(\frac{dS}{dt})^{irr}$ / kW/K	$(\frac{dS}{dt})^{irr}_{cryo}$ / kW/K
C-1	250	0	-	0.16	0
H-1	0	1710	452.5	0.49	0
M-1	0	0	-	0.56	0
C-2	-60	0	-	0.04	0
H-2	0	13270	815.8	1.48	0
R-1	0	9560	1342.8	13.68	0
C-3	8760	0	-	1.32	0
H-3	0	-20030	863.2	0.23	0
C-4	-190	0	-	0.10	0
F-1	0	-4500	251.3	5.92	2.40
D-1 (c)	0	-1300	235.4	5.68	1.17
D-1 (r)	0	2260	351.4	-	-
P-1	-1	0	-	0.001	0
H-4	0	-180	309.8	0.11	0
D-2 (c)	0	-17540	287.1	13.28	2.00
D-2 (r)	0	18160	322.9	-	-
E-1	-120	0	-	0.13	0
V-1	-10	0	-	0	0
E-2	-30	0	-	0.05	0
E-3	-370	0	-	0.74	0
H-5	0	-40	295.2	0.03	0
H-6	0	50	281.8	0.05	0
H-7	0	610	275.6	0.61	0
Sum	8230	2030	-	44.66	5.57

7.4.3 Comparison of the initial and optimal process

The total entropy production of the propane dehydrogenation process was reduced with 53%, or 50.6 kW/K, by finding the optimal operating conditions. Six units produced the majority of the total entropy in both the initial and optimal process: H-2, R-1, C-3, F-1, D-1 and D-2. Each of these contributions, from both processes, ise shown in Fig. 7.2. The entropy production due to the

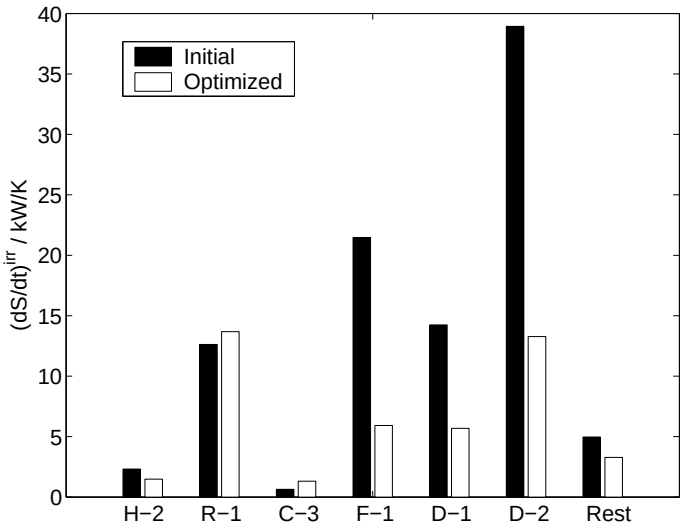

Figure 7.2. Entropy production in the 5 most significant units and the rest of the process, both in the initial and optimal process.

cryogenic process units, all of these located in the separation part (F-1, D-1 and D-2), decreased with 75% or 16.8 kW/K. The reactor, on the other hand, experienced a small increase in the entropy production. Though the pressure drop was smaller in the optimal reactor, the heat transfer was nearly doubled and the net effect was an increase in the entropy production of the reactor.

The recycle of propylene and propane changed from 0.717 mol/s and 99.4 mol/s to 10.5 mol/s and 27.9 mol/s, respectively. The net work added to the process doubled, increasing with 4190 kW, while the heat added decreased with the 3720 kW.

7.5 Discussion

The most important result of this study is that we were able to formulate and solve an optimization problem using the entropy production of a chemical process as the objective function. We divide the discussion into three parts: The most important results are discussed first. A discussion of the method is then given, before we in the last part discuss aspects of the underlying models.

7.5.1 Process optimization results

From the initial process, we know the variables that have the greatest impact on the entropy production of the process. There is little knowledge of whether the initial process is reasonable, however. The operating conditions of the initial process were not taken from a real, existing process, but were rather obtained through qualified guesses. Based on the experience from the work presented in Chapter 6 we set the inlet pressure of the reactor to 5.0 atm, the inlet temperature to 1100 K and the temperature in the furnace to 1300 K. Furthermore, to condense most of the ethylene, propylene and propane present in the process stream at a temperature around 230 K, the pressure had to be approximately 12-18 atm. We worked with a process where the cooling cycles were based on propane, and 230 K was the coldest temperature available for the cold streams. The fractional recoveries of the light key component in D-1 and D-2 were both 0.99, which was reasonable compared to the number of trays in each column. The other operating conditions were chosen to fit in with the key operating conditions explained above. To summarize, we chose in the outset operating conditions that we intuitively believed would make the initial process energy efficient.

The optimal state must be explained on this background. In order to understand which operating conditions were the most important ones for reduction of the entropy production, we examine first the reactor. The entropy production in the reactor changed very little from the initial to the optimal process. Even though the molar flow rate to the reactor, F_6, decreased a lot, the volumetric flow rate was almost doubled due to the lower pressure, so the number of reactor tubes also nearly doubled, from 72 to 124. The production of propylene in the reactor had to be nearly constant. A lower molar flow rate gave thus a higher conversion of propane. By lowering the inlet pressure to its minimum value, the equilibrium composition was shifted toward the product side. Combined with a higher ambient temperature, reaction (II) produced less methane and ethylene, giving thereby a higher selectivity.

After the reactor, the compressor C-3 increased the pressure to the maximum pressure allowed, 25 atm, while in C-4 the pressure decreased to 19 atm. This was a direct consequence of the upper bounds put on the variables (cf. Tab. 7.2). The reason for this increase in pressure is clear: In the condenser (F-1), a lot of heat had to be removed at cryogenic conditions. By increasing the pressure, the corresponding equilibrium temperature increased from 230.0 K to 251.3 K. In terms of entropy production this meant large savings. Furthermore, the higher conversion and selectivity in the reactor changed the inlet composition to F-1, shifting it toward purer hydrogen. This made the fraction of vapor exiting the condenser increase, so less cooling was needed.

The feed composition to the distillation D-1 changed very little by the optimization. The reduction in entropy production in this unit was mainly due to the reduced molar flow through the column and the high pressure, which increased the cryogenic temperature of the top partial condenser.

In the pump/expander (P-1), the pressure was also at its maximum allowed value of 18 atm. This must also be seen as an attempt to reduce the need for cryogenic cooling in the condenser of the distillation D-2. A lower reflux ratio and a higher temperature in the condenser reduced the cryogenic contribution from 7.8 kW/K to 2.0 kW/K (cf. Tabs. 7.3 and 7.4). However, the reduced cryogenic cooling cannot explain the reduction of 25.7 kW/K in the entropy production of D-2. A reduction of about 36% in the flow rate through the column explains a third of the total reduction. The main part of the reduction, came as a result of a lower reflux ratio (from 46 to 18) and a radical change of feed composition from $x_{\mathrm{F,C_3H_6}} = 0.42$ to $x_{\mathrm{F,C_3H_6}} = 0.74$. This reduced the separation task of the column; the bottom product changed purity from $x_{\mathrm{B,C_3H_6}} = 0.007$ to $x_{\mathrm{B,C_3H_6}} = 0.27$. We observed the same behavior in a diabatic distillation column (Røsjorde and Kjelstrup 2004) (see Chapter 3).

The reduced entropy production translated into changes in the work and heat added to the process. The work increased with a factor of 2 because of the optimization, while the heat decreased with an almost equal amount (it would have been equal had all the exiting streams been entirely fixed). In Tabs. 7.3 and 7.4 we gave the temperatures at which each flow of heat were added to the process. The general tendency was that heat was supplied to the process at lower temperatures (except those with cryogenic conditions), while heat was released at higher temperatures. For instance, in the heat exchanger H-3, where 20000 kW of heat was released, the temperature increased from 718.3 K to 863.2 K. The reduced entropy production can be realized in practice by

installing heat engines at each exiting heat flow to produce work, or by using this heat to reduce the external heating in other parts of the process (or other processes).

To obtain further improvements in the entropy production, more variables could be added to the optimization (unit design), the process could be more integrated, and units could be upgraded. For instance, note the extremely low temperatures on stream 21 and 22 were hydrogen and light hydrocarbons were expanded from high pressures to 1 atm. These streams could be part of a heat exchanger network designed to take advantage of the heat consumed/released in the process (Gundersen and Naess 1990). The design and operation of the heat exchanger network may be included in the optimization. This requires, however, a very different mathematical treatment.

According to Fig. 7.2, the reactor and the distillation columns produced most of the entropy in the process. Similar results, from an exergy analysis carried out on a TAME-producing process, were recently reported by Rivero et al. (2004). Further improvements of the energy efficiency can be obtained by allowing better versions of the most inefficient units. In the reactor, the ambient temperature could be allowed to vary along the reactor (Nummedal et al. 2004). In processes where the overall heat transfer coefficient and heat transfer area in the reactor are lower than in the neighboring heat exchangers, a flat ambient temperature profile in the reactor may not be efficient (Johannessen and Kjelstrup 2004a). By replacing the adiabatic distillation columns D-1 and D-2 with diabatic columns (Chapter 3) or heat-integrated distillation columns (Chapters 4 and 5) large reductions in the entropy production of the process are expected.

To summarize, the higher efficiency of the optimal process compared to the initial process can be attributed mainly to three conditions:

- Lower total recycle.
- Higher pressure in the separation equipment.
- Increased selectivity in the reactor.

We do not know how wide or narrow the optimal state is, but the progress of the numerical optimization from initial to optimal state, suggested that it was the three above conditions that also affected the entropy production the most. Changes in many temperatures, for instance, resulted in only small changes

in the entropy production. The sensitivity of the entropy production in the optimal state should be studied in more detail.

To the authors' knowledge, this is the first time a minimization of the entropy production has been carried out for a chemical process. It is difficult to extract general knowledge from this kind of optimization. How the different contributions will affect the total entropy production depends very much on the choice of models and model parameters. It is interesting to see however, that there is a possibility for larger gains, to be found through optimization. This illustrates that there is a potential for similar optimizations to ensure high energy efficiency of chemical processes.

7.5.2 The models

The reactor was modeled as a one-dimensional plug-flow reactor with side firing. Of the two reactions, only one reaction rate was founded on experimental results. The predictive ability of the reactor was thus probably low. The rate of the second reaction was chosen to never dominate the first reaction, since the purpose of including the second reaction was to introduce impurities.

In a real dehydrogenation reactor, coking is a common problem. To reduce the formation of coke the partial pressure of hydrocarbons is often reduced by adding water to the reaction mixture. This affects the chemistry of the reactor, and moreover, it introduces more load on the compressors and heat exchangers downstream. By neglecting the presence of water we make the process more energy efficient than it really is. Similarly, by neglecting the entropy that is created in the furnace chamber when fuel is burnt to provide the high temperature needed in the reactor, we underestimate the entropy production of the reactor. An improved model should most of all correct for this. Each process unit was modeled according to Appendix B and Røsjorde and Kjelstrup (2004), Johannessen and Kjelstrup (2004b). We modeled the reactor and distillation columns in more detail than the other units since most of the irreversibilities in the process were caused here.

It was necessary to use an equation of state different from the ideal gas law in order to obtain information about the vapor-liquid equilibrium. We used the Soave-Redlich-Kwong equation of state (Prausnitz et al. 1999) to describe the mixture of the five components setting the binary interaction coefficients zero. For the sake of consistency we used the SRK equation of state in all the units of the process, and to obtain thermodynamic properties as enthalpy and

entropy (Prausnitz et al. 1999). We assumed that the SRK equation of state described the vapor phase as well as the liquid phase. Since we were more interested in general features than actual numbers, we believe that this was a fair assumption.

Both distillation columns were modeled assuming equilibrium between the vapor and liquid that left each tray. This assumption gave a too high performance of the columns. No fluid dynamics were accounted for inside the columns and this also contributed to make the separation too efficient compared to a real column. A more detailed model should be a rate-based model (see Chapter 2) with for instance a pressure drop equation.

The heat exchangers and compressors were modeled in a crude way, mainly to get estimates of the heat and work required and the entropy production of the unit. No detailed models were adopted and the only specification done regarding the heat exchangers was that the average pinch was equal to 50 K. Even with this number, which was maybe too large, the entropy production of the heat exchangers was less than 10% of the total entropy production. The compressors and expanders had an efficiency of 0.8, but they did also contribute very little to the total entropy production of the process.

In all analysis based on minimization of the entropy production, an underlying assumption is that all flows of heat and materials can be transformed into useful work via Carnot engines. This is not a realistic assumption even if one would use realistic heat engines. A water stream with a temperature 3 K higher than the environment would probably not be used to produce work. In some processes, it could be used for heating purposes though. When the entropy production is minimized, the entropy content in the streams of heat and material that leaves the process is reduced, but if we do not take advantage of this, the real savings will be much smaller. It may therefore be wise to also consider the use of objective functions where this assumption is eliminated.

To summarize, most of the units are lacking the level of detail necessary to predict the behavior of the real process. Some simplifications were done in order to make the optimization converge fast, while other, more critical assumptions were done due to lack of better models (i.e. the reaction rate expression). Most of the models of the units seem to have underestimated the entropy production. It is not the absolute value of the entropy production that matter, however, but rather how it varies.

7.5.3 The method

Problem formulation: It is essential that the variables and constraints of the optimization problem are chosen with great care. In order to have a fair comparison between the initial and optimized process, conditions of the material input and output streams must not change significantly. This introduces special artifacts. In a chemical process, several material streams may enter and exit, and it is in general not possible to keep the composition of all these streams fixed. The input streams can be kept constant, however. By introducing heat exchangers and compressors at all output streams, the thermodynamic state of the output streams can also be kept constant. This was the purpose of the units V-1, E-2, E-3, H-5, H-6 and H-7. They would not necessarily be present in reality. As the composition and flow rate of the output streams follow from the way the process is operated, a minimization of the entropy production will tend to reduce the entropy carried with the exiting material streams. The total entropy production of the process may be written as:

$$\left(\frac{dS}{dt}\right)^{\text{irr}} = \sum F^{\text{out}} S^{\text{out}} - \sum F^{\text{in}} S^{\text{in}} - \sum \frac{Q}{T} \tag{7.9}$$

where $-\sum Q/T$ represents the entropy increase due to heat flows entering or leaving the process (somewhat simplified form). The second term is the entropy carried with the process input streams, which is fixed. Clearly, minimizing the entropy production will favor output streams with low entropy content. In this study, the change in $\sum F^{\text{out}} S^{\text{out}}$ from the initial to the optimized process was only 60 W/K, which is around 0.1% of the total entropy production in the process. Clearly, the constraint on the production counteracts the tendency to lower this term too much, but in bigger processes with more exiting streams and additional degrees of freedom, this might not be so.

Instead of fixing the design of all the units in the process, we chose in some instances to keep other properties fixed. For the reactor, the number of tubes was for instance calculated to give a residence time of 5 seconds. Also, in the heat exchangers, the total heat transfer area was not set; areas would have to be found afterward, from the specified temperature difference between hot and cold side, ΔT=50 K. The units became less sensitive toward changes in the flow rate in this manner, and a larger freedom in the optimization was obtained.

To have a physically meaningful optimization problem, all units had to be modeled such that the entropy production of each unit always was positive.

This is why we in the model of the reactor had to *create* an expression for the reaction rate of the second reaction instead of using the expression reported in the literature. Based on experimental data, Loc et al. (1996) reported an expression for the reaction rate for the forward reaction. To ensure that the entropy production of the reactor always was positive, the backward reaction also had to be included in the expression for the reaction rate.

A similar problem may arise in the heat exchangers, since we did not specify any internal model for the heat exchange between the process stream and heat exchange fluid. According to Eq. (7.25) one term in the entropy production of the heat exchanger was $-Q/T_{\mathrm{u}}$, where T_{u} was calculated from the temperature of the process stream and the desired temperature difference. The temperature T_{u} was thus not calculated from any internal model and might thus be unphysical, leading to negative entropy production in the heat exchangers. Since the entropy productions of the heat exchangers were small (and positive) compared to those in the reactor and separation parts, we believe that the way T_{u} was calculated was good enough.

Solution method: In order to find the solution of the optimization problem in a reasonable amount of time, several limitations and simplifications had to be set. This was partly due to the choice of numerical solver and partly due to a desire to use less than a few days of computational time to find the optimum.

The superstructure of the process was fixed during the study. To include the different interconnections and alternative units as variables gives a highly complex optimization problem. At the present stage in the method development this was not seen as necessary. We concentrated instead on the effect of finding the best operating conditions.

Since the superstructure was fixed, we had to make sure that all process streams had the phase (liquid or vapor) that the surrounding units were designed to handle. This was most critical in condenser (F-1) where the temperature was one of the variables in the optimization: For a given pressure and temperature, the output of the condenser might be vapor, liquid or an equilibrium between the two. If the liquid output disappeared (too low pressure/high temperature), the downstream branch of the process would not be needed, and no propylene product would be produced. Similarly, in the heat exchangers and compressors/expanders a phase change in the unit was not allowed. This forced us to put narrow constraints on the variables in order to minimize the chance of failure. Upper and lower bounds were put on the variables, and for four of the variables these bounds were active in the optimal state. The four variables

were P_5, P_8, P_{10} and P_{15}; the first attained the value of the lower bound, while the three last attained the values of the upper bound. This means that a lower minimum would have been found if these bounds had been less restrictive.

A penalty function was used to make the condenser (F-1) very unattractive for too high temperatures, cf. Eq. (7.7). This was a way to transform a discrete constraint (liquid present or not?) into a continuous constraint. During the optimization, very few guesses on the operating conditions activated the penalty function. Without it, though, the numerical solver would not have found any solutions.

Fixing the superstructure and placing upper and lower bounds on the variables were thus essential in order for the numerical solver to work. In addition, to speed up the time used to find the optimal state, we reduced the computational complexity as described below.

In a real process, the number of components and units will most likely be much bigger than what we used in this study. There are no upper limits to the two numbers inherent in the way we formulate or solve the optimization problem. The time needed to numerically find the optimum scales almost linearly with the number of units included in the process. For each additional unit there usually are one or two additional variables, and hence the size of the Jacobian increases accordingly. The number of components, on the other hand, influences the computational speed more dramatically. When modeling distillation columns, the number of equilibrium calculations we have to carry out depends on the number of trays and the number of components. Therefore we sought to reduce the time used for equilibrium calculations where it was possible. In the condenser (F-1) this was done by assuming the relative volatility independent of composition, while we in the PP-splitter (D-2) assumed the system to be binary. To further increase the computational speed, we compiled a table with the entropy production of D-2 at different operating conditions, which was used during the optimization instead of the model of D-2 itself.

The above simplifications introduce errors in our overall process model, but the advantage gained by increased computational speed surpass, at this point in the development, the disadvantage of reduced realism.

To develop the methodology based on minimization of the entropy production, it seems necessary to include both a heat exchanger network (see e.g. Gundersen and Naess (1990)) and allow the superstructure of the process to vary (see e.g. Grossmann and Daichendt (1996)). Furthermore, a very interesting

possibility is to perform entropy production minimizations with an additional constraint on the operating or capital cost. Several of these optimizations would give valuable information of the additional cost associated with increasing the energy efficiency of a process, as recently demonstrated by Toffolo and Lazzaretto (2002).

7.6 Conclusion

We have shown in this work that it is meaningful to use the entropy production in a chemical process as objective function in an optimization that aims to find the most energy efficient state of operation and, in some aspects, design. A process where propylene was produced in a dehydrogenation reactor from propane was studied. A plausible initial process was chosen as reference, inspired by Lindes design. The optimal process gave a large reduction in entropy production, for feasible new operating conditions. In both the initial and optimal process, the most inefficient units were the reactor, partial condenser and the two distillation columns. The results show that there was a large gain possible in the separation part of the process, by reducing the recycle stream. A higher conversion of propane and selectivity toward propylene in the reactor also contributed to reduce the entropy produced in the distillation column separating propylene from propane. Finally, we found that a higher operating pressure in parts of the process reduced the need for cryogenic heat exchange.

Assumptions and models, introduced to have reasonable computational times in the initial phase, can now be improved. Most important is to include water among the species in the process and implement the corresponding expressions for the reaction rates in the two reactions. To improve the energy efficiency of the process further, a reasonable strategy will be to include a heat exchanger network and a variable superstructure in the optimization. Future stages in the development of these procedures should include economic optimizations.

Acknowledgments

Statoil's VISTA program is thanked for the financial support to Audun Røsjorde.

Appendix A: Process stream data

The phase state, temperature, pressure, flow rate and composition of all the streams in the process are given in this appendix. Tables 7.5 and 7.6 give process data for the initial and optimized process, respectively. The phase of each process stream is marked with a 'g' or 'l' (gas or liquid) immediately after the stream number in both tables.

Table 7.5. Data for the initial process streams.

Stream no.	T / K	P / atm	F / mol/s	z_{H_2}	z_{CH_4}	$z_{C_2H_4}$	$z_{C_3H_6}$	$z_{C_3H_8}$
1 (g)	275.0	1.0	100.0	0.010	0.010	0.010	0.010	0.960
2 (g)	321.8	3.0	100.0	0.010	0.010	0.010	0.010	0.960
3 (g)	500.0	3.0	100.0	0.010	0.010	0.010	0.010	0.960
4 (g)	393.1	3.0	200.2	0.005	0.005	0.005	0.009	0.976
5 (g)	416.5	5.0	200.2	0.005	0.005	0.005	0.009	0.976
6 (g)	1100.0	5.0	200.2	0.005	0.005	0.005	0.009	0.976
7 (g)	940.9	3.3	291.1	0.260	0.059	0.059	0.263	0.359
8 (g)	1036.5	10.0	291.1	0.260	0.059	0.059	0.263	0.359
9 (g)	500.0	10.0	291.1	0.260	0.059	0.059	0.263	0.359
10 (g)	527.5	15.0	291.1	0.260	0.059	0.059	0.263	0.359
11 (g)	230.0	15.0	99.3	0.746	0.131	0.052	0.034	0.037
12 (l)	230.0	15.0	191.8	0.009	0.022	0.063	0.381	0.526
13 (g)	246.3	15.0	19.6	0.084	0.212	0.599	0.071	0.034
14 (l)	313.8	15.0	172.2	0.000	0.000	0.002	0.417	0.582
15 (l)	313.8	15.0	172.2	0.000	0.000	0.002	0.417	0.582
16 (l)	300.0	15.0	172.2	0.000	0.000	0.002	0.417	0.582
17 (l)	309.1	15.0	72.0	0.000	0.000	0.000	0.990	0.010
18 (g)	317.1	15.0	100.2	0.000	0.000	0.000	0.007	0.993
19 (g)	261.1	3.0	100.2	0.000	0.000	0.000	0.007	0.993
20 (l)	307.2	1.0	72.0	0.000	0.000	0.004	0.986	0.010
21 (g)	145.1	1.0	19.6	0.084	0.212	0.599	0.071	0.034
22 (g)	132.5	1.0	99.3	0.746	0.131	0.052	0.034	0.037
23 (l)	310.0	1.0	72.0	0.000	0.000	0.004	0.986	0.010
24 (g)	310.0	1.0	19.6	0.084	0.212	0.599	0.071	0.034
25 (g)	310.0	1.0	99.3	0.746	0.131	0.052	0.034	0.037

Table 7.6. Data for the optimal process streams.

Stream no.	T / K	P / atm	F / mol/s	z_{H_2}	z_{CH_4}	$z_{C_2H_4}$	$z_{C_3H_6}$	$z_{C_3H_8}$
1 (g)	275.0	1.0	100.0	0.010	0.010	0.010	0.010	0.960
2 (g)	311.3	2.3	100.0	0.010	0.010	0.010	0.010	0.960
3 (g)	493.8	2.3	100.0	0.010	0.010	0.010	0.010	0.960
4 (g)	437.5	2.3	138.4	0.007	0.007	0.007	0.083	0.895
5 (g)	432.7	2.0	138.4	0.007	0.007	0.007	0.083	0.895
6 (g)	1099.0	2.0	138.4	0.007	0.007	0.007	0.083	0.895
7 (g)	1019.0	1.1	230.0	0.369	0.037	0.037	0.415	0.141
8 (g)	1366.3	25.0	230.0	0.369	0.037	0.037	0.415	0.141
9 (g)	460.0	25.0	230.0	0.369	0.037	0.037	0.415	0.141
10 (g)	446.4	19.0	230.0	0.369	0.037	0.037	0.415	0.141
11 (g)	251.3	19.0	110.9	0.753	0.066	0.039	0.111	0.031
12 (l)	251.3	19.0	119.2	0.013	0.011	0.036	0.698	0.242
13 (g)	265.4	19.0	8.7	0.179	0.149	0.457	0.188	0.026
14 (l)	321.6	19.0	110.5	0.000	0.000	0.003	0.738	0.259
15 (l)	321.5	18.0	110.5	0.000	0.000	0.003	0.738	0.259
16 (l)	309.8	18.0	110.5	0.000	0.000	0.003	0.738	0.259
17 (l)	317.1	18.0	72.0	0.000	0.000	0.000	0.990	0.010
18 (g)	322.9	18.0	38.4	0.000	0.000	0.000	0.273	0.727
19 (g)	250.0	2.3	38.4	0.000	0.000	0.000	0.273	0.727
20 (l)	314.3	1.0	72.0	0.000	0.000	0.004	0.986	0.010
21 (g)	153.6	1.0	8.7	0.179	0.149	0.457	0.188	0.026
22 (g)	141.2	1.0	110.9	0.753	0.066	0.039	0.111	0.031
23 (l)	310.0	1.0	72.0	0.000	0.000	0.004	0.986	0.010
24 (g)	310.0	1.0	8.7	0.179	0.149	0.457	0.188	0.026
25 (g)	310.0	1.0	110.9	0.753	0.066	0.039	0.111	0.031

Appendix B: Models of the unit operations

The studied process had units of many different types: Compressor/expander, normal and cryogenic heat exchanger, mixer, reactor, partial condenser, and binary and multicomponent distillation columns. Equations that model the plug-flow reactor and binary tray distillation column are given elsewhere (Røsjorde and Kjelstrup 2004, Johannessen and Kjelstrup 2004b). Below we give the equations for the other process unit operations.

Compressors/expanders

Given the state of the inlet process stream, a compressor or expander is modeled once the outlet pressure is specified (Seader et al. 1999). We assume that the compression and expansion of a fluid is done adiabatically and with a certain efficiency, $\eta_{c/e}$, equal to 0.7 (Perry and Green 1997). To find the state of the output process stream, we start by calculating the temperature $T_{\text{out}}^{\text{isen}}$ that makes the operation reversible. Since we use the equation of state to calculate the molar entropy and enthalpy, this temperature must be found by solving the following equation numerically:

$$s(T_{\text{out}}^{\text{isen}}, P_{\text{out}}, \mathbf{z}) = s(T_{\text{in}}, P_{\text{in}}, \mathbf{z}) \tag{7.10}$$

where $\mathbf{z}$ is a vector with mole fractions of the fluid. We assume that no phase change occurs in the compressor/expander. The composition of the process stream entering/leaving is therefore unaltered.

Knowing $T_{\text{out}}^{\text{isen}}$ we can calculate the enthalpy of the process stream, $h(T_{\text{out}}^{\text{isen}}, P_{\text{out}}, \mathbf{z})$. To account for irreversible phenomena in the compressor, an efficiency is introduced, relating the enthalpy of the reversible process stream to the enthalpy of the real output process stream (McCabe et al. 1993):

$$h(T_{\text{out}}, P_{\text{out}}, \mathbf{z}) = \frac{h(T_{\text{out}}^{\text{isen}}, P_{\text{out}}, \mathbf{z}) - h(T_{\text{in}}, P_{\text{in}}, \mathbf{z})}{\eta_{\text{c}}} + h(T_{\text{in}}, P_{\text{in}}, \mathbf{z}) \tag{7.11}$$

A similar expression exists for expanders, with η_{c} replaced by $1/\eta_{\text{e}}$. The mechanical work that is related to the compressor or expander is:

$$W = F(h(T_{\text{out}}, P_{\text{out}}, \mathbf{z}) - h(T_{\text{in}}, P_{\text{in}}, \mathbf{z})) \tag{7.12}$$

The entropy production rate of an adiabatic compressor or expander is at steady state the difference in entropy carried with the process stream in and out:

$$\left(\frac{dS}{dt}\right)_{\text{comp/exp}}^{\text{irr}} = F(s(T_{\text{out}}, P_{\text{out}}, \mathbf{z}) - s(T_{\text{in}}, P_{\text{in}}, \mathbf{z})) \tag{7.13}$$

Cryogenic heat exchange

When heat is removed from a process stream that has a lower temperature than the environment ($T < T_0$) we speak of cryogenic heat exchange. It requires the use of a refrigerating cycle. One possibility is to use the small cycle shown in Fig. 7.3 which absorbs heat at low temperature and releases it at higher temperatures with the help of mechanical work (Seader et al. 1999). We assume that the temperature in the evaporator is equal to the cryogenic

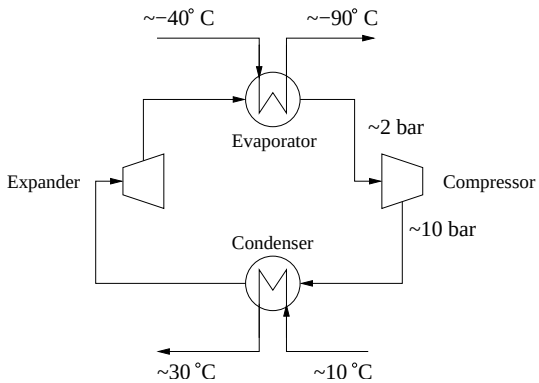

Figure 7.3. Flow sheet of the cryogenic heat exchanger cycle.

temperature that is the desired one for the process stream, T_{low}. In reality, it should be even lower, to ensure a non-zero thermal driving force between the utility fluid and process stream.

Clausius-Clapeyrons equation gives the relation between the boiling point and pressure of a fluid (Atkins 1998). For ideal gases:

$$\frac{d\ln P}{dT} \approx \frac{\Delta_{\text{vap}} H}{RT^2} \tag{7.14}$$

For the utility fluid we assume that the heat capacity of vapor and liquid is independent of temperature and equal to 70 J/K mol and 112 J/K mol, respectively (values for propane taken from Aylward and Findlay (1994)). Integration of the above equation from the normal boiling point of propane, $T_{\text{b}} = 231.05$ K, to the current temperature gives:

$$\ln\left(\frac{P}{P_0}\right) \approx -\frac{\Delta_{\text{vap}} H_0}{R}\left(\frac{1}{T} - \frac{1}{T_{\text{b}}}\right) + \frac{\Delta C_p}{R}\left(\ln\frac{T}{T_{\text{b}}} + \frac{T_{\text{b}}}{T} - 1\right) \tag{7.15}$$

where $\Delta_{\text{vap}}H_0$ is the heat of vaporization at T_{b}, equal to 18.8 kJ/mol and $\Delta C_p = C_p^{\text{vap}} - C_p^{\text{liq}}$, the difference between the heat capacity of vapor and liquid. The vapor pressure of propane corresponding to a temperature of T_{low} can now be found from the above equation.

In the condenser, heat is released at a high temperature, T_{high}, assumed to always be 40°C. For the utility fluid to reach such a high temperature, it must be compressed to a pressure found from Clausius-Clapeyrons equation above to be $P_{\text{high}} = 10.5$ atm. We assume that the compressor is operated adiabatically, without a phase change, and with an efficiency, $\eta_{\text{c}} = 0.8$. The reversible output temperature, $T_{\text{comp}}^{\text{isen}}$, that results from a compression of the utility fluid from P_{low} to P_{high} is calculated from (Atkins 1998):

$$\begin{aligned}\Delta S &= \int_{T_{\text{low}}}^{T_{\text{comp}}^{\text{isen}}} (\frac{\partial S}{\partial T})dT + \int_{P_{\text{low}}}^{P_{\text{high}}} (\frac{\partial S}{\partial P})dP \\ &= C_p^{\text{vap}} \ln\left(\frac{T_{\text{comp}}^{\text{isen}}}{T_{\text{low}}}\right) - R\ln\left(\frac{P_{\text{high}}}{P_{\text{low}}}\right) = 0\end{aligned} \tag{7.16}$$

The real output temperature from the compressor, T_{comp}, is found from the isentropic output temperature, correcting with the efficiency:

$$T_{\text{comp}} = T_{\text{low}} + \frac{T_{\text{comp}}^{\text{isen}} - T_{\text{low}}}{\eta_{\text{c}}} \tag{7.17}$$

The work supplied to the compressor is now readily calculated from the energy balance:

$$W_{\text{comp}} = F_{\text{u}} C_p^{\text{vap}} (T_{\text{comp}} - T_{\text{low}}) \tag{7.18}$$

Since the temperature of the refrigerant is higher than the environment temperature, it is possible to transfer heat to the environment (or an other process stream) in a condenser. For simplicity we assume that the condenser lowers the temperature of the utility fluid from T_{comp} (super-heated vapor) to T_{high} (vapor at boiling point) before the entire utility stream is condensed without lowering the temperature further. The amount of heat transferred out of the refrigeration cycle is thus:

$$Q_{\text{cond}} = F_{\text{u}}(-\Delta_{\text{vap}}H_0 + (T_{\text{high}} - T_{\text{b}})C_p^{\text{liq}} - (T_{\text{comp}} - T_{\text{b}})C_p^{\text{vap}}) \tag{7.19}$$

where F_{u} is the flow rate of the utility fluid (determined from the energy balance over the evaporator, Eq. (7.21)).

The final piece of equipment in the refrigeration cycle is an expansion valve. It is assumed to operate isenthalpic (Joule-Thompson valve). When a liquid

phase at the boiling point enters, the output phases may be a vapor phase in equilibrium with a liquid phase. The fraction of liquid, q, out from the expansion valve follows from the energy balance across the valve:

$$q = 1 - \frac{C_p^{\text{liq}}(T_{\text{high}} - T_{\text{low}})}{\Delta_{\text{vap}}H_0 + \Delta C_p(T_{\text{low}} - T_{\text{b}})} \tag{7.20}$$

Finally, to find the flow rate of the utility fluid, we transform the energy balance over the evaporator:

$$F_{\text{u}} = \frac{Q_{\text{evap}}}{q(\Delta_{\text{vap}}H_0 + (T_{\text{low}} - T_{\text{b}})\Delta C_p)} \tag{7.21}$$

We have assumed that the evaporator operates at $T = T_{\text{low}}$ and the condenser at $T = T_{\text{high}}$. The entropy production in these four units then sum up to:

$$\left(\frac{dS}{dt}\right)_{\text{cryo}}^{\text{irr}} = -\frac{Q_{\text{evap}}}{T_{\text{low}}} - \frac{Q_{\text{cond}}}{T_{\text{high}}} \tag{7.22}$$

A simplification has been made when we assume that the condenser operates at the same temperature, when in fact the vapor that enters is super-heated. The effect is that Eq. (7.22) becomes the same as when the compressor operates reversibly. Note that the introduction of an efficiency in the compressor still serves the purpose of making the real work, W, bigger than the reversible work.

Heat exchangers

We specify no geometry of the heat exchangers in the process. The overall heat transferred is given when the inlet and outlet state of the process stream is specified:

$$Q_{\text{hx}} = F(h(T_{\text{out}}, P, \mathbf{z}) - h(T_{\text{in}}, P, \mathbf{z})) \tag{7.23}$$

To estimate the entropy production in the heat exchanger, we introduce the average temperature of the heating/cooling medium, $\overline{T}_{\text{u}}$, from:

$$\overline{T}_{\text{u}} = \overline{T} + \Delta T \tag{7.24}$$

where $\overline{T} = (T_{\text{out}} + T_{\text{in}})/2$. In this study ΔT was set to $\pm$ 50 K. This average utility temperature give the approximate expression for the entropy production:

$$\left(\frac{dS}{dt}\right)_{\text{hx}}^{\text{irr}} = F(s(T_{\text{out}}, P, \mathbf{z}) - s(T_{\text{in}}, P, \mathbf{z})) - \frac{Q_{\text{hx}}}{\overline{T}_{\text{u}}} + \left(\frac{dS}{dt}\right)_{\text{irr}}^{\text{cryo}} \tag{7.25}$$

where $(\frac{dS}{dt})_{\text{irr}}^{\text{cryo}}$ is the extra entropy produced if $\overline{T}_{\text{u}}$ is below the environmental temperature. To arrive at the above expression, we have used that:

$$\int \frac{dQ_{\text{hx}}}{T_{\text{u}}} \approx \frac{Q_{\text{hx}}}{\overline{T}_{\text{u}}} \tag{7.26}$$

This approximation enables us to estimate the entropy production of the heat exchanger without integrating any local model.

Mixer

The mixer is a simple unit, which we assume is operated adiabatically. We require that all streams entering have the same pressure. The thermodynamical state of the single output stream is thus fully determined by what enters, and can easily be determined from the energy balance and the mass balance:

$$F_{\text{out}} h(T_{\text{out}}, P, \mathbf{z}_{\text{out}}) - \sum_{i=1}^{\#str} F_i h(T_i, P, \mathbf{z}_i) = 0 \tag{7.27}$$

$$F_{\text{out}} \mathbf{z}_{\text{out}} - \sum_{i=1}^{\#str} F_i \mathbf{z}_i = 0 \tag{7.28}$$

The entropy production of the mixer is:

$$\left(\frac{dS}{dt}\right)_{\text{mixer}}^{\text{irr}} = F_{\text{out}} s(T_{\text{out}}, P, \mathbf{z}_{\text{out}}) - \sum_{i=1}^{\#str} F_i s(T_i, P, \mathbf{z}_i) \tag{7.29}$$

The subscript i represents the different streams that enter the mixer.

Partial condenser

By removing heat from a process stream in vapor phase, liquid may be formed containing the majority of the heavy components. The light components remain in the vapor phase (McCabe et al. 1993). For a given state of the inlet process stream, we want to determine the state of the outlet stream. First we have to find out whether the output phase will be vapor, liquid, or vapor and liquid in equilibrium. If the latter is the case, we have to determine the composition of each phase. The condition for equilibrium is:

$$y_j = K_j x_j \tag{7.30}$$

where K_j is the relative volatility of component j (McCabe et al. 1993), found from the equation of state. A mass balance over the unit gives a constraint on the relation between x_j and y_j:

$$z_j = f y_j + (1 - f) x_j \tag{7.31}$$

where f is the fraction of the process stream that is still vapor phase at the outlet of the condenser. By introducing Eq. (7.30) into Eq. (7.31) we find an expression for the composition of the condensed phase:

$$x_j = \frac{z_j}{1 + f(K_j - 1)} \tag{7.32}$$

Unfortunately, it is not possible to solve the above equation analytically for x_j. The relative volatility depends on the pressure, temperature and composition in a nontrivial way. Attempts to solve the problem numerically often fail or take excessive amount of computer time. We therefore simplify and assume that K_j is independent of composition.

We calculate $\mathbf{K}$=[K_1,...,K_5] with the following choice for the compositions: Liquid consisting of nearly pure heavy component and vapor consisting of nearly pure light component. These compositions are close to those we expect at equilibrium, so we assume they give reasonable values for $\mathbf{K}$. With a constant $\mathbf{K}$, we can calculate $\mathbf{x}$ from Eq. (7.32) by guessing the value of f. The right value of f is found when the sum of the mole fractions equals one:

$$\sum_{j=1}^{5} x_j = 1 \tag{7.33}$$

If no value of f between 0 and 1 fulfills Eq. (7.33) only pure vapor or pure liquid exist. The sum of mole fractions is then either greater or less than one. On closer inspection, we find the following separation:

$$\begin{aligned} &\sum_{j=1}^{5} x_j > 1 \rightarrow f = 0 \qquad \text{(liquid only)} \\ &\sum_{j=1}^{5} x_j < 1 \rightarrow f = 1 \qquad \text{(vapor only)} \end{aligned} \tag{7.34}$$

The heat removed by the condenser is:

$$Q_{\text{cond}} = F((1 - f) h^{\text{V}}(T_{\text{out}}, P, \mathbf{y}) + f h^{\text{L}}(T_{\text{out}}, P, \mathbf{x}) - h^{\text{V}}(T_{\text{in}}, P, \mathbf{z})) \tag{7.35}$$

The entropy production of the partial condenser is found from a balance over the unit. Again we introduce an average utility temperature, $\overline{T}_{\mathrm{u}}$, as in the heat exchangers (see Section 7.5.2):

$$\left(\frac{dS}{dt}\right)_{cond}^{\mathrm{irr}} = F((1-f)s^{\mathrm{V}}(T_{\mathrm{out}},P,\mathbf{y}) + fs^{\mathrm{L}}(T_{\mathrm{out}},P,\mathbf{x}) - s^{\mathrm{V}}(T_{\mathrm{in}},P,\mathbf{z})) - \frac{Q_{\mathrm{cond}}}{\overline{T}_{\mathrm{u}}} + \left(\frac{dS}{dt}\right)_{\mathrm{irr}}^{\mathrm{cryo}} \tag{7.36}$$

When $\overline{T}_{\mathrm{u}} > T_0$, heat is removed at temperature above the environment and the cryogenic contribution to the entropy production is zero.

Multicomponent distillation

Modeling multicomponent distillation is different from modeling binary distillation mainly in one respect: In binary distillation, there is a one-to-one correspondence between the equilibrium composition (given by one mole fraction) and temperature at a certain pressure. This is not so in multicomponent distillation models.

In binary distillation we can perform a number of equilibrium calculations and construct tables with the composition and corresponding temperature. When more than two components (n) are present in the distillation, such an approach is very impractical. It requires the compilation of $(n-1)$-dimensional tables. The most practical way is then to solve the equations for equilibrium simultaneously as the modeling is done. This, however, requires much more computational time, compared to binary systems.

In binary distillation it is common to specify the top and bottom product purity, but in multicomponent distillation this easily gives impossible systems. As is more common in modeling of multicomponent distillation (McCabe et al. 1993), we specify the reflux ratio, RR, and the distillate flow rate, D, reducing the chance of setting invalid specifications. Instead of using a total condenser at the top of the column, we use a partial condenser. The reason is that the lightest components do not exist in liquid phase unless temperature is extremely low and the pressure is high. It is much more energy efficient to allow these components to remain in the vapor phase. This means that the composition of the reflux stream is not the same as the vapor leaving the first tray.

The interior of the column can be modeled using the MESH-equations (mass-,

equilibrium-, summation- and energy-equations). The equations were solved using the numerical solver *fsolve* from Matlab. For each iteration the following steps were done:

1. The liquid compositions $\mathbf{x}$ (4 of 5 components, tray 0 to $N+1$) as well as $\mathbf{T}$ (0 to N+1), $\mathbf{L}$ (1 to N), y_{D} (distillate composition) and x_{N+1} were guessed. In total this gave 6N+14 variables.

2. The last liquid mole fraction was calculated from $\sum x_j$=1.

3. Since RR and D were specified, we calculated $L_0 = RR \cdot D$.

4. With $\mathbf{L}$ and $\mathbf{x}$ we used the mass and component balances to calculate $\mathbf{V}$ and $\mathbf{y}$.

5. The net heats released/consumed, Q, on each tray were then calculated from the energy balance knowing $\mathbf{T}$, $\mathbf{x}$, $\mathbf{y}$, $\mathbf{L}$ and $\mathbf{V}$.

6. Eqs. (7.37), (7.38) and (7.39) represented 6N+14 constraints to be fulfilled.

Equilibrium between the vapor and liquid leaving each tray is ensured by requiring the fugacity of the components in each phase to be equal:

$$\phi^{\mathrm{L}}_{i,j} x_{i,j} - \phi^{\mathrm{V}}_{i,j} y_{i,j} = 0 \qquad \begin{cases} i \in [0, N+1] \\ j \in [1, n-1] \end{cases} \tag{7.37}$$

where ϕ is the fugacity coefficient of either the liquid or the vapor phase and the indexes i and j represents the tray and component number, respectively. The fugacity coefficients can be obtained from the equation of state (Prausnitz et al. 1999). The energy balance on each tray is:

$$Q_i = V_i H^{\mathrm{V}}_i + L_i H^{\mathrm{L}}_i - V_{i+1} H^{\mathrm{V}}_{i+1} - L_{i-1} H^{\mathrm{L}}_{i-1} = 0 \tag{7.38}$$

except at the feed tray where an additional term representing the feed stream enters. Finally, the composition of the liquid leaving the bottom is equal to the composition of the vapor entering (total reboiler):

$$y_{N+1,j} - x_{N,j} = 0 \qquad j \in [1, n-1] \tag{7.39}$$

The entropy production of the distillation column is calculated from:

$$\begin{aligned}\left(\frac{dS}{dt}\right)^{\text{irr}}_{\text{dist}} =& V_1 s^{\text{V}}(T_1, P, \mathbf{y}_1) - L_0 s^{\text{L}}(T_0, P, \mathbf{x}_0) + L_N s^{\text{L}}(T_N, P, \mathbf{x}_N) \\ &+ V_{N+1} s^{\text{V}}(T_{N+1}, P, \mathbf{y}_{N+1}) - F s^{\text{L}}(T_{\text{F}}, P, \mathbf{x}_{\text{F}}) + Q_{\text{cond}} X_{\text{cond}} \\ &+ Q_{\text{reb}} X_{\text{reb}} + \left(\frac{dS}{dt}\right)^{\text{irr}}_{\text{cryo}}\end{aligned} \tag{7.40}$$

where X_{cond} and X_{reb} are the average driving forces for heat transfer in the condenser and reboiler, respectively:

$$X \approx \frac{1}{\overline{T}} - \frac{1}{\overline{T} + \Delta T} \tag{7.41}$$

Here $\overline{T}$ is the average temperature in the condenser/reboiler and ΔT is the average temperature difference to the cooling/heating fluid. This model was explained in Chapter 4. The cryogenic addition to the entropy production was only included if the temperature in the partial condenser at the top of the column dropped below 298 K.

Chapter 8

Conclusions

The entropy production in single and connected process units was numerically analyzed and minimized in this thesis. An emphasis has been made to study chemical processes, which have been, to the author's knowledge, relatively little studied in this manner before. In Chapter 2, we gave a brief demonstration of the benefits of using nonequilibrium thermodynamics in some selected examples of unit operations in chemical industry. The strength of this theory lies in its ability to describe transport processes and the irreversibilities associated with them in a consistent and systematic manner. In the rest of the thesis, we took advantage of the framework offered by nonequilibrium thermodynamics where it was convenient.

In Chapters 3, 4 and 5, we studied two improved distillation concepts without including any upstream or downstream process units. Given the input and output state of the material streams, the entropy production of the ideal diabatic column, separating mixtures of propylene and propane, was minimized in Chapter 3. The areas of heat exchange on each tray were used as variables in the optimization, constrained to a certain total heat transfer area. In the optimal state, we found that most of the heat transfer area, and thus the heat transfer itself, was located close to the top and bottom of the column. This may ease an implementation in practice. Furthermore, it was also shown that variations in the feed composition had a large impact on the minimum value of the entropy production, while variations in the feed temperature had a much smaller effect, an observation that may be important when the column is connected with other units.

Another concept for distillation, is the heat-integrated distillation column (HIDiC), extensively studied by Nakaiwa et al. (2003). By operating the rectifying section of the column at a pressure higher than the stripping section, direct heat transfer may take place between the two sections. Two important parameters governing this heat transfer are the ratio between the two pressures and the total rate of heat transfer per Kelvin (UA_{total}) between the sections. In Chapter 4, we studied how different values of these parameters affected the entropy production of the HIDiC, given that the UA_{total} was evenly distributed among the trays. The column that had the lowest entropy production was found at the maximum value allowed for UA_{total} (2000 kW/K) and at a pressure ratio of 2.14. Compared to the adiabatic distillation column doing the same separation task, this was a reduction of 37%, a large value. We also observed that for values of UA_{total} below 300 kW/K, no HIDiCs had a lower entropy production than the adiabatic column. This has not been reported before the present study.

To understand the energy efficiency of the HIDiC better, we studied columns where UA_{total} was allowed to distribute itself among the trays in an optimal way. Again, the column with the lowest entropy production was found at the maximum value of UA_{total} (2000 kW/K), but at a somewhat lower pressure ratio of 1.88. The entropy production of this column was 1.66 kW/K, or 48% lower than that of the adiabatic column. A lower bound on UA_{total} was found around 150 kW/K, below which the HIDiC under consideration had a higher entropy production than the adiabatic column. The results from Chapter 4 were thus confirmed. The columns that had entropy productions close to the optimal value showed different distributions of UA_{total}. One particular distribution had UA located only at the two topmost and the bottommost pair of trays. This lead us to suggest a change in the design of the HIDiC, from heat integration between all trays in rectifying and stripping section, to heat integration between tray 1 and N only. Initial calculations showed that with the same UA_{total}, the entropy production could become as low as 1.42 kW/K. No lower bound on UA_{total} was observed in the column with the newly proposed design.

The two final chapters of this thesis were concerned with minimizing the entropy production of process units in connection. In Chapter 6, we optimized a plug-flow reactor with heat exchangers before and after the reactor, using the reactor inlet temperature, ambient temperature and length as variables. Two different kinds of profiles for the ambient temperature of the reactor were compared. It was found that both a flat and a varying ambient temperature profile

gave very similar results when the entropy production of the three units were minimized. This finding was taken advantage of in Chapter 7 (see below). Furthermore, the results showed that most of the heating of the process stream should take place in the heat exchanger up-front, while cooling should take place after the reactor. The reactor itself was operated nearly adiabatically.

The combined experience from the previous chapters were put together in Chapter 7, where we minimized the entropy production of a process where propylene of high purity was produced from propane. For a fixed production of propylene, we found the operating conditions of the process that gave the lowest total entropy production. The units were modeled using experience from Chapters 3-6. In several units, heat had to be removed at cryogenic conditions, and the associated irreversibilities were included in the total entropy production of the process. In the optimal state, several characteristic features describing the process were found, of which two were the recycle of propane and propylene, and conversion and selectivity in the reactor. Most of the entropy was produced in the reactor and the separation part of the process (one partial condenser and two tray distillation columns). This confirmed the importance of developing more energy efficient distillation concepts, like the ideal diabatic column and the HIDiC, and to study the interplay between the parts in the total process in this manner.

A matter of considerable importance for the analysis and minimizations of the entropy production carried out in Chapters 3-7, was the development and customization of the computational tools that were used. The different systems that were studied required different problem formulations and consequently different numerical solution methods. In Chapter 3, we managed to formulate the optimization problem in a way that did not require the use of constraints, and since the entropy production always could be written as the sum of many positive terms, we applied a nonlinear regression method with great success. A similar method was used to model the HIDiC in Chapter 4, where a set of equations were solved by minimizing the square of a set of residuals. In Chapter 5, however, we had to perform a minimization with an equality constraint and a sequential quadratic programming method were used. Since such methods calculate the Jacobian of the objective function and the constraints at each iteration, the objective function and the constraints must be continuous. The objective of the studies presented in Chapters 6 and 7 was to further develop the framework for entropy production minimization to handle more than just single process units. Due to the stability and speed of the sequential quadratic programming methods, we chose to use this technique also for process opti-

mization, even if that meant that the superstructure of the processes had to be fixed (to have continuous objective function and constraints).

We succeeded in developing a framework for numerical analysis and minimization of the entropy production of both single process units and chemical processes. The value of the developed methodology, as well as similar methods, lies not necessarily in the quantitative predictions of operation and design of units and processes. The qualitative information that an engineer or scientist may learn from this kind of method is also of great importance. It may serve as a guideline for research related to the unit or process in question, for instance by helping to identify where in a unit or process there are big losses, and why these losses occur. We stress the fact that this methodology is *complementary* to other design tools and principles. It is our belief that entropy production minimizations should be carried out parallel to economical optimizations and controllability studies in order to maximize the benefits.

Many of our models lacked the level of detail necessary to use the descriptions offered by nonequilibrium thermodynamics. For instance, it was not possible to make a nonequilibrium model of the distillation columns, without more advanced models for the fluid dynamics on each tray. This prevented us from using the local fluxes and forces to explain the various transport phenomena in the different process units. At the same time, we recognize that the ability to understand the optimal solutions in terms of fluxes and forces, probably is the greatest feature of our methodology. The knowledge of local conditions, enabled by nonequilibrium thermodynamics, would be very helpful in understanding and developing further the design of a process unit. To some degree only, this was illustrated here (Chapter 2). More work in this direction will be interesting.

As the framework of our methodology is quite general, it is easy to change objective function, add/change process units, increase the number of chemical components etc. Our experience has made it clear that other objective functions than the entropy production of a process could be more tuned toward practical applications. In particular, to minimize the work needed by a process could be of great interest to those who design a new process. We chose to always use the entropy production as our objective function due to its fundamental meaning. Even though work is related to the entropy production as explained in the introductory chapter of this thesis, interpretation of the results in terms of entropy production can allow a fundamental link to molecular events. The work in this thesis can be pursued in this direction.

Adding more units and components might lead to results that are interesting mainly to an engineer working on specific industrial applications. However, to develop the methodology of minimizing the entropy production further in a direction of general interest, we propose the following improvements:

- To introduce more detailed models (local descriptions) to take advantage of the understanding enabled by nonequilibrium thermodynamics.
- To include heat exchanger network.
- To vary the superstructure in order to find better process alternatives doing the same task.

It is evident that processes where large amounts of energy is transformed are among the most important candidates for entropy production minimization. With raising energy prices this kind of analysis and optimization may become more important. Two such processes today are air separation, where oxygen and nitrogen are separated at very low temperatures, and hydrogen liquefaction, where gaseous hydrogen is cooled and condensed over several stages. Both these processes are known to consume a lot of high quality energy with the present technology.

Bibliography

Agrawal, R. and Herron, D. 1997. Optimal thermodynamic feed conditions for distillation of ideal binary mixtures. *AIChE Journal* **43**(11), 2984–2996.

Amdam, R., Gran, H., Hansen, S. and Sogner, K.: 2002. *Markedsøkonomiens utvikling.* Fagbokforlaget Vigmostad & Bjørke AS. Oslo, Norway.

Atkins, P. W.: 1998. *Physical Chemistry.* 6 edn. Oxford.

Aylward, G. and Findlay, T.: 1994. *SI Chemical data.* Wiley.

Baker, R. W. 2002. Future directions of membrane gas separation technology. *Ind. eng. chem. res* **41**, 1393–1411.

Bauer, M. H. and Stichlmair, J. 1998. Design and economic optimization of azeotropic distillation processes using mixed-integer nonlinear programming. *Comput. Chem. Eng.* **22**, 1271–1286.

Bedeaux, D. 1986. Nonequilibrium thermodynamics and statistical physics of surfaces. *Adv. Chem. Phys.* **64**, 47–109.

Bedeaux, D. and Kjelstrup, S. 2003. Irreversible thermodynamics - A tool to describe phase transitions far from equilibrium. *Chem. Eng. Sci.* **59**, 109.

Bedeaux, D. and Mazur, P. 2001. Mesoscopic non-equilibrium thermodynamics for quantum systems. *Physica A* **298**, 81–100.

Bejan, A.: 1996a. *Entropy Generation Minimization. The Method of Thermodynamic Optimization of Finite-Size Systems and Finite-Time Processes.* CRC Press. New York.

Bejan, A. 1996b. Entropy generation minimization: The new thermodynamics of finite-size devices and finite-time processes. *J. Appl. Phys.* **79**, 1191–1218.

Bejan, A. and Vargas, J. V. C. 1995. Optimal allocation of a heat exchanger inventory in heat driven refrigerators. *Int. J. Mass Transfer* **38**, 2997–3004.

Bejan, A., Tsatsaronis, G. and Moran, M.: 1996. *Thermal Design and Optimization.* John Wiley & Sons, Inc.. New York.

Bohnet, M. (ed.): 2003. *Ullmann's encyclopedia of industrial chemistry.* 6 edn. Wiley.

Bryson, A. and Ho, Y.: 1975. *Applied Optimal Control. Optimization, estimation and control.*. Wiley. New York.

Budiman, A. and Ishida, M. 1998. Optimal side heating and cooling in a distillation column. *Energy* **23**(5), 365–371.

Chemical Manufacturers Association: 1998. *U.S. Chemical industry statistical handbook.* Arlington, Virginia.

Coleman, B. and Truesdell, C. 1960. On the reciprocal relations of Onsager. *J. Chem. Phys.* **53**, 28–31.

Cornelissen, R. L. and Boerema, C.: 2001. Exergy scan, the new method for cost effective fuel saving. *in* A. Ozturk and Y. Gogus (eds), *Proceedings of ECOS 2001.* Istanbul, Turkey. pp. 725–731. ISBN 975-97568-2-2.

Daubert, T. E. and Danner, R. P.: 1992. *Physical and Thermodynamic Properties of Pure Chemicals. Data Compilation.* Hemisphere. Washington.

De Groot, S. and Mazur, P.: 1984. *Non-Equilibrium Thermodynamics.* Dover. London.

De Koeijer, G. and Kjelstrup, S. 2000. Minimizing entropy production in binary tray distillation. *Int. J. Appl. Thermodynamics* **3**, 105–110.

De Koeijer, G. and Kjelstrup, S.: 2002. Application of rate equations for heat and mass transfer to distillation of ethanol and water. *in* J. Grievink and J. van Schijndel (eds), *Computer-Aided Chemical Engineering, Vol. 10, Proceedings of ESCAPE 2002.* The Hague, The Netherlands. pp. 235–240. ISBN 0-444-51109-1.

De Koeijer, G. and Rivero, R. 2003. Entropy production and exergy loss in experimental distillation columns. *Chem. Eng. Sc.* **58**(8), 1587–1597.

De Koeijer, G., Johannessen, E. and Kjelstrup, S. 2004a. The second law optimal path of a four-bed SO_2 converter with five heat exchangers. *Energy* **29**(4), 525–546.

De Koeijer, G., Kjelstrup, S., Salamon, P., Siragusa, G., Schaller, M. and Hoffmann, K. 2002. Comparison of entropy production rate minimization methods for binary diabatic tray distillation. *Ind. Eng. Chem. Res.* **41**, 5826–5834.

De Koeijer, G. M. and Kjelstrup, S.: 2003. Application of irreversible thermodynamics to distillation. *in* N. Houbak, B. Elmegaard, B. Qvale and M. Moran (eds), *Proceedings of ECOS 2003.* number ISBN 87-7475-297-9. Department of mechanical engineering, DTU. Copenhagen, Denmark. pp. 1205–1212.

De Koeijer, G., Røsjorde, A. and Kjelstrup, S. 2004b. Distribution of heat exchanghers in optimum diabatic distillation columns. *Energy* **29**(12-15), 2425–2440.

Demirel, Y.: 2002. *Nonequilibrium Thermodynamics. Transport and Rate Processes in Physical and Biological Systems.* Elsevier.

Dennis, J.: 1977. *State of the art in numerical analysis.* Academic Press. chapter Nonlinear Least-Squares.

Edgar, T. F., Himmelblau, D. M. and Lasdon, L. S.: 2001. *Optimization of chemical processes.* 2 edn. McGraw-Hill. Singapore.

Engelien, H. K., Larsson, T. and Skogestad, S. 2003. Implementation of optimal operation for heat integrated distillation columns. *Chem. Eng. Res. Des: TransIChemE* **81**(A2), 277–281.

Fang, G. and Ward, C. 1999. Examination of the statistical rate theory expression for liquid evaporation rates. *Phys.Rev.E* **59**, 441–453.

Fogler, H.: 1992. *Elements of Chemical Reaction Engineering.* 2 edn. Prentice-Hall, New York.

Fonyo, Z. 1974a. Thermodynamic analysis of rectification I. Reversible model of rectification. *Int. Chem. Eng.* **14**(1), 18–27.

Fonyo, Z. 1974b. Thermodynamic analysis of rectification II. Finite cascade models. *Int. Chem. Eng.* **14**(2), 203–210.

Froment, G. F. and Bischoff, K. B.: 1990. *Chemical Reactor Analysis and Design.* 2. edn. Wiley.

Gmehling, J. and Onken, U.: 1980. *Vapor-liquid equilibrium data collection.* Vol. 1. DECHEMA Chemistry Data Series. Frankfurt, Germany.

Graveland, A. J. G. G. and Gislof, E. 1998. Exergy analysis: An efficient tool for process optimization and understanding. *Comput. Chem. Eng.* **22**, S545–S552.

Grossmann, I. E. and Daichendt, M. M. 1996. New trends in optimization-based approaches to process synthesis. *Comput. Chem. Eng.* **20**, 665–683.

Gundersen, T. and Naess, L. 1990. The synthesis of cost optimal heat exchanger networks. *Heat Recovery Systems & CHP* **10**, 301–328.

Hafskjold, B.: 2002. *Thermal Nonequilibrium Phenomena in Fluid Mixtures, eds. W. Kohler and S. Wiegand.* Lecture Notes in Physics. Springer. Berlin. chapter Computer Simulations of Thermal Diffusion in Binary Fluid Mixtures.

Hafskjold, B. and Ratkje, S. K. 1995. Criteria for local equilibrium in a system with transport of heat and mass. *J. Stat. Phys.* **78**, 463–494.

Heyen, G. and Kalitventzeff, B. 1997. Methodology for optimization of operation to reduce site-scale energy use in production plants. *Appl. Therm. Eng.* **17**, 1005–1014.

High, K. A. and Roche, R. D. L. L. 1995. Parallel nonlinear optimization techniques for chemical process design problems. *Comput. Chem. Eng.* **19**, 807–825.

Hinderink, A. P., Kerkhof, F. P. J. M., Lie, A. B. K., Arons, J. D. S. and van der Kooi, H. J. 1996. Exergy analysis with a flowsheeting simulator-ii. application: Synthesis gas production from natural gas. *Chem. Eng. Sci.* **51**, 4701–4715.

Hostrup, M., Gani, R., Kravanja, Z., Sorsak, A. and Grossmann, I. 2001. Integration of thermodynamics insights and minlp optimization for the synthesis, design and analysis of process flowsheets. *Comput. Chem. Eng.* **25**, 73–83.

Ishikawa, T., Chung, W. and Lu, B. 1980. *Adv. Cryog. Eng.* **25**, 671.

Jimenez, E. S., Salamon, P., Rivero, R., Rendon, C., Hoffmann, K. H., Schaller, M. and Andresen, B.: 2003. Simulation based optimization of a diabatic distillation column. *in* N. Houbak, B. Elmegaard, B. Qvale and M. Moran (eds), *Proceedings of ECOS 2003*. number ISBN 87-7475-297-9. Department of mechanical engineering, DTU. Copenhagen, Denmark. pp. 1513–1520.

Johannessen, E. and Kjelstrup, S.: 2002. Entropy production minimization in plug flow fixed-bed reactors. *in* G. Tsatsaronis, M. Moran, F. Cziesla and T. Bruckner (eds), *Proceedings of ECOS 2002*. number ISBN 3-00-009533-0. Institute for Energy Engineering, TU Berlin. Berlin, Germany. pp. 1352–1360.

Johannessen, E. and Kjelstrup, S. 2004a. A highway in state space for reactor with minimum entropy production. *Submitted.*

Johannessen, E. and Kjelstrup, S. 2004b. Minimum entropy production rate in plug flow reactors. An optimal control problem solved for SO_2 oxidation. *Energy* **29**(12-15), 2403–2423.

Johannessen, E., Nummedal, L. and Kjelstrup, S. 2002. Minimizing the entropy production in heat exchange. *Int. J. Heat Mass Transfer* **45**, 2649–2654.

Kauchali, S., McGregor, C. and Hildebrandt, D. 2000. Binary distillation re-visited using the attainable region theory. *Comp. Chem. Eng.* **24**, 231–237.

King, C.: 1980. *Separation Processes*. 2 edn. McGraw-Hill, New York.

Kirk-Othmer: 1994. *Encyclopedia of Industrial Chemistry*. 4 edn. Wiley.

Kjelstrup, S. and Bedeaux, D.: 2001. *Elements of Irreversible Thermodynamics for Engineers*. number ISBN 975-97568-1-1. Int. Centre of Applied Thermodynamics, Instanbul.

Kjelstrup, S. and De Koeijer, G. 2003. Transport equations for distillation of ethanol and water from the entropy production rate. *Chem. Eng. Sci.* **58**(7), 1147–1161.

Kjelstrup, S., Johannessen, E., Røsjorde, A., Nummedal, L. and Bedeaux, D. 2000. Minmizing the entropy production for the methanol producing reaction in a methanol reactor. *Int. J. Appl. Thermodynamics* **3**, 147–153.

Kjelstrup, S., Tsuruta, T. and Bedeaux, D. 2003. The inverted temperature profile across a vapour/liquid surface analyzed by molecular computer simulations. *J. Colloid Interface Sci.* **256**, 451–461.

Kotas, T.: 1995. *The Exergy Method of Thermal Plant Analysis*. repr. edn. Krieger Publishing Company.

Kravanja, Z. and Glavic, P. 1997. Cost targeting for hen through simultaneous optimization approach: a unified pinch technology and mathematical programming design of large hen. *Comput. Chem. Eng* **21**, 833–853.

Krishna, R. and Wesselingh, J. 1997. The Maxwell-Stefan approach to mass transfer. *Chem. Eng. Sc.* **52**(6), 861–911.

Linnhoff, B.: 1979. *Thermodynamic analysis in the design of process networks.* PhD thesis. University of Leeds.

Loc, L., Gaidai, N., Kiperman, S. and Thoang, H. 1996. Kinetics of propane and n-butane dehydrogenation over platinum-alumina catalysts in the presence of hydrogen and water vapor. *Kinetics and Catalysis* **37**(6), 851–857.

Lucia, A., Xu, J. and Layn, K. M. 1996. Nonconvex process optimization. *Comput. Chem. Eng.* **20**, 1375–1398.

Marechal, F. and Kalitventzeff, B. 1997. Effect modelling and optimization, a new methodology for combined energy and environment synthesis of industrial processes. *Appl. Therm. Eng.* **17**, 981–992.

Maslow, A. H.: 1970. *Motivation and personality.* Harper & Row.

McCabe, W., Smith, J. and Harriot, P.: 1993. *Unit Operations of Chemical Engineering.* 5 edn. McGraw-Hill. New York.

Merkel, A. 1998. The role of science in sustainable development. *Science* **281**, 336–337.

Nakaiwa, M.: 2004. Personal communication.

Nakaiwa, M., Huang, K., Naito, K., Endo, A., Akiya, T., Nakane, T. and Takamatsu, T. 2001. Parameter analysis and optimization of ideal heat integrated distillation columns. *Comput. Chem. Eng.* **25**, 737–744.

Nakaiwa, M., Huang, K., Ohmori, T., Akiya, T. and Takamatsu, T. 2003. Internally heat-integrated distillation columns: A review. *Trans IChemE.*

Nakaiwa, M., Owa, M., Akiya, T., Kawasaki, S., Lueprasitsakul, V., Yajima, K. and Takamatsu, T. 1986. Design procedure for a plate-to-plate heat-integrated distillation column. *Kagaku Kogaku Ronbunshu* **12**(5), 535–541.

Net Resources International Limited: 2002. Industry projects. Website. http://www.chemicals-technology.com/projects/tarragona/.

Nevers, N. D. and Seader, J. D. 1984. Mechanical lost work, thermodynamic lost work, and thermodynamic efficiencies of processes. *Lat. Am. J. Heat Mass Transf.* **8**, 77–105.

Nocedal, J. and Wright, S. J.: 1999. *Numerical Optimization.* Springer. New York.

Null, H. R. 1976. Heat pumps in distillation. *Chem. Eng. Prog.* **78**, 58–64.

Nummedal, L., Costea, M. and Kjelstrup, S. 2003. Minimizing the entropy production rate of an exothermic reactor with constant heat transfer coefficient: The ammonia reactor. *Ind. Chem. Eng. Res.* (42), 1044–1056.

Nummedal, L., Røsjorde, A., Johannessen, E. and Kjelstrup, S.: 2002. Minimization of the entropy production in the primary steam reformer. *in* J. Grievink and J. van Schijndel (eds), *Computer-Aided Chemical Engineering, Vol. 10, Proceedings of ESCAPE 2002*. The Hague, The Netherlands. ISBN 0-444-51109-1.

Nummedal, L., Røsjorde, A., Johannessen, E. and Kjelstrup, S. 2004. Second law optimization of a tubular steam reformer. *Chem. Eng. Proc.*

Olivier, M.-L.: 2003. A new model for non-equilibrium mass and heat transfer at a liquid-gas interface. *in* N. Houbak, B. Elmegaard, B. Qvale and M. Moran (eds), *Proceedings of ECOS 2003*. number ISBN 87-7475-297-9. Department of mechanical engineering, DTU. Copenhagen, Denmark. pp. 1221–1229.

Olujic, Z., Fakhri, F., Rijke, A. d., Graauw, J. d. and Jansens, P. 2003. Internal heat integration - the key to an energy-conserving distillation column. *Journal of Chemical Technology and Biotechnology* **78**(2-3), 241–248.

Onsager, L. 1931a. Reciprocal relations in irreversible processes. I.. *Phys. Rev.* **37**, 405–426.

Onsager, L. 1931b. Reciprocal relations in irreversible processes. II.. *Phys. Rev.* **38**, 2265–2279.

Papalexandri, K. P. and Pistikopoulos, E. N. 1998. A decomposition-based approach for process optimization and simultaneous heat integragtion: Application to an industrial process. *Trans IChemE* **76**, 273–286.

Perez-Madrid, A., Rubi, J. and Mazur, P. 1994. Browinan motion in the presence of a temperature gradient. *Physica A* **212**, 231.

Perry, R. and Green, D.: 1997. *Perry's Chemical Engineers Handbook*. 7 edn. McGraw-Hill, New York.

Peters, M. S. and Timmerhaus, K. D.: 1991. *Plant design and economics for chemical engineers*. McGraw-Hill. Singapore.

Prausnitz, J., Lichtenthaler, R. and de Azevedo, E.: 1999. *Molecular thermodynamics of fluid-phase equlibria*. 3 edn. Prentice Hall PTR. New Jersey.

Prigogine, I.: 1955. *Thermodynamics of Irreversible Processes*. Charles C. Thomas. Springfield.

Pujado, P. and Vora, B. 1990. Make C_3-C_4 olefins selectively. *Hydrocarbon processing* pp. 65–70.

Rao, S. S.: 1996. *Engineering optimization: Theory and practice*. John Wiley and Sons. New York.

Ray, S. and Sengupta, S. P. 1996. Irreversibility analysis of a sieve tray in a distillation column. *International Journal of Heat and Mass Transfer* **39**(7), 1535–1542.

Reguera, D. and Rubi, J. 2001. Kinetic equations for diffusion in the presence of entropic barriers. *Phys.Rev. E* **64**, 061106.

Resasco, D. E. and Haller, G. L.: 1994. *Catalysis.* A specialist periodical report. The Royal Society of Chemistry. London. chapter 9.

Rivero, R.: 1993. *L'Analyse d'Exergie: Application à la Distillation Diabatique et aux Pompes à Chaleur à Absorption.* PhD thesis. Institut National Polytechnique de Lorraine, Nancy, France.

Rivero, R. 2001. Exergy simulation and optimization of adiabatic and diabatic binary distillation. *Energy* **26**, 561–593.

Rivero, R., Cachot, T., Ramadane, A. and Goff, P. L. 1994. Diabatic or quasi reversible distillation. *Int. Chem. Eng.* **34**, 240–242.

Rivero, R., Garcia, M. and Urquiza, J. 2004. Simulation, exergy analysis and application of diabatic distillation to a tertiary amyl methyl ether production unit of a crude oil refinery. *Energy* **29**, 467–489.

Rodriguez-Toral, M. A., Morton, W. and Mitchell, D. R. 2001. The use of new sqp methods for the optimization of utility systems. *Comput. Chem. Eng.* **25**, 287–300.

Røsjorde, A. and Kjelstrup, S. 2004. The second law optimal state of a diabatic binary tray distillation column. *Accepted in Chem. Eng. Sci.*

Røsjorde, A., Fossmo, D. W., Kjelstrup, S., Bedeaux, D. and Hafskjold, B. 2000. Nonequilibrium molecular dynamics simulations of steady-state heat and mass transport in condensation: I. Local equilibrium. *J. Colloid Interf. Sci.* **232**, 178–185.

Røsjorde, A., Johannessen, E. and Kjelstrup, S.: 2003. Minimizing the entropy production in two heat exchangers and a reactor. *in* N. Houbak, B. Elmegaard, B. Qvale and M. Moran (eds), *Proceedings of ECOS 2003.* number ISBN 87-7475-297-9. Department of mechanical engineering, DTU. Copenhagen, Denmark. pp. 1297–1304.

Røsjorde, A., Kjelstrup, S., Bedeaux, D. and Hafskjold, B. 2001. Nonequilibrium molecular dynamics simulations of steady-state heat and mass transport in condensation: II. Transfer coefficients. *J. Colloid Interf. Sci.* **240**, 355–364.

Røsjorde, A., Nakaiwa, M., Huang, K., k. Iwakabe and Kjelstrup, S.: 2004. Second law analysis of an internal heat-integrated distillation column. *in* R. Rivero, L. Monroy, R. Pulido and G. Tsatsaronis (eds), *Proceedings of ECOS 2004.* number ISBN 968-489-027-3. Instituto Mexicana del Petroleo. Guanajuato, Mexico. pp. 107–115.

Rytter, E. and Bölt, H.: 2000. An improved process for catalytic dehydrogenation of propane to propylene. *Proceedings of CatCon.* Houston, USA.

Sauar, E., Rivero, R., Kjelstrup, S. and Lien, K. M. 1997. Diabatic column optimization compared to isoforce columns. *Energy Convers. Mgmt.* **38**, 1777–1783.

Schaller, M., Hoffman, K. H., Siragusa, G., Salamon, P. and Andresen, B. 2001. Numerically optimized performance of diabatic distillation columns. *Comput. Chem. Eng.* **25**, 1537–1548.

Schaller, M., Hoffmann, K. H., Rivero, R., Andresen, B. and Salamon, P. 2002. The influence of heat transfer irreversibilities on the optimal performance of diabatic distillation columns. *J. Non-equilib. Thermodyn.* **27**(3), 257–269.

Schechter, R. S.: 1967. *The variational method in engineering.* McGraw-Hill, New York.

Seader, W. D., Seader, J. D. and Lewin, D. R.: 1999. *Process design principles: synthesis, analysis, and evaluation.* Wiley.

Smith, J. and Van Ness, H.: 1987. *Introduction to Chemical Engineering Thermodynamics.* 4th edn. McGraw-Hill, Inc.

Smith, R.: 1995. *Chemical process design.* McGraw-Hill.

Sorin, M., Hammache, A. and Diallo, O. 2000. Exergy based approach for process synthesis. *Energy* **25**, 105–129.

Sun, L., Olujic, Z., deRijke, A. and Jansens, P.: 2003. Industrially viable configurations for a heat-integrated distillation column. *Proceedings of the 5th International Conference on Process Intensification for Chemical Industry.* Maastricht, The Netherlands. pp. 151–166.

Sundaram, K. M. and Froment, G. F. 1977. Modeling of thermal cracking kinetics - I. *Chem. Eng. Sci.* **32**, 601–608.

Szargut, J., Morris, D. R. and Steward, F. R.: 1988. *Exergy Analysis of Thermal, Chemical, and Metallurgical Processes.* Hemisphere. New York.

Taylor, R. and Krishna, R.: 1993. *Multicomponent Mass Transfer.* Wiley. New York.

Toffolo, A. and Lazzaretto, A. 2002. Evolutionary algorithms for multi-objective energetic and economic optimization in thermal system design. *Energy* **27**, 549–567.

Umeda, T., Itoh, J. and Shiroko, K. 1978. Heat exchange system syntesis. *Chem. Eng. Prog.* **74**, 70–76.

Van der Lee, P. E. A., Terlay, T. and Woudstra, T. 2001. A new approach to optimizing energy systems. *Comput. Methods Appl. Mech. Engrg.* **190**, 5297–5310.

Vilar, J. and Rubi, J. 2001. Thermodynamics beyond local equilibrium. *Proc. Natl. Acad. Sci. USA* **98**, 11081.

Weast, R. C. and Astle, M. J. (eds): 1982. *CRC Handbook of Chemistry and Physics.* 62 edn. CRC Press. Boca Raton, Florida.

Wendt, M., Konigseder, R., Li, P. and Wozny, G. 2003. Theoretical and experimental studies on startup strategies for a heat-integrated distillation column system. *Chem. Eng. Res. Des: TransIChem* **81**(A1), 153–161.

Wesselingh, J. A. 1997. Non-equilibrium modelling of distillation. *Chem. Eng. Res. Des: TransIChem* **75**(A), 529–538.

Wilkendorf, F., Espuna, A. and Puigjaner, L. 1998. Minimization of the annual cost for complete utility systems. *Chem. Eng. Res. Des: TransIChemE* **76**, 239–245.

Zamora, J. M. and Grossmann, I. E. 1998a. Continuous global optimization of structured process system models. *Comput. Chem. Eng.* **22**, 1749–1770.

Zamora, J. M. and Grossmann, I. E. 1998b. A global minlp optimization algorithm for the synthesis of heat exchanger networks with no stream splits. *Comput. Chem. Eng.* **22**, 367–384.